MECHANISM OF SMOLDERING COMBUSTION IN CELLULOSIC MATERIALS

By

N. Albert Moussa

B. S., Stanford University (1971)
M. S., Massachusetts Institute of Technology (1972)

Submitted in Partial Fulfillment
of the Requirements for the

Degree of Doctor of Science

at the
Massachusetts Institute of Technology

October 1975
(i.e. February, 1976)

Signature Redacted

Signature of Author.....
Department of Mechanical Engineering

Signature Redacted

Certified by.....
T. K. Toong
Thesis Supervisor

Signature Redacted

Accepted by.....
Warren M. Rohsenow
Chairman, Departmental Committee
on Graduate Students

ARCHIVES

MAR 16 1976
LIBRARIES

MECHANISM OF SMOLDERING COMBUSTION IN CELLULOSIC MATERIALS

N. Albert Moussa

Submitted to the Department of Mechanical Engineering in October 1975 in partial fulfillment of the requirement for the degree of Doctor of Science

ABSTRACT

A coordinated theoretical and experimental investigation of the mechanism of smoldering in cellulosic materials has been conducted.

Both steady and transient smoldering have been observed for single cylindrical cellulosic elements, mounted horizontally in quiescent oxygen/nitrogen environments of varying pressures and compositions. In the region of steady smoldering, the measured propagation speed and maximum temperature in the smoldering zone depend on the oxygen partial pressure and mole fraction in the environment. However, independent of the environment, the speed is uniquely related to the maximum temperature. In the region of transient smoldering, an extinguishment limit is observed at well-defined combinations of oxygen mole fraction and partial pressure.

It is postulated that cellulose, upon heating, decomposes to yield char and volatiles. The char reacts with oxygen, diffusing from the surroundings, to provide the heat needed for pyrolysis. The overall kinetic parameters for cellulose pyrolysis and for char-oxidation (appropriate for this study) were determined by comparing the observed temperature-speed relationship and extinguishment limit with the corresponding theoretical predictions. On the basis of these overall

kinetic parameters, steady smoldering speeds and corresponding temperatures are computed for various oxygen mole fractions and partial pressures. The predicted values agree quite well with measurements.

Thesis Supervisor: T. Y. Toong

Title: Professor of Mechanical Engineering

ACKNOWLEDGMENTS

The author expresses his gratitude to Professor T. Y. Toong for suggesting the subject of this thesis, securing the financial support and for his guidance through its completion.

Various discussions with Dr. C. A. Garris, Messrs. F. Wong, M. Ortiz and J. P. Patureau are appreciated. Dr. Garris' contribution to the mathematical formulation of the pyrolysis model for a semi-infinite slab and Messrs. M. Ortiz and M. Atlas' help in conducting some of the experiments are gratefully acknowledged.

The criticism and suggestions of the following members of the author's thesis committee are appreciated: Professors J. P. Appleton, J. B. Howard and G. Tesoro.

This work was supported by the National Bureau of Standards under Grant No. 4-9014 and by the Sloan Basic Research fund made available to the Department of Mechanical Engineering through the Union Carbide Corporation, Linde Division.

MECHANISM OF SMOLDERING COMBUSTION

IN CELLULOSIC MATERIALS

TABLE OF CONTENTS

ABSTRACT	i
ACKNOWLEDGMENTS	iii
LIST OF TABLES	iv
LIST OF FIGURES	v
CONCLUSIONS	1
SUMMARY OF RESULTS	3
CHAPTER 1: INTRODUCTION	5
CHAPTER II: EXPERIMENTAL INVESTIGATIONS	10
2.1 Experimental Apparatus	12
2.1.1 Pressure Vessel	12
2.1.2 Gas Analysis	16
2.2 Reproducibility of the Results	17
2.3 Qualitative Description of Smoldering	21
2.4 Effects of Environmental Parameters	22
2.4.1 Transitions to Extinguishment or Flaming	25
2.4.2 Steady Smoldering Results	30
2.5 Effects of Fuel Parameters	39
2.6 Smoldering Behavior of Non-Cellulosic Polymers	47
2.7 Experimental Results	49

CHAPTER III: THEORETICAL ANALYSES AND COMPARISONS WITH EXPERIMENTS 51

3.1 Pyrolysis Study 54

3.1.1 Overall Mechanism of Cellulose Pyrolysis 54

3.1.2 Mathematical Formulations 62

3.1.3 Closed-form Approximate Eigenvalue 67

3.1.4 Comparison of Theory and Experiment 79

3.1.5 Conclusions from the Pyrolysis Study 82

3.2 Char-Oxidation Study 84

3.2.1 Overall kinetics of Char-oxidation 86

3.2.2 Reaction Rate Accounting for Kinetics and Diffusion Considerations 89

3.2.3 Energy Balance 97

3.2.4 Comparison of Theory with Experiment 104

3.3 Smoldering Behavior: Theory and Experiment 108

3.4 Conclusions 119

RECOMMENDATIONS 121

REFERENCES 122

APPENDIX 2.1 EXPLORATORY EXPERIMENTS ON SMOLDERING 128

APPENDIX 2.2 LISTING OF EXPERIMENTAL RESULTS FOR VARIOUS ENVIRONMENTS 131

APPENDIX 2.3 INVESTIGATION OF THE HAZARDS FROM SMOLDERING FIRES 138

APPENDIX 3.1 REACTION OF A POROUS CHAR LAYER WITH AMBIENT OXYGEN 146

APPENDIX 3.2 NON DIMENSIONAL PARAMETERS OF INTEREST TO THIS STUDY 150

APPENDIX 3.3 OXYGEN DIFFUSION FLUX TO CHAR SURFACE 151

APPENDIX 3.4 HEAT TRANSFER CORRELATION FOR THE BOUNDARY LAYER THICKNESS 154

APPENDIX 3.5 COMPUTOR PROGRAMS 156

APPENDIX 3.6 NUMERICAL VALUES EMPLOYED IN THE THEORETICAL CALCULATIONS 164

LIST OF TABLES

Table No.	Title
2.2.1	Reproducibility of Steady Smoldering Results
2.2.2	Reproducibility of Runs in Borderline Region, Leading to Self-Extinguishment
2.4.1	Induction Times Between the Onset of Smoldering and the Transition to Flaming
2.4.2	Induction Times Between the Onset of Smoldering and the Transition to Extinguishment
2.5.1	Diameter and Density of Cylindrical Cellulosic Materials used in Fig. 2.5.1
2.5.2	Effects of Sample Orientation in the Gravity Field
3.1.1	Comparison of the Kinetic Parameters Reported for the Two-Reaction Pyrolysis Model
3.1.2	Comparison of the Experimental Conditions of the Present Study and those of Aldrich [3.1] and Emmons [3.2]

LIST OF FIGURES

Figure No.	Title
2.1.1	Schematic Diagram of Pressure Vessel
2.1.2	Pressure Line
2.3.1	Description of Steady Smoldering in Cylindrical Cellulosic Materials Mounted Horizontally
2.3.2	Correlations of Visual Observations with Temperature Measurements at Center and at Surface of a Cotton Yarn; Smoldering in Standard Atmospheric Conditions
2.4.1	Occurrence of Steady or Transient Smoldering Followed by Flaming or Extinguishment as Functions of Ambient Oxygen Mole Fractions and Partial Pressures, Cellulosic Samples Mounted Horizontally
2.4.2	Steady Smoldering Speed versus Ambient Oxygen Mole Fraction as a Function of its Partial Pressure, Cellulosic Samples Mounted Horizontally
2.4.3	Steady Smoldering Speed versus Ambient Oxygen Partial Pressures as a Function of Mixture Pressures, Cellulosic Samples Mounted Horizontally
2.4.4	Steady Smoldering Speed versus Mixture Pressure as a Function of Ambient Oxygen Partial Pressure, Cellulosic Samples Mounted Horizontally

2.4.5 Steady Smoldering Speed versus Ambient Oxygen Partial Pressure at a Constant Oxygen Mole Fraction, Cellulosic Samples Mounted Horizontally

2.4.6 Steady Smoldering Maximum Temperature versus Ambient Oxygen Mole Fraction at a Constant Oxygen Partial Pressure, Cellulosic Samples Mounted Horizontally

2.4.7 Steady Smoldering Maximum Temperature versus Ambient Oxygen Partial Pressure at a Constant Oxygen Mole Fraction, (Cellulosic Samples Mounted Horizontally)

2.4.8 Reaction Zone Length versus Ambient Oxygen Mole Fraction at a Constant Oxygen Partial Pressure, Cellulosic Sample Mounted Horizontally

2.5.1 Steady Smoldering Speed and Maximum Temperature versus Density. Diameter for Cellulosic Materials Mounted Horizontally, in Standard Atmospheric Conditions

3.1.1 Postulated Reaction Schemes of Cellulose Pyrolysis

3.1.2 Overall Specific Reaction Rate for Cellulose Pyrolysis versus Temperature for Two Sets of Kinetic Parameters

3.1.3 Physical Description of the Stationary Pyrolysis Zone. External Heat Flux (q_s) is Imposed at x = o. Virgin Material is Entering Zone and Char and Volatiles are Leaving it

3.1.4 Steady Smoldering Speed, V, versus Imposed Heat Flux as a Function of the Thermicity of the Pyrolysis Reactions

3.1.5	Interface Temperature versus Imposed Heat Flux as a Function of the Thermicity of the Pyrolysis Reactions
3.1.6	Exponential Integral Function, Ei(x), for a Range of Values of Interest
3.1.7	Approximate and Exact Pyrolysis Speed versus Imposed Heat Flux
3.1.8	Approximate and Exact Interface Temperature versus Imposed Heat Flux
3.1.9	Comparison of Theory and Experiment for the Steady Smoldering Temperature-Speed Relationship. Theory gives Approximate and Exact Solutions. Horizontal Cellulosic Samples were tested in Various Oxygen Mole Fractions (X_{o_2}) and Partial Pressures (P_{o_2})
3.2.1	Flow Field around Smoldering Cellulosic Element
3.2.2	(a) Kinetics-Limited Regime (b) Diffusion-Limited Regime
3.2.3	Heat Flux Generated by Char-Oxidation Reaction versus Temperature for Ambient Oxygen Mole Fraction = 0.21 and Partial Pressure = 15.7 cm Hg
3.2.4	Schematic for the Energy Balance over the Smoldering Element
3.2.5	Balance of Heat Fluxes versus Temperature
3.3.1	Comparison of Theory and Experiment for the Steady Smoldering Speed and Temperature versus Ambient Oxygen Mole Fraction at a Constant Oxygen Partial Pressure, Cellulosic Samples are Mounted Horizontally

3.3.2 Comparison of Theory and Experiment for the Steady Smoldering Speed and Temperature versus Ambient Oxygen Partial Pressure at a Constant Oxygen Mole Fraction, Cellulosic Samples are Mounted Horizontally

3.3.3 Calculated Boundary Layer Thickness versus Oxygen Mole Fraction or Mixture Pressure at a Constant Oxygen Partial Pressure, P_{O_2}

3.3.4 Predicted Ratio of Diffusion to Chemical Times versus Ambient Oxygen Mole Fraction at a Constant Oxygen Partial Pressure, P_{O_2}

3.3.5 Predicted Ratio of Diffusion to Chemical Times versus Ambient Oxygen Partial Pressure at a Constant Oxygen Mole Fraction, X_{O_2}

CONCLUSIONS

On the basis of the agreement between theory and experiments, it can be concluded that the mechanism proposed in this thesis can interpret the main observed features of smoldering combustion. In this mechanism, cellulose, upon heating, decomposes to yield char and volatiles. The char reacts with oxygen, diffusing from the surroundings, to yield the heat needed for pyrolysis.

The main features of smoldering determined by experiments and interpreted on the basis of this mechanism are the following:

(1) the occurrence of either steady or transient smoldering depending on the ambient oxygen mole fraction and partial pressure which govern the heat generated by char-oxidation.

(2) In the region of steady smoldering, the propagation speed and the maximum temperature in the smoldering zone depend more on the ambient oxygen mole fraction than on its partial pressure. This is caused by the greater effect of the mole fraction on oxygen diffusion to the char. However, independent of the mole fraction or partial pressure of oxygen, the temperature-speed relationship is governed by the pyrolysis and thermophysical characteristics of the fuel.

(3) In the region of transient smoldering, an extinguishment limit occurs at well defined combinations of oxygen partial pressures and mole fractions at which the heat generated can not sustain pyrolysis.

It is also concluded that for the purposes of studying smoldering, the use of overall kinetic schemes for cellulose pyrolysis and char-oxidation is adequate. Furthermore, the overall kinetic parameters for pyrolysis can be determined by comparing the observed steady smoldering temperature-speed relationship with that predicted on the basis of specific kinetic parameters. Similarly, the overall kinetic parameters for char-oxidation can be determined by comparing the observed extinguishment limit with that predicted on the basis of specific kinetic parameters, combined with the kinetic parameters determined for pyrolysis.

SUMMARY OF RESULTS

The coordinated experimental and theoretical investigation of this study determined that:

(1) Both steady and transient smoldering occur depending on the pressure and composition of the environment.

(2) In the region of transient smoldering, an extinguishment limit occurs at well-defined oxygen mole fractions and partial pressures.

(3) In the region of steady smoldering, the speed depends strongly on the oxygen mole fraction and weakly on its partial pressure; and the corresponding dependencies of the temperature are weak and negligible. However, independent of the environment, the speed is uniquely related to the temperature for a specified fuel.

(4) The overall kinetic parameters for cellulose pyrolysis and char-oxidation (appropriate for this study) were determined by critical comparisons of theory and experiment.

In addition, the theoretical phase of this investigation yielded a closed-form approximate experssion for the smoldering speed, as a function of an imposed heat flux or the temperature at the interface (between the pyrolysis and char zone) and the kinetic and thermophysical parameters of the system. According to this expression, the speed will increase with:

- an increase in fuel thermal conductivity
- a decrease in fuel heat capacitance
- faster kinetics for the pyrolysis reaction of the fuel

Furthermore, the experimental phase demonstrated the following:

1. In the region of steady smoldering:
   - the speed is inversely related to the product of density x diameter
   - the effect of sample orientation in the gravity field on the speed is small (when compared to the corresponding effect in the case of flaming).
   - the reaction zone length is of the size of the fuel element diameter ($\pm$ 30%) for various environmental parameters.
   - the amount of char residue, left after the smoldering wave has spread over an element, varies significantly with the environmental parameters.
2. In the region of transient smoldering:
   - a flaming limit occurs at well-defined combinations of oxygen mole fractions and partial pressures.
   - the induction time, from the initiation of smoldering to a transition to flaming or extinguishment, varied significantly with the environmental parameters.
3. For non-cellulosic materials, smoldering was observed for char-forming polymers (namely, wool and polyurethane) and was not observed for non-char-forming polymers (namely, nylon, polyester and polystyrene).
4. The hazards from smoldering fires in dwellings include the loss of visibility (long before the tolerance limits in carbon monoxide and oxygen are reached) and the transition to flaming (for some materials) when sufficient air flow is imposed on the smoldering zone.

Chapter I

INTRODUCTION

Unwanted fires have caused an annual toll of about 12,000 deaths, many sufferings due to personal injury, and a direct property damage of about two billion dollars. Furthermore, the indirect wastage might well be two to three times this amount [1.1]*. Thus, the need for research to help understand fires and reduce their potential hazards has been well recognized. In fact, many studies on flame spread and mass fires are well underway [1.2 - 1.4].

Statistics show that 75% of unwanted fires in dwellings are smoldering during their initial stage [1.5] and, when the fuel and environment characteristics are favorable, a transition to flaming may occur and the fire goes out of control. Smoldering can be defined as a flameless mode of combustion, usually accompanied by the evolution of smoke, heat and light (usually referred to as glow). Despite its seemingly important role in fire hazards in dwellings, little attention has been given to its study. Its hazards have been identified mainly in factories, and consequently the smoldering of inductrial dust deposits has been investigated in the past [1.6, 1.7]. However, a mechanism has not as yet been developed, to describe the smoldering behavior from a knowledge of the characteristics of the fuel and the environment;

---

* Numbers in brackets denote references at end of manuscript.

thus, the motivation of this doctoral thesis.

The purpose of this thesis is to investigate, by theory and experiment, the mechanism of smoldering in cellulosic materials. Cellulosic materials were chosen because of their commercial importance and their high availability in dwellings. The main hazards associated with smoldering fires have also been identified in this study.

On the basis of the results obtained in this thesis, more effective means of fire protection can be developed. Furthermore, this thesis is of interest to other fields of study, namely the pyrolysis and combustion of solid refuse in incinerators and power plants, and the generation of carcinogens in cigarette smoldering.

The problem of industrial smoldering fires, has been recognized in the past. In 1954, Cohen and Luft [1.6] listed the rates of propagation of smoldering in still air for a range of dusts, including Magnesium, coal, cocoa, Lycopodium*, wood, sawdust and Pyrites. Temperature measurements in the smoldering zone were also reported in some instances. Approximate expressions were given for the dependencies of (1) the smoldering speed on the depth of the dust layer; and (2) the minimum depth of the dust layer for sustained smoldering on the particle size of the dust.

In 1956, Palmer [1.7] measured smoldering rates and temperatures in several types of dust trains and in rigid fiberboards, under imposed air flow and in still air. The dusts included cork, grass, and beech and deal sawdusts. He also determined the minimum depth of dust deposit

* erect or creeping plants with evergreen leaves.

required for sustained smoldering. A transition from smoldering to flaming, under the effect of imposed air flow, was occasionally reported.

In 1962, (the late) Sir Egerton initiated another interest in smoldering. He studied [1.8] the smoldering of cigarettes "with a view to elucidating the dependence of temperatures, consumption rates, etc., upon cigarette structure and smoking parameters. Information obtained by special methods included: peripheral surface temperatures by cine radiation-pyrometry; internal temperature contours, at various times, by cine x-ray photography of the melting of minute inclusions; external distribution of hot gases by schlieren photography; and consumption patterns for a variety of smoking conditions. Considerations of unidimsional theory and of the smouldering of an adiabatic analogue, using graphite particles, yielded a working model for cigarettes. Some conclusions were that all 'available' smoke derives from the outermost annulus containing one half to one third of the total volume; particle temperatures there exceed 900°C and surface temperatures reach 1200 °C. The inner cylinder - three quarters of the total radius - smolders chiefly by natural convection, which is relevant to the smoker only in that it acts as pilot and maintains the shape of the smoldering zone and the passage of gases through it." [1.8]

In 1967, Kinbara et al [1.9] studied the smoldering in the following samples: (1) circular rods of rolled paper, (2) circular incense sticks, (3) strips of cardboard and (4) piles of cardboard tightly bound with thread. They generated empirical formulae for the vertically-downward-smoldering speed in terms of the ambient temperature (T_o) and the radius or the breadth and thickness of the samples. They

also developed a theory on the basis of the following assumptions: (1) the heat produced by the combustion of a solid body per unit time is proportional to the rate of air supplied by diffusion which is assumed proportional to the difference between the body temperature and the ambient temperature; and (2) this heat is inversely proportional to $(T_i - T_a)$, where T_i is the temperature at which the solid material ignites instantaneously. This theory yielded good agreement with the empirical formulae for the smoldering speed.

Of the four studies summarized above, that of Kinbara et al simulates best the conditions of smoldering fires in dwellings. Namely, they considered cellulosic materials and geometries that can be found in dwellings. Similar situations were investigated in the present study, however, the emphasis is very different from that of Kinbara et al.

Kinbara et al made a priori assumptions, on the processes occurring during smoldering, to predict the speed. In this thesis, a mechanism of smoldering is proposed to account for these processes. Specifically, Kinbara et al's assumption, of the existence of an ignition temperature at which the material ignites instantaneously was not invoked in this study. Instead, the pyrolysis behavior of cellulose was taken into consideration. Furthermore, Kinbara et al's assumption that the heat produced was proportional to the rate of arrival of oxygen was not invoked either. Instead, the heat generated was calculated for the reaction of oxygen with the products of pyrolysis including both kinetics and diffusion considerations. Finally, to verify the mechanism

proposed in this thesis, the effects of the composition and pressure in the environment of the smoldering sample were determined experimentally. This yielded information so far unavailable in the literature.

In the following text, the experimental investigation of environment and fuel parameters on the smoldering behavior of cellulosic materials are presented in chapter II. Then, a mechanism of smoldering is proposed, in chapter III, and the experimental results are discussed in light of this mechanism. The rationale and main findings of each chapter are given in the introductory paragraphs to each chapter. The recommendations for future research are given in a separate section. Qualitative investigations of the smoldering behavior under various conditions and the hazards associated with smoldering fires are given in Appendices 2.1 and 2.3. A listing of the raw data is given in Appendix 2.2. Analysis and calculations supporting the theoretical section of chapter III are given in Appendices 3.1 to 3.5.

CHAPTER II

EXPERIMENTAL INVESTIGATIONS

The purpose of this chapter is to determine experimentally the effects of environment and fuel characteristics on smoldering in cellulosic materials. Critical comparisons of these results with the theoretical predictions are presented in the following chapter and have shed light on the mechanism of smoldering.

The first of these factors, the environment, is mainly characterized by its composition, pressure, temperature and relative humidity, and externally imposed thermal or flow fields. The second factor, the fuel, is mainly characterized by geometry, size, density, porosity, thermophysical properties, initial temperature and orientation in the gravity field.

To understand the rationale behind this experimental investigation, one must refer to the theory presented in chapter III. The theory describes how environment and fuel influence processes involved in smoldering such as heat transfer, pyrolysis, buoyancy, oxygen diffusion and oxidation reactions.

To make this study tractable, it was decided to use a simple geometry and a simple configuration. Specifically, a single cylindrical element placed in a horizontal plane in an infinite natural-convective field, with minimum interactions with the surroundings, was selected*.

---

* Some qualitative observations for other geometries, are given in Appendix 2.1.

Under these conditions, smoldering tests were conducted to measure the speed and the temperature-time profile* as a function of:

- environmental parameters, namely oxygen mole fraction and partial pressure, and mixture pressure

or

- fuel parameters, namely density, diameter and sample orientation in the gravity field.

Under the conditions of this study, it was observed that the environmental parameters determined a region of steady-smoldering, and a region of transient smoldering followed by extinguishment or flaming. Extinguishment and flaming limits occurred at critical combinations of oxygen mole fraction and partial pressure.

In the region of steady-smoldering it was found that:

1. the speed and maximum temperature in the smoldering zone increased strongly and weakly with increasing oxygen mole fraction, respectively
2. the speed increased weakly with increasing oxygen partial pressure, and the corresponding changes in the maximum temperature were negligible**.
3. the temperature-speed relationship was unique for a specified fuel regardless of the environmental parameters.
4. the reaction zone length obtained from the temperature-time profile (as described in section 2.2.4) was of the size of the fuel element diameter ($\pm$ 30%),for various environmental

---

* These parameters are also important to hazards assessment as described in Appendix 2.3.

** Because only two environmental parameters are independent, the effects of the mixture pressure can be deduced from those of the two other parameters.

parameters.

5. the speed was inversely related to the product of density x diameter, regardless of the particular value of each parameter. On the other hand, the temperature increased (though weakly) with this product.
6. the effects of sample orientation on the speed is small (as compared to its effects in the case of flaming).

This chapter presents a description of the apparatus, the experimental procedure and the main qualitative features of smoldering, a discussion of reproducibility of the results, and finally, the effects of environmental and fuel parameters on the smoldering behavior.

2.1 EXPERIMENTAL APPARATUS

The main components of the experimental apparatus are the pressure vessel and the gas-analysis instrumentation. The rationale behind choosing each component is presented below, followed by its description.

2.1.1 Pressure Vessel

In the design of an enclosure to study the mechanism and hazards of smoldering fires, three possible configurations were studied; viz., (a) a screen* with an exhaust hood, (b) a scaled-down room** with on/off exhaust capability and (c) a cylindrical pressure vessel. Preliminary designs have been undertaken on all three configurations. (In fact, the screen with an exhaust hood was set-up for some exploratory experiments). An analysis of these configurations was performed, taking into account the

* The purpose of the screen is to minimize any disturbances from the surroundings.

** Made of Transite sheets with windows.

following: safety of experimenter, capability for exercising controls on critical variables, adaptability to instrumentation, construction time and costs, flexibility for future changes, operational convenience and limitation on field of vision. It was found that the pressure vessel was the most desirable.

A prefabricated pressure vessel was obtained and its main features are illustrated in Fig. 2.1.1. The vessel consists of a 1/2"-thick (1.27 cm) steel shell 3'-diameter (0.91 m) and 4'6" long (1.4 m), with dome-shaped ends and a swinging door. Three 6"-diameter (15 cm) windows are available for visual observation and picture-taking. A number of pipe connections and feedthroughs are also available. The vessel can withstand vacuum of a few centimeters of H_2O and pressures of up to 100 psi (~ 7 atmospheres), thus allowing the study of the effects of oxygen concentration and pressure. A Sutorbuilt pump and a Worthington compressor are available for this purpose, as is shown in Fig. 2.1.1. Furthermore, a Forge blower can quickly flush the vessel through a 3-1/2" (8.9 cm) valve.

Figure 2.1.2 illustrates in detail the pressure line in the vessel. It should be noted that redundant safety components are present such as the safety valve and two automatic switches to turn off the compressor in case of pressure build-up in the line. Should pressure build up in the vessel, a solenoid valve can shut off the air flow from the compressor. A safety valve is also available in the vessel itself to release such a pressure build-up.

The vessel was implemented with a 0.05 mm wire frame to support fuel samples with minimum quenching, and with zone boxes to measure the temperature at various locations in the vessel. Chromel-Almel thermocouples were used (wire diameter = 0.002" or 0.05 mm and bead diameter

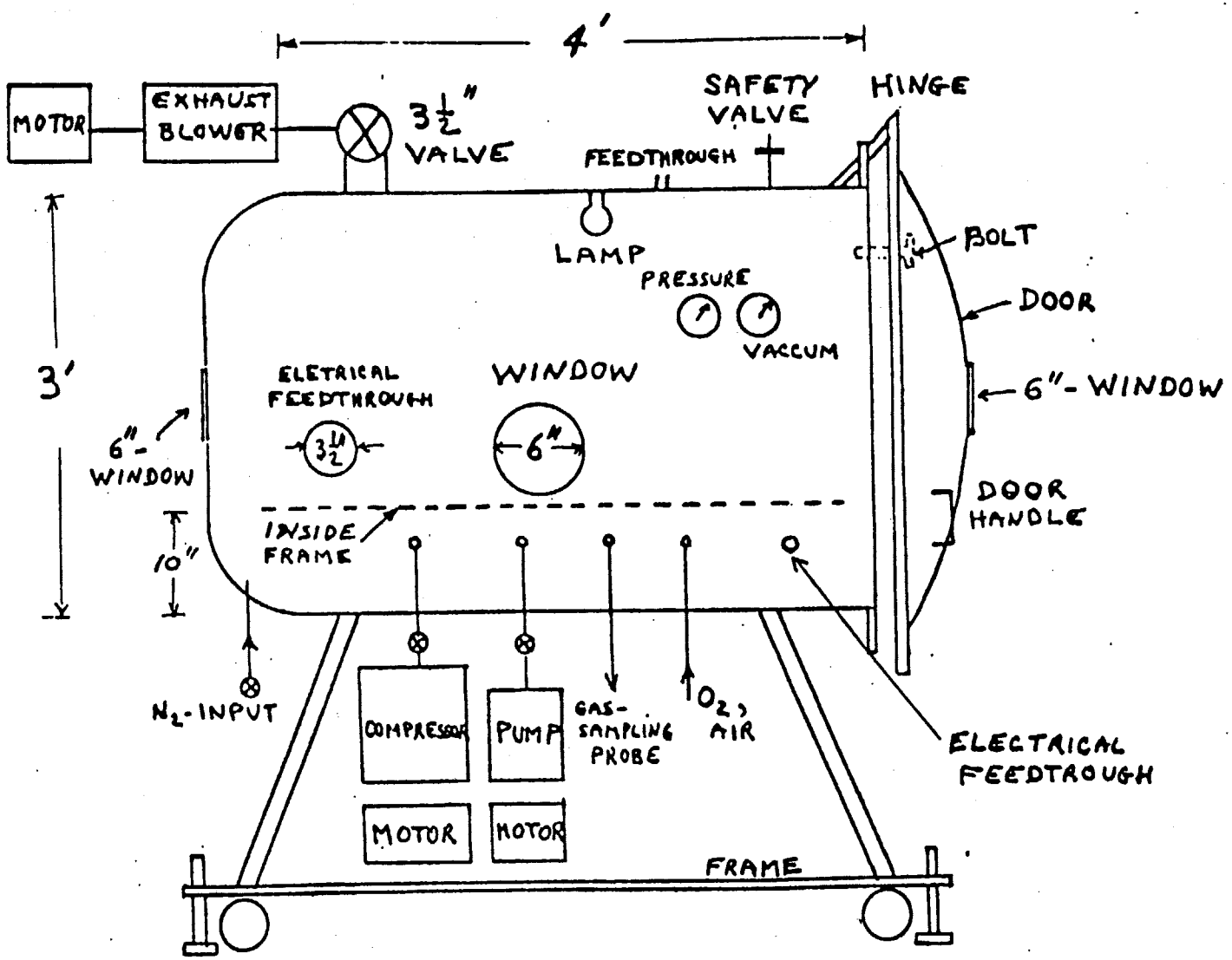


Fig. 2.1.1 Schematic Diagram of Pressure Vessel

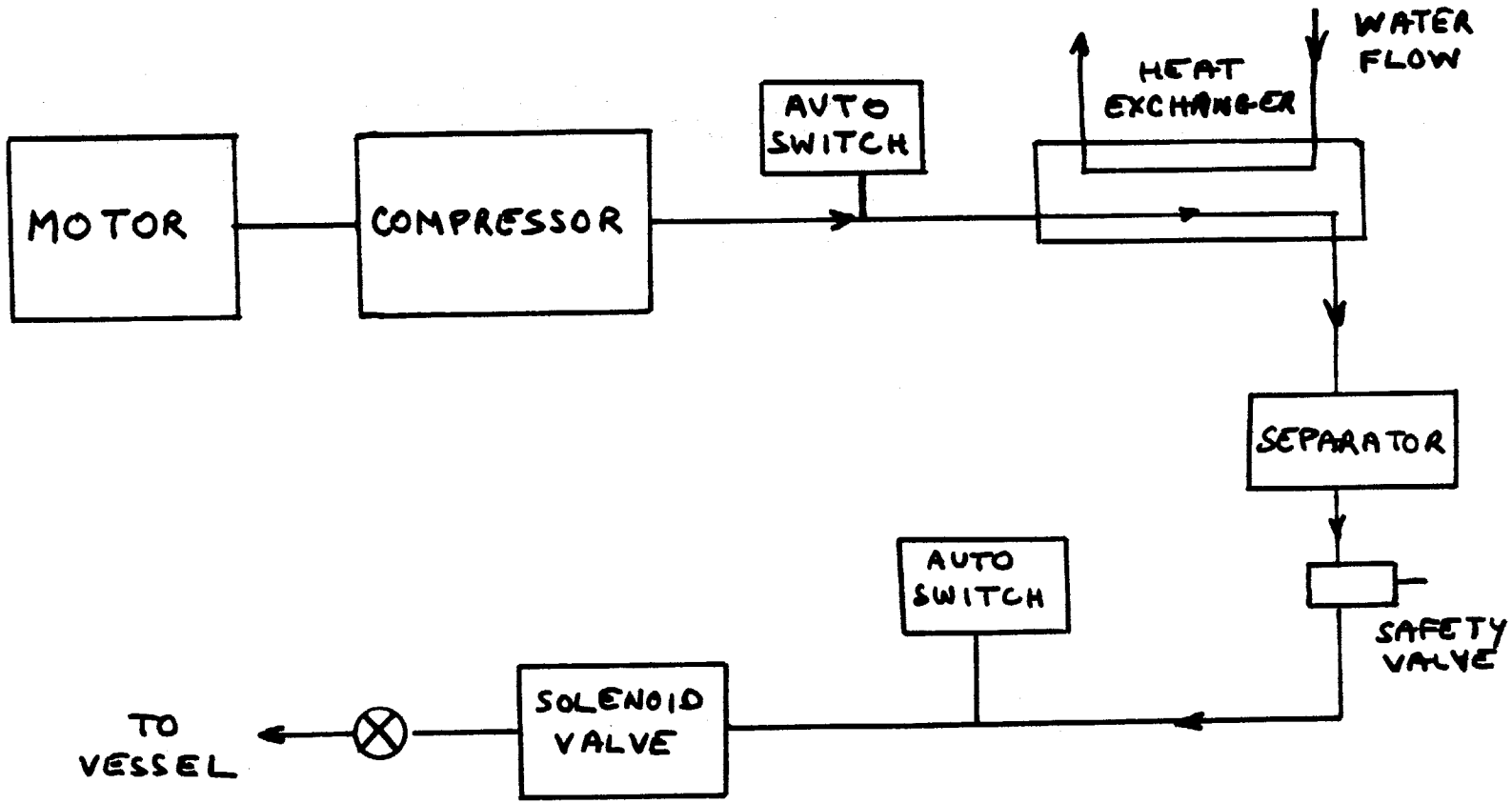


FIG. 2.1.2 PRESSURE LINE

= 0.004" to 0.006" or 0.1 to 0.15 mm). A heating coil was used as the ignition source, providing up to about 6 cal/cm^{2}s.

2.1.2 Gas Analysis

As has been discussed by Fristrom [2.1], the most frequent cause of death in fires is by CO poisoning. Hence, the analysis of CO evolution during experiments is of basic imoortance. Further, to evaluate the flashover hazard of smoldering combustion, monitoring the buildup of unburned hydrocarbons is essential. For both the life hazard of asphyxiation and the explosion hazard, monitoring the oxygen concentration during the experiments is also of fundamental importance. It was therefore desired to continuously monitor the evolution of CO, HC, and O_2 during some experiments at different strategic locations. For this purpose, a non-dispersive infra-red CO and HC analyzer (Model GSM 300A, purchased from Horriba, Ind.) and a polarographic oxygen analyzer (Beckman Model 777) were used, see Appendix 2.3.

2.2 REPRODUCIBILITY OF THE RESULTS

The reproducibility of the results presented in this chapter are affected by two main factors:

1. Uncertainty introduced by the experimental method due to poor contact between thermocouple and a porous yarn, and due to subjective visual monitoring of the location of the smoldering zone.
2. Parameters uncontrolled in each experiment such as ambient temperature and relative himidity, sample initial temperature and inherent non-uniformities in the sample properties. The effects of these parameters is expected to be especially important in the borderline regions between steady smoldering and transient smoldering leading to extinguishment or flaming.

First, the overall effect of the two factors was examined in the region of steady smoldering. Table 2.2.1 illustrates the results for the speed and the maximum temperatures at the center and at the surface of the yarn, under the same running conditions but for tests conducted on different days and with different samples. The mean and the standard deviation calculated for these results are the following:

- speed = 1.27 cm/min $\pm$ 6%
- maximum inside temperature = 940 °K $\pm$ 6%
- maximum surface temperature = 810 °K $\pm$ 7%

While the standard deviation appears large, the trends in our data were still apparent, and thus, the reproducibility was regarded as adequate.

Secondly, scatter has been observed on many occasions (as expected) in the borderline regions between steady smoldering and transient smolder-

TABLE 2.2.1

Reproducibility of Steady Smoldering Results

Run	Date	P	X_{O_2}	P_{O_2}	R.H.	T_d	T_s	T_i	V
		cmHg	%	cmHg	%	°C	°K	°K	cm/min
A2	1/9/74	75.7	21.	15.9	43	20.5	860	-	1.27
16	1/22/75	76.9	21.	16.1	28	25.0	890	950	1.40
18	1/28/75	76.8	21.	16.1	36	17.0	790	-	1.27
22	3/18/75	77.4	21.	16.3	25	23.5	780	980	1.23
23	3/21/75	75.3	21.	15.8	28	20.5	770	860	1.34
A3	5/13/75	76.4	21.	16.0	61	23.5	-	-	1.17
40	7/17/75	76.7	21.	16.1	66	30.0	740	986	1.19
71	7/17/75	76.7	21.	16.1	47	22.5	-	-	1.27

P = Mixture pressure
X_{O_2} = Oxygen mole fraction
P_{O_2} = Oxygen partial pressure
RH = Relative Humidity
T_d = Air dry temperature
T_s = Surface temperature of the yarn
T_i = Temperature at center of yarn
V = Steady smoldering Speed

ing leading to flaming or extinguishment. For example, the flame obtained(either spontaneously or by an induced air flow) may or may not self-sustain under otherwise identical conditions. Furthermore, extinguishment occured after induction times* varying by a factor of five for two runs at the same oxygen mole fraction and partial pressure, as illustrated in Table 2.2.2. Note that the two runs vary only in the relative humidity and possibly in some uncontrolled variations of the heating rate ** and the sample properties. Accordingly, scatter is expected in the induction times presented in section 2.4.1. Such scatter cannot be determined, as yet, because of insufficient data in these borderline regions.

---

* The induction time is the time interval between the onset of smoldering and extinguishment or the appearance of a flame.

** Such as variations in the thermal contact between the sample and the heating coil.

Table 2.2.2

Reproducibility of Runs in Borderline Region, Leading to Self-Extinguishment

Run #	Date	P cm Hg	X_{o_2} %	P_{o_2} cm Hg	T_{air} °C	RH %	$T^*_{c,max}$ °C	d_e **	T_e sec
11	12-6-74	99.7	14.4	14.3	22	10	____	17	1600
21	3-13-75	99.4	14.4	14.3	22	47	610	3.5	300

*$T_{c,max}$ = Maximum temperature reached inside yarn

**d_e = distance travelled by smoldering wave before extinguishment, in yarn diameters

fT_e = time to extinguishment measured from interruption of external heating to extinguishment.

2.3 QUALITATIVE DESCRIPTION OF SMOLDERING

Smoldering can be defined as a flameless combustion process usually accompanied by the evolution of heat, smoke and light (the latter is referred to as glow).

The main features of steady smoldering are illustrated in Fig. 2.3.1 for the case of a cellulosic yarn (8.6 mm diameter) placed in a horizontal plane in an infinite natural-convective field with minimum interactions with the surroundings. Note the existence of four regions, namely:

1. the virgin material
2. a pyrolysis zone marked by yarn discoloration and outflow of greyish gases (smoke) forming a laminar plumethat eventually* becomes turbulent and disperses in the surroundings
3. a char-oxidation zone emitting visible glow (with cyclic variations in the intensity of the emission) and with invisible gaseous reaction products (i.e., the visible smoke comes out from the pyrolysis zone)
4. a zone of highly porous residual char and/or ash. This residue can be forced to react (as noted by glow and mass loss) when additional heat or oxygen or both are provided.

It is of note that when the glow zone† is separated (using a blade) from the pyrolysis zone, it continues to glow till burn-out, while

* The height of the plume at the point of transition to turbulence changes with the environmental mixture pressure, as expected.

† i.e., the zone emitting glow

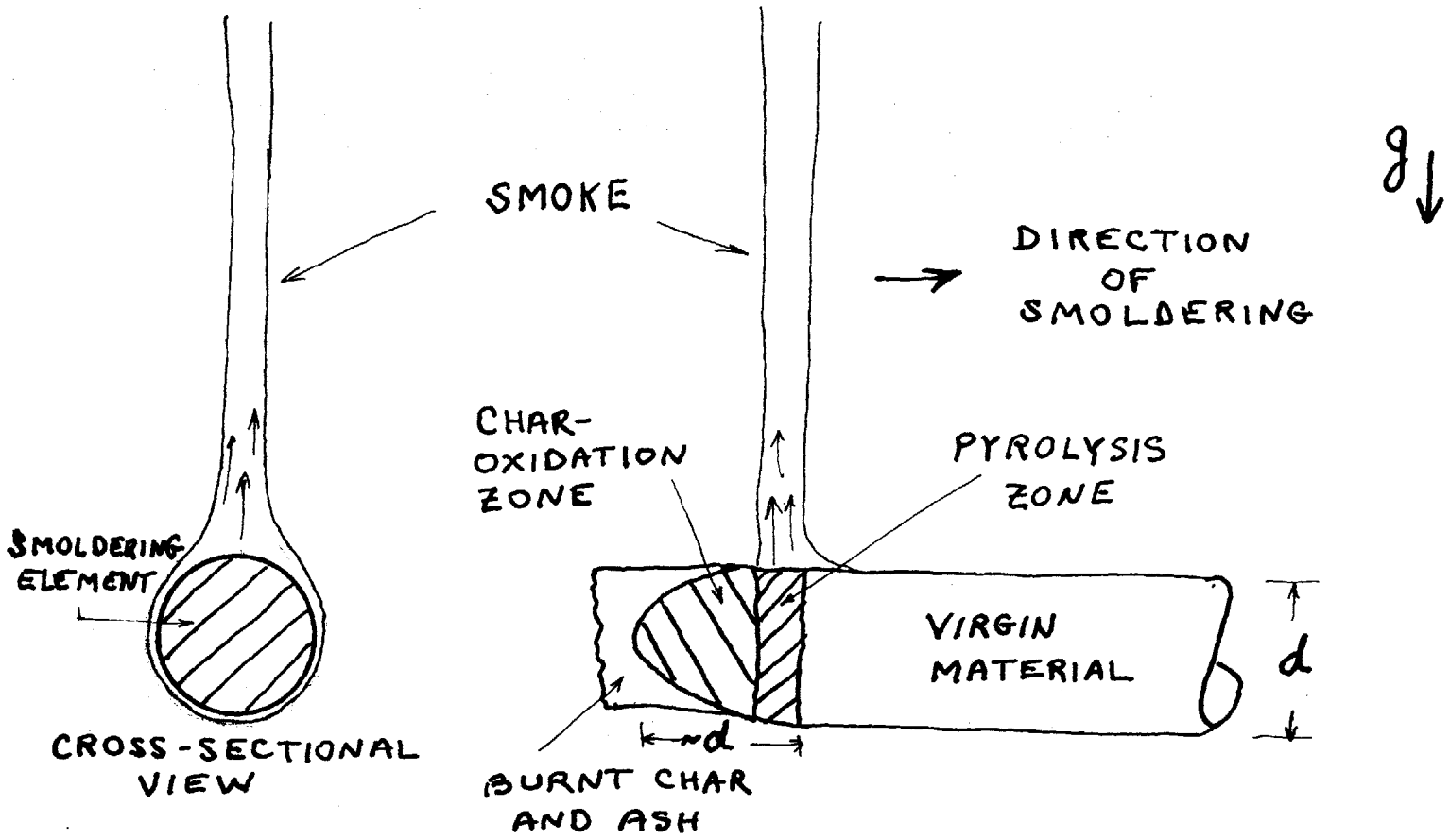


FIG. 2.3.1 DESCRIPTION OF STEADY SMOLDERING IN CYLINDRICAL CELLULOSIC MATERIALS

pyrolysis stops immediately (i.e., no outflow of greyish gases). This experiment suggests that the glow zone is needed to provide the heat necessary for pyrolysis. This fact has been incorporated in the theory as described in chapter III.

A typical temperature-time profile for this sample is illustrated in Fig. 2.3.2 with visual correlations of the different zones with temperature. The temperature at the surface of the yarn is lower than that at the center (possibly because of heat losses). Thus, the spreading is not strictly unidimensional even for such a sample with simple geometry and small thickness.

As the geometry becomes complicated and the thickness increases (to a few centimeters such as for piles of single samples or for cotton waddings), additional processes are observed such as erratic glow, expansion of the fuel bed and curling of the char. However, for a variety of cylindrical materials (listed in section 2.5), the main observed smoldering features are the same as those for the yarn described in this section.

2.4 EFFECTS OF ENVIRONMENTAL PARAMETERS

Smoldering tests are conducted in quiescent environments of varying compositions and pressures to determine the effects of the environment on critical, steady-state smoldering parameters such as speed, reaction temperature and reaction zone length and on the occurence of transitions to flaming or extinguishment. The rationale behind these experiments will become evident in the theoretical discussion of section 3.2

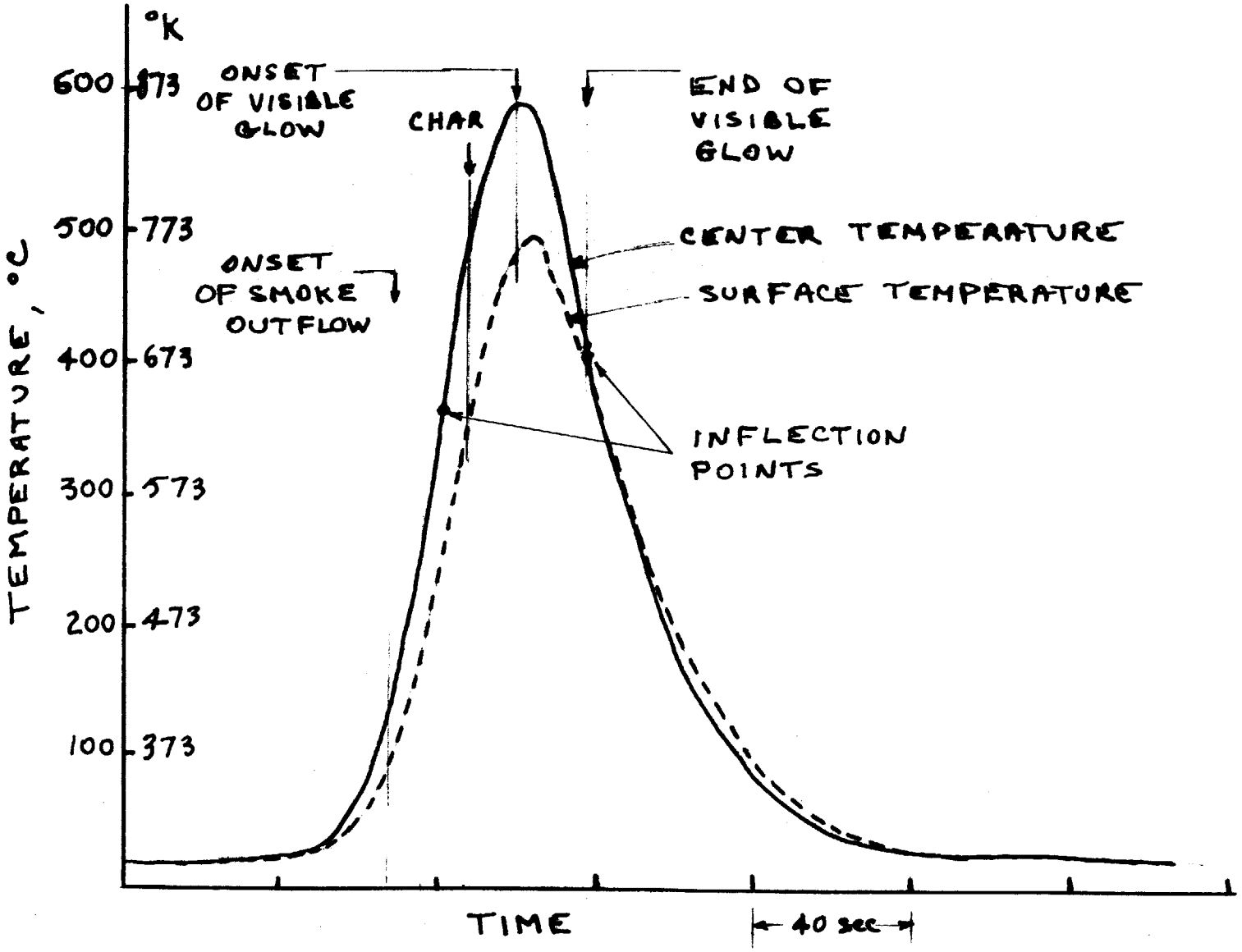


Figure 2.3.2 Correlations of Visual Observations with Temperature Measurements at Center and at Surface of a Cotton Yarn, Smoldering in Standard Atmospheric Condtions

The fuel element used was a commercial cylindrical (four ply) cotton yarn with the following description: a violet color, a diameter = 8.6 mm and a density = 0.06 g/cm^3. It was obtained by the J. O. Hammett Company, Lynchburg, Virginia. (Material Code No. = 71936, Code Name = Cotton Roving). The main qualitative features of the smoldering of this yarn are similar to those of other cylindrical cellulosic elements and were presented in the preceding section. A comparison of the smoldering speed of this yarn with the other elements is given in section 2.5.

The tests were conducted in the pressure vessel described in section 2.1. The yarn was supported in a horizontal plane by a wire frame that caused negligible quenching*. For these conditions, the pressure vessel could be considered as an infinite enclosure, and the accompanying flow field was dominated by the smoldering fire.

The composition of the ambient "air" was changed by replacing specified amounts of air with nitrogen or oxygen. The range of environmental parameters investigated was limited by the occurrence of leaks into or from the pressure vessel and by the capacity of the vacuum pump. The ambient relative humidity and temperature were not controlled and their effects were discussed in section 2.2. A heater coil providing about 1 cal/cm^2-sec was used to initiate the smoldering and was turned off as soon as the smoldering zone "appeared" to be spreading.

---

* The effects of sample orientation in the gravity field are discussed in section 2.5

Temperature measurements were made by the use of chromel-alumel thermo-couples (wire diameter = 0.002" or 0.05 mm and bead diameter = 0.004" to 0.006" or 0.1 to 0.15 mm). For measuring surface temperatures, the thermocouple was wound once around the roving to insure a good thermal contact and to reduce conductive heat losses through the leads.

The smoldering was considered self-sustaining if the entire material was consumed, i.e., if spreading occurs over a length of at least 60 diameters. Such a long sample is needed to ensure that no transition to flaming or to extinguishment will occur. Such spontaneous transitions have been observed long after the initiation of smoldering as discussed in the following section.

The results presented in this section are discussed and compared with theory in chapter 3. The theory has indicated the importance of the oxygen mole fraction and partial pressure depending on the rate-limiting regime of char-oxidation(section 3.2.2). Thus, these two parameters were used in correlating the results in the following sections. Furthermore, a comprehensive listing of the data is given in Appendix 2.2

2.4.1 Transitions to Extinguishment or Flaming

Three qualitatively different results were observed after the initiation of a smoldering wave as described in the previous section:

1. steady-smoldering.
2. transient smoldering followed by flaming
3. transient smoldering followed by extinguishment

These results occurred in three separate regions determined by the environmental parameters, as illustrated in Fig. 2.4.1. Note the existence of an extinguishment limit (the dashed line) at critical combinations of oxygen partial pressures and mole fractions. Below this limit, extinguishment occurs. Above this limit, there exists a region of steady smoldering bounded (apparently) by a second limit (the dashed-dotted line), above which spontaneous transitions to flaming occur*. The solid lines indicate the theoretical predictions of the extinguishment limit and will be discussed in section 3.2.4.

Note that for each transition, an induction time can be defined as the time from onset of smoldering to the appearance of a flame or to extinguishment. Such induction times are illustrated in Tables 2.4.1 and 2.4.2. The large variations observed in these times are expected depending on how close the environmental conditions are from those of the flaming or extinguishment limits. One expects longer induction times as these limits are approached. The study of such transient behavior was not the purpose of this thesis, however, and is recommended for future work.

---

* The flaming limit was not studied extensively in this thesis because the occurrence of a flame ignited the instrumentation employed in the vessel (due to high oxygen concentrations) and caused considerable damage. The flame was yellow-orange and flashed with a speed about three orders of magnitude higher than that of smoldering.

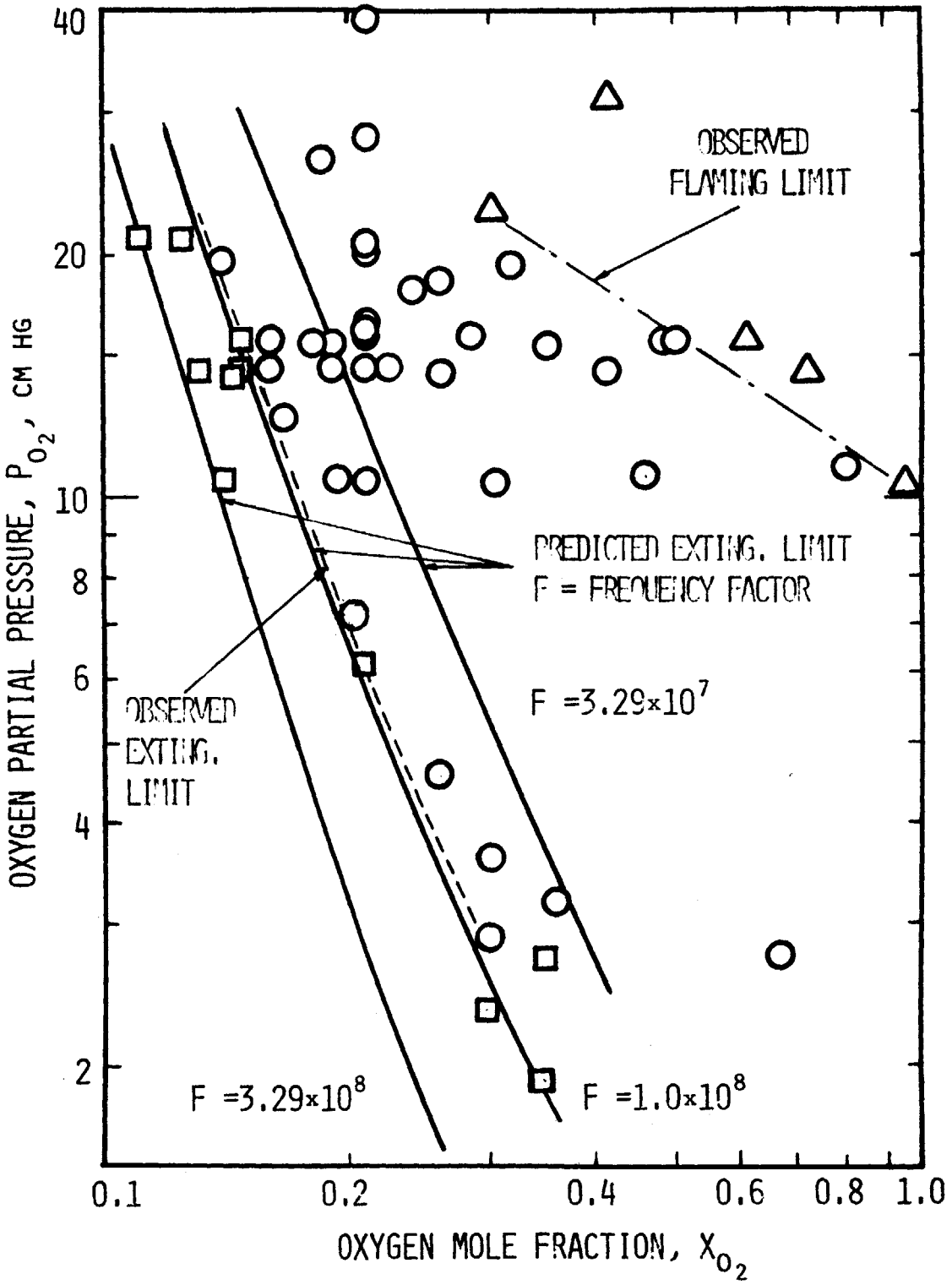


Figure 2.4.1 Occurrence of Steady (○) or Transient Smoldering Followed by Flaming (△) or Extinguishment (□) as functions of Ambient Oxygen Mole Fractions and Partial Pressures, Cellulosic Samples Mounted Horizontally

Table 2.4.1

Induction Times Between the Onset of Smoldering and the Transition to Flaming

Run #	P	X_{O_2}	P_{O_2}	Time
	cm Hg	%	cm Hg	sec
2	75.7	30.	23.	~ 1
9	76.0	42.	32.	< 1
25	26.	60.	15.7	850
26	11.0	95.	10.5	110
42	20.	72.	14.4	~ 1

Table 2.4.2

Induction Times Between the Onset of Smoldering and the Transition to Extinguishment

Run #	P	X_{O_2}	P_{O_2}	Time
	cm Hg	%	cm Hg	sec
T2	76.	14.1	10.7	230
11	99.7	14.4	14.3	1600
20	106.6	14.8	15.8	140
21	99.4	14.4	14.3	300
27	190.	11.1	21.	100
37	170.	12.4	21.	~ 60
45	10.9	21.	2.3	100
48	30.	21.	6.2	1200
65	7.9	30.	2.3	420

2.4.2 Steady-Smoldering Results

This section presents the effects of environmental parameters on the steady-smoldering characteristics, under the testing conditions described in section 2.4. Interpretations of these results are given in section 3.3 , after the theory has been introduced.

The steady-smoldering characteristics considered are the speed, the maximum reaction temperature and the reaction zone length. The environmental parameters considered are the oxygen partial pressure (P_{o_2}) and mole fraction (X_{o_2}) and the mixture pressure (P)*. The results are reported below:

Smoldering Speed

In the region of steady smoldering investigated in this study, Fis. 3.4.2 through 3.4.5. illustrate that the speed increases:

1. with increase in oxygen mole fraction at any constant oxygen partial pressure
2. with increase in oxygen partial pressure at any constant mixture pressure
3. with decrease in mixture pressure at any constant oxygen partial pressure
4. with increase in oxygen partial pressure when the oxygen mole fraction is held constant

Note that only two of the environmental parameters are independent and are thus sufficient to describe the environment. The results

---

* Note that only two of these parameters are independent

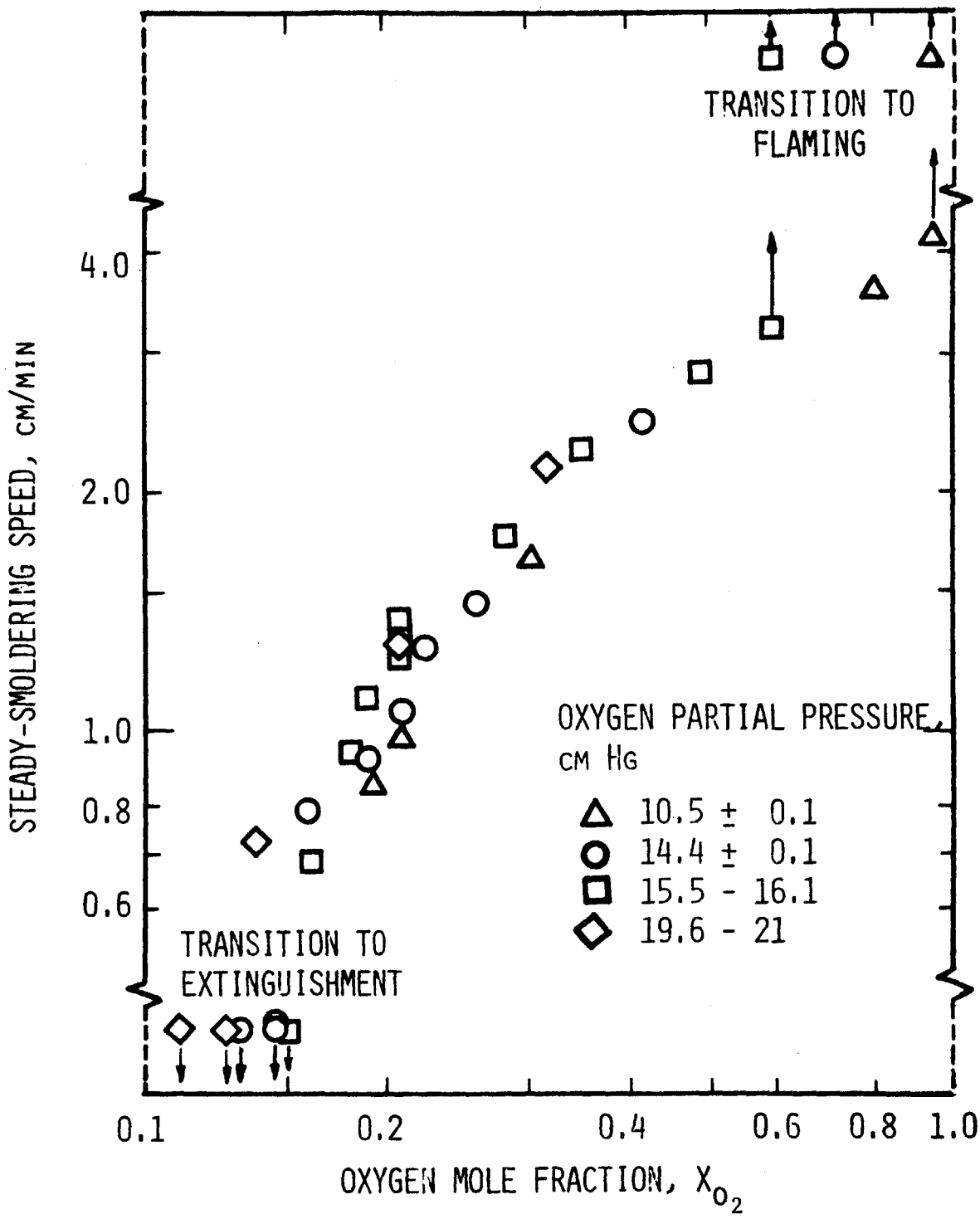


FIGURE 2.4.2 Steady Smoldering Speed versus Ambient Oxygen Mole Fraction as a Function of O_2 Partial Pressures (Cellulosic Samples Mounted Horizontally)

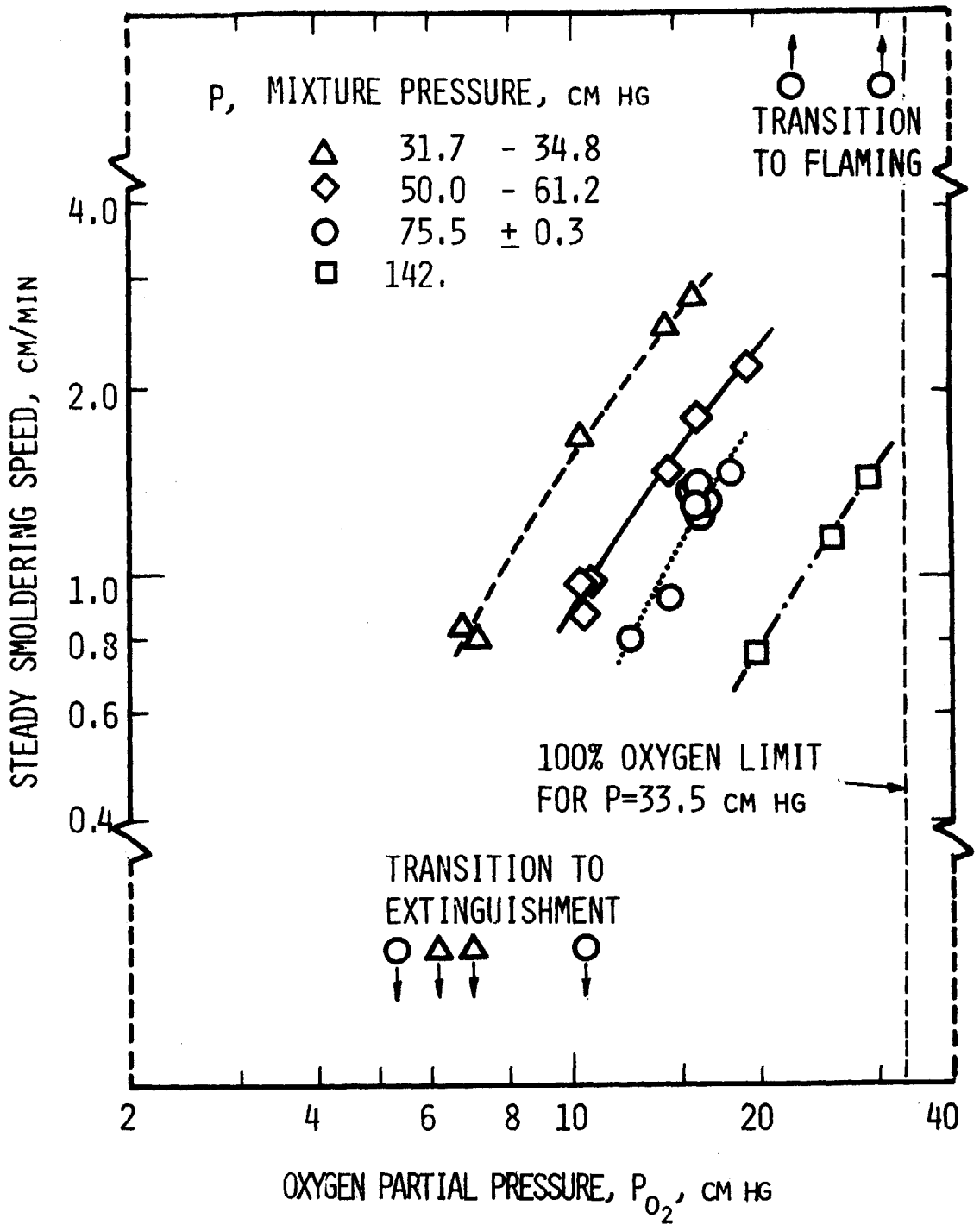


FIGURE 2.4.3 Steady Smoldering Speed versus Ambient Oxygen Partial Pressures as a Function of Mixture Pressures (Cellulosic Samples Mounted Horizontally)

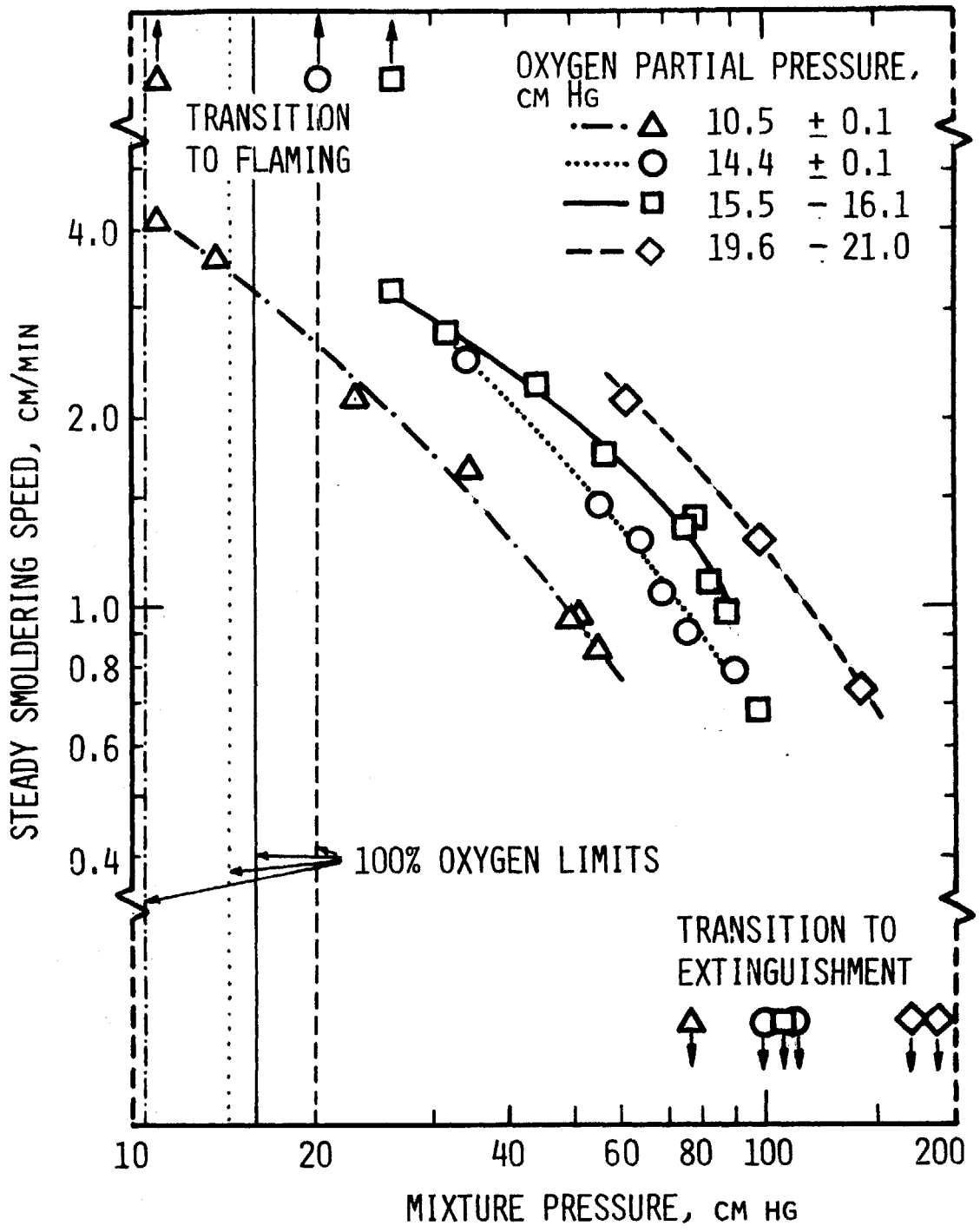


FIGURE 2.4.4 Steady Smoldering Speed versus Mixture Pressure as a Function of Ambient Oxygen Partial Pressure, Cellulosic Samples Mounted Horizontally

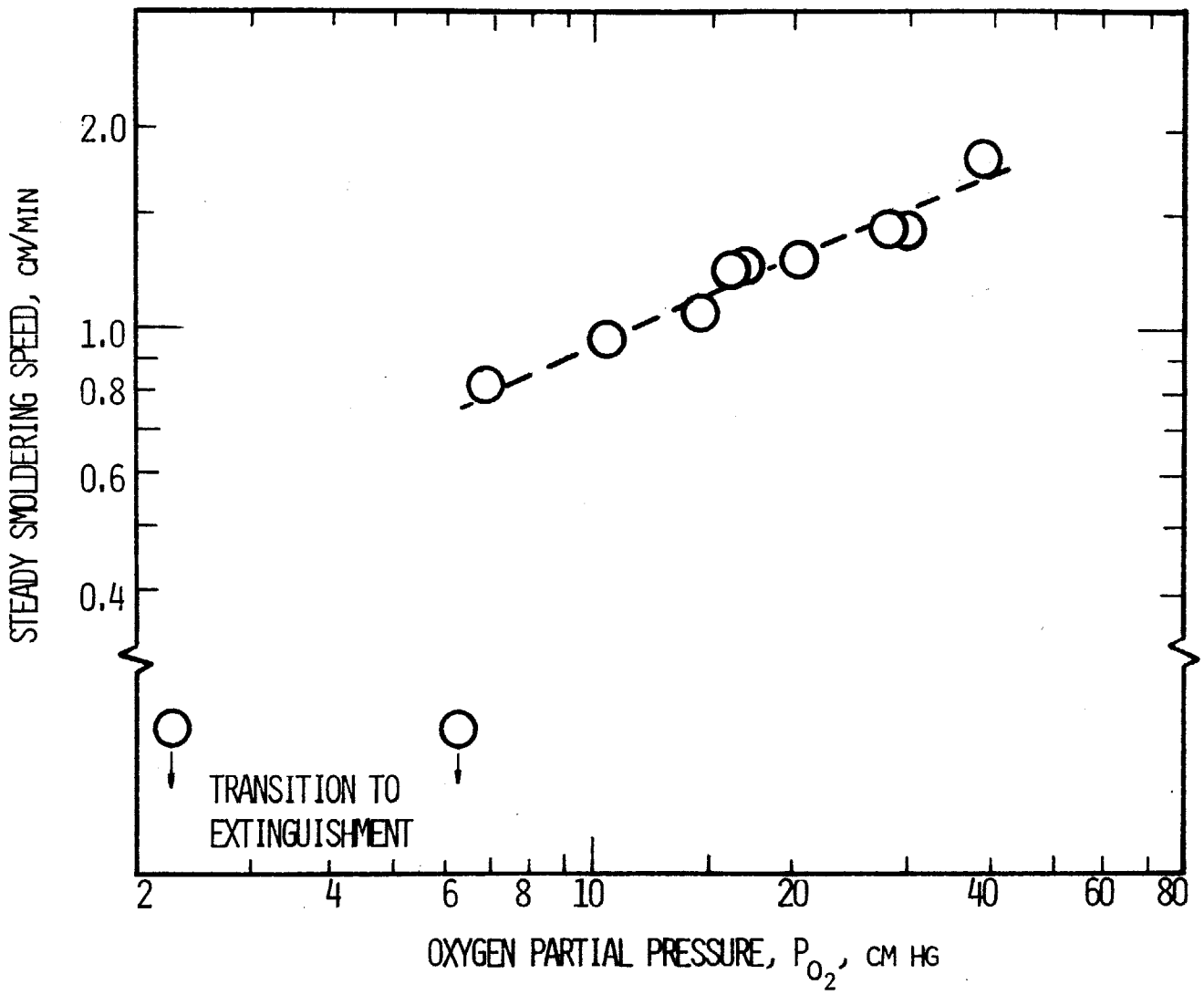


FIGURE 2.4.5 Steady Smoldering Speed versus Ambient Oxygen Partial Pressure at 21 percent Oxygen Mole Fraction, Cellulosic Samples Mounted Horizontally

are shown for three parameters, however, to compare the importance of the speed dependency on each parameter. Clearly, one can conclude that the speed is a strong function of the oxygen mole fraction when any of the other two parameters is held constant; and, the speed is a weak function of the oxygen partial pressure (or the mixture pressure) when the oxygen mole fraction is held constant. These features can be interpreted by the mechanism proposed in this thesis as presented in section 3.3.

In Figs. 3.4.2 - 3.4.5, it should be also noted that:

(1) the smoldering temperature, reaction length and % char residue vary for each of these runs, as presented in the following sections.

(2) steady smoldering occurs in a region limited by the occurrence of transitions to flaming or extinguishment at critical combinations of the environmental parameters (as discussed in section 2.4.1).

(3) the 100% oxygen limits are marked where the abscissa permits

Maximum Temperature in the Smoldering Zone

Temperature-time histories were measured with thermocouples placed in the center of the smoldering yarn. The maximum temperature in the smoldering zone is given in Fig. 2.4.6 and 2.4.7 as a function of the oxygen mole fraction while the partial pressure is held constant, and vice versa. These figures show also the transitions to flaming and extinguishment that were discussed in section 2.4.1.

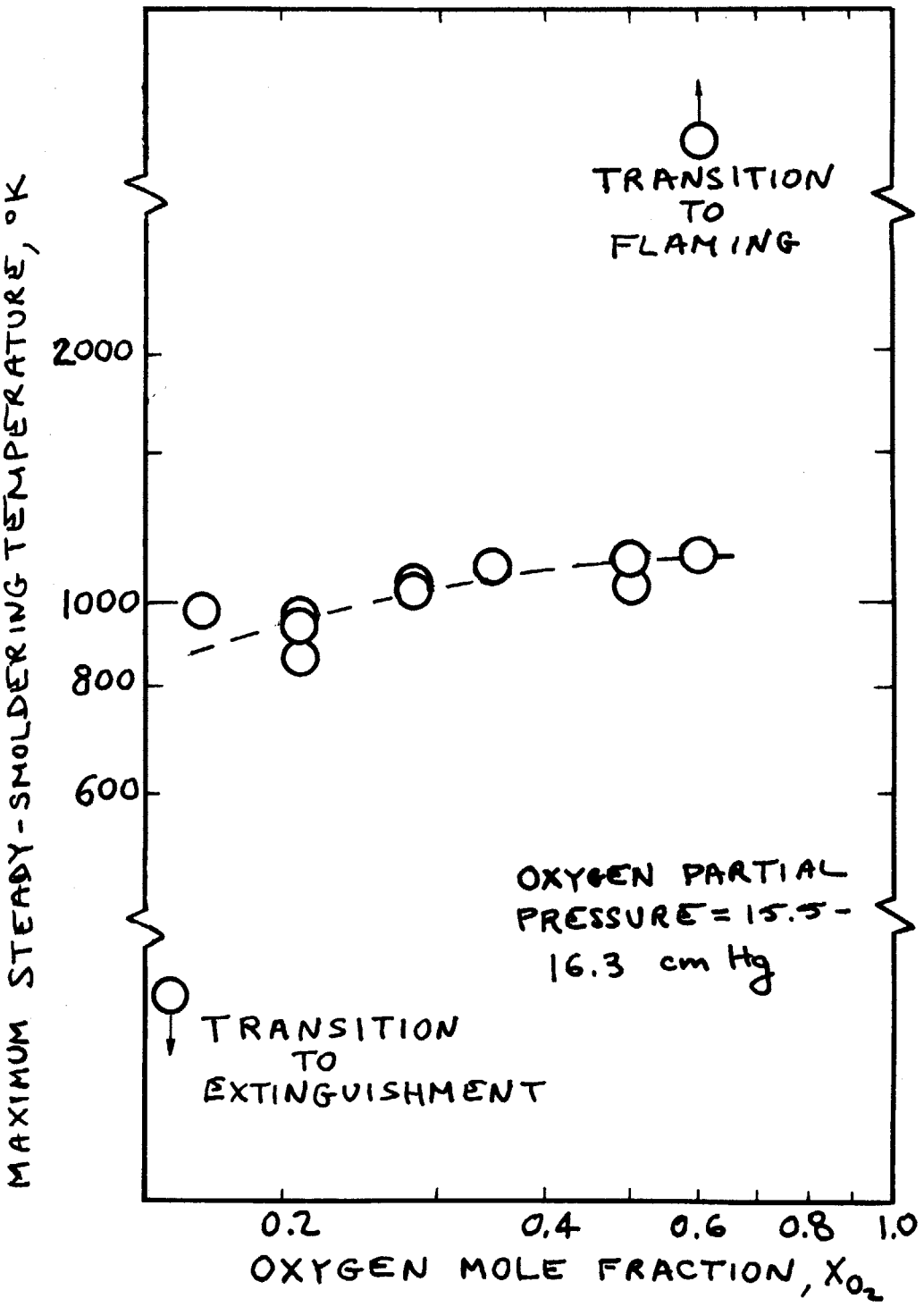


FIGURE 2.4.6 Steady Smoldering Maximum Temperature versus Ambient Oxygen Mole Fraction at a Constant Oxygen Partial Pressure, Cellulosic Samples Mounted Horizontally

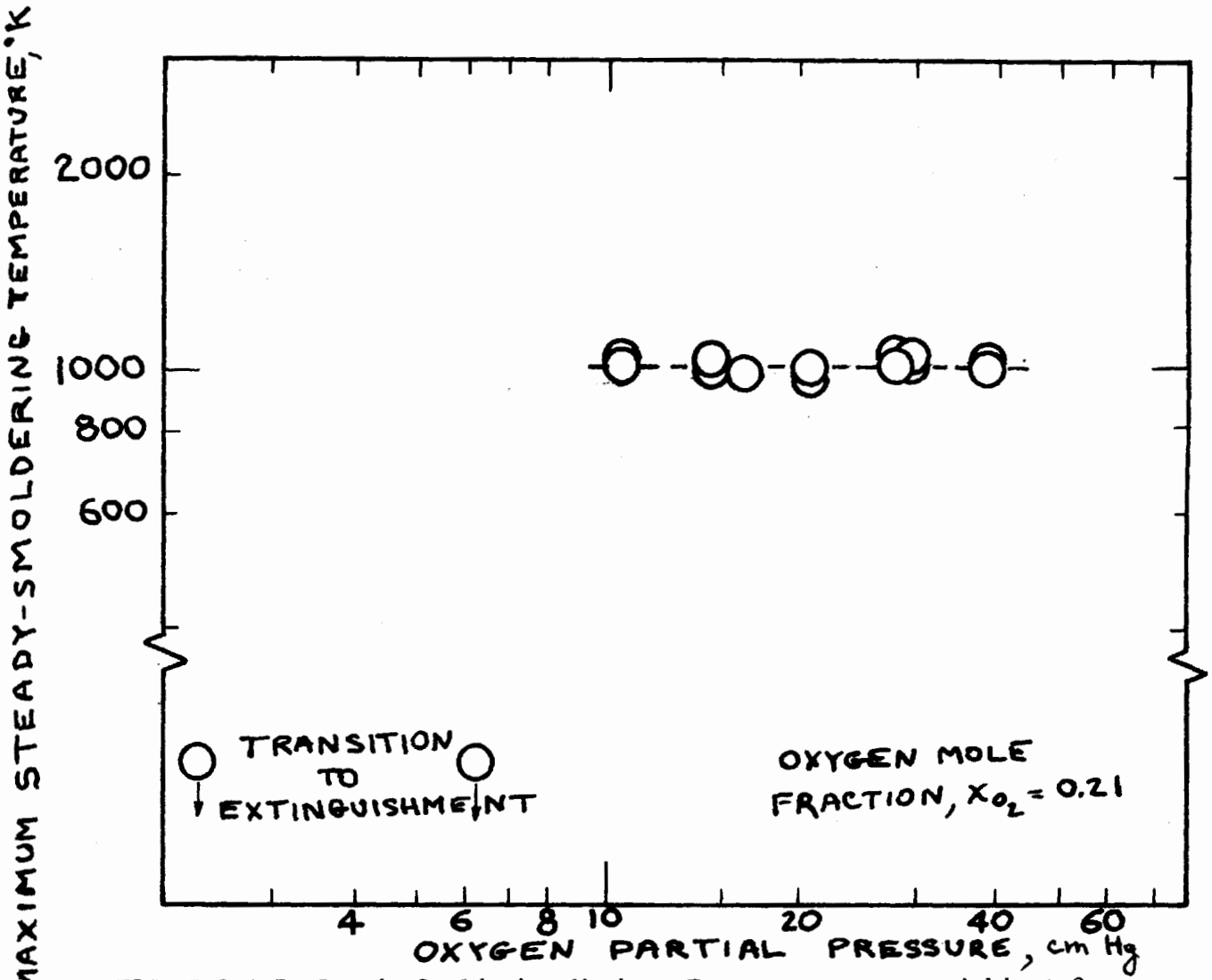


FIGURE 2.4.7 Steady Smoldering Maximum Temperature versus Ambient Oxygen Partial Pressure at a Constant Oxygen Mole Fraction, (Cellulosic Samples Mounted Horizontally)

Note that the temperature depends weakly on the oxygen mole fraction and negligibly on the oxygen partial pressure. These features can be interpreted by the mechanism proposed in this thesis as presented in section 3.3. (The temperature dependence on the mixture pressure can be deduced easily by inspection of Figs. 2.4.6 and 2.4.7. Thus, it is not given).

The temperature was also measured at the surface of the yarn This temperature was always lower than that at the yarn center (see Appendix 2.2). It is believed that a measurement at the yarn center is a better representation of the reaction temperature than one at the yarn surface due to the following reasons:

1. the heat losses to the surroundings from the thermocouple bead are smaller when it is placed at the yarn center than at its surface.
2. at low oxygen mole fraction ($\sim$ 0.14 see Fig 2.4.6), heat losses cause partial extinguishment at the yarn surface, while its insider continues to react. This is deduced from visual inspection of the sample after smoldering. One notices virgin material at some parts of the yarn surface, while the inside is completely charred.

Reaction Zone Length

In Fig. 2.3.1 a reaction zone was visually identified and was found to correlate roughly with the length between the two inflection points in the temperature profile illustrated in Fig. 2.3.2. Clearly, between these inflection points, the temperature profile differs markedly from that of the heating (or cooling) of an inert slab,

indicating significant heat generation in this zone.

The reaction zone lengths, between the two inflection points, were measured from temperature-time profiles for various environmental conditions, as illustrated in Fig . 2.4.8 . Large uncertainties in these measurements are expected because the small curvature in the profiles make the inflection points difficult to determine. Because of these uncertainties, no trend is apparent for the dependence of the reaction zone length. However one can conclude that this length is of the size of the yarn diameter,* regardless of the environmental conditions. This finding is used in the theoretical development in section 3.2.3.

2.5 EFFECTS OF FUEL PARAMETERS

The purpose of this section is to measure the effects of fuel parameters such as diameter and density on the smoldering speed and the maximum temperature in the smoldering zone. Such results can be compared at least qualitatively with the theory presented in chapter III. The effects of sample orientation in the gravity field is also investigated in this section.

In addition to these parameters, other fuel characteristics may influence the smoldering process, such as, the air permeability, the thermophysical properties and the surface conditions. These parameters have not been investigated in this study, however.

A number of cylindrical cellulosic fuels of varying density and diameters were tested. These fuels included commercial materials such as threads, yarns and strings, and cylinders made by compaction of "pure" α-cellulose fibers and powders. Two α-cellulose were used:

---

* The yarn diameter is specified by the dashed line in Figs. 2.4.8

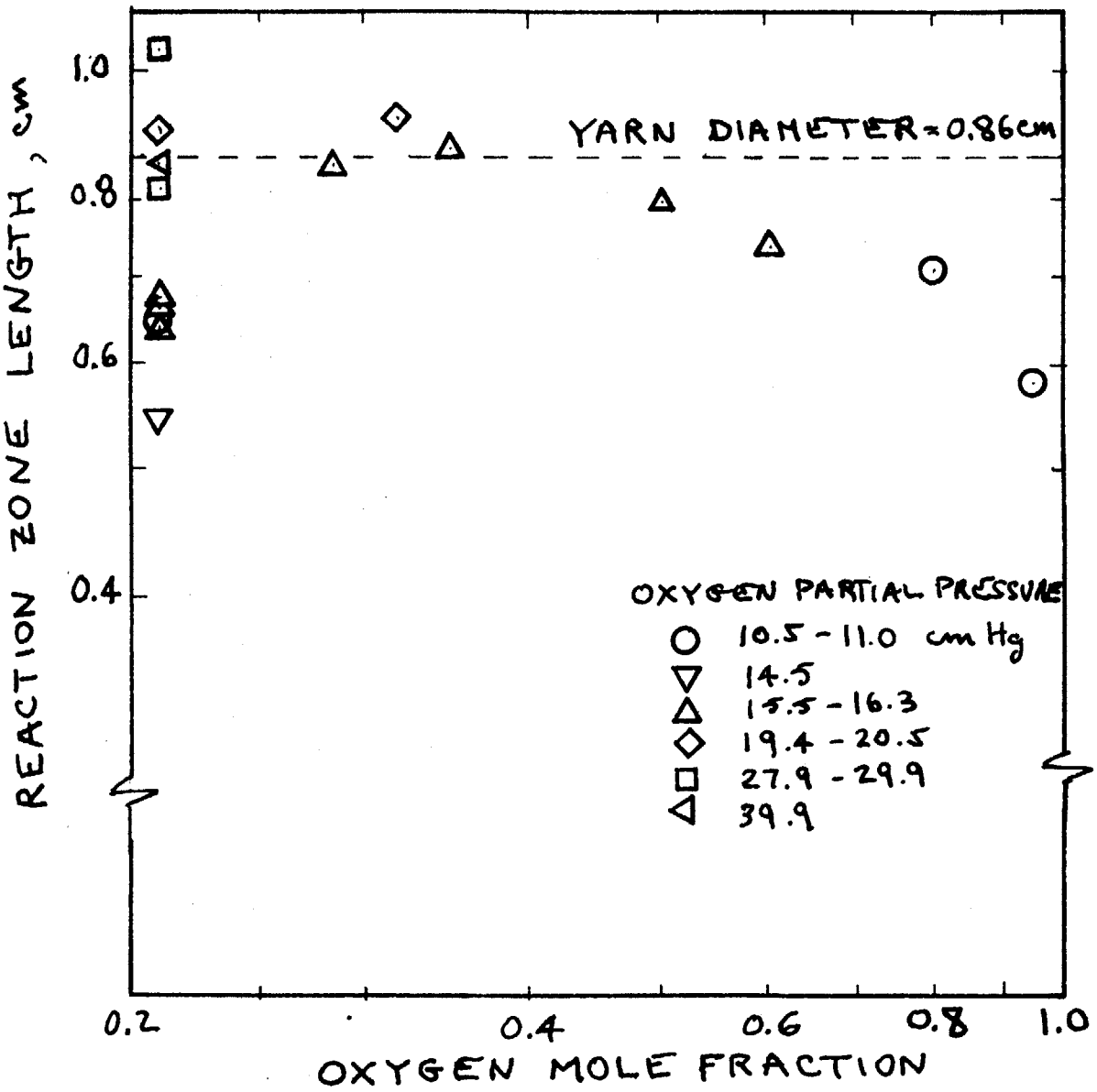


FIGURE 2.4.8 Reaction Zone Length versus Ambient Oxygen Mole Fraction at Constant Oxygen Partial Pressures, Cellulosic Sample Mounted Horizontally

- Sulfa Flox^{R} fibers, a highly purified wood cellulose, obtained from thd Brown Co., Berlin, N. H. The fibers were wetted before compaction to facilitate their adhesion.
- Avicel^{R} ph 101, a microcrystalline cellulose powder yielding less than 250 ppm "Residue on Ignition", obtained from FMC Corp., Marcus Hook, Penn. This powder was compacted without wetting. (This material did not self-sustain smoldering, however).

The tests were conducted in standard atmospheric conditions with the samples placed in a horizontal plane with minimum interactions with the surroundings. The steady smoldering speed was inversely proportional to the product of density and diameter, as illustrated in Fig. 2.5.1. On the other hand, the steady smoldering maximum temperature increased (though weakly) with this same product. (The variations in densities and diameters for the samples are listed in Table 2.5.1). It is remarkable that the steady smoldering results for these fuels, which vary in air permeability, surface conditions and possibly in chemical compositions*, correlate well on the basis of the product of density and diameter alone. This product can be thought of as the mass per unit surface area of oxygen arrival to the sample. The dependence on this product suggests the importance of oxygen mass transfer in smoldering.

---

* Because some are dyed and some are glossy (indicating the presence of some surface chemical finishes), and one material is 99.5% pure α-cellulose.

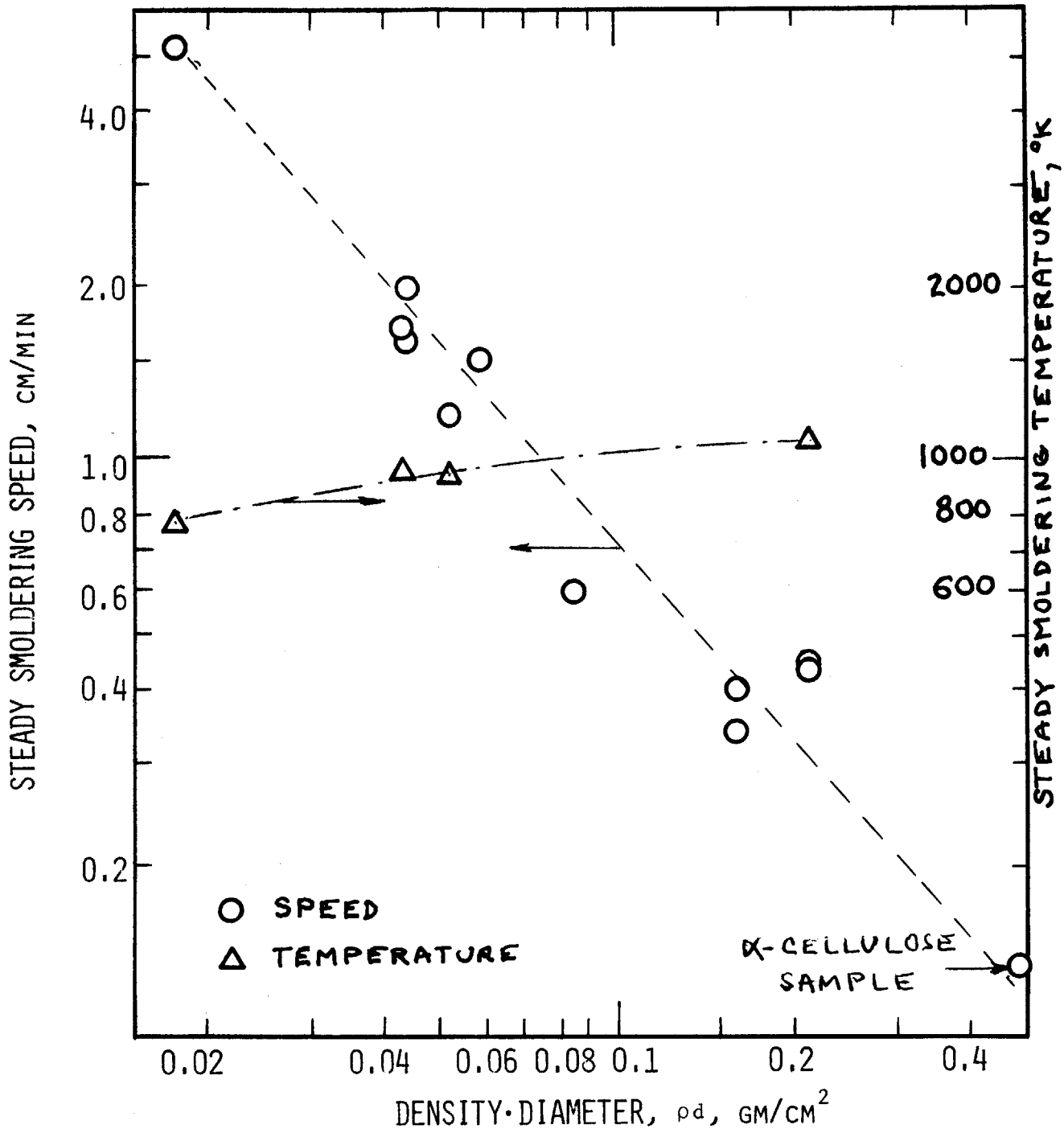


FIGURE 2.5.1 Steady Smoldering Speed and Maximum Temperature versus Density. Diameter for Cellulosic Materials Mounted Horizontally, in Standard Atmospheric Conditions

TABLE 2.5.1

Diameter and Density of

Cylindrical Cellulosic Materials

Used in Fig. 2.5.1

Material Description	Diameter d_f, mm	Density ρ, g/cm^3
Roving	8.6	0.06
α-cellulose cylinder	6.0	0.81
String	3.8	0.35
Twine	2.8	0.57
Twine	2.5	0.34
Twine	2.1	0.78
Yarn	1.7	0.26
Twine	1.5	0.39
Twine	1.3	0.33
Thread	0.4	0.44

To investigate the effects of sample orientation in the gravity field, some of the tests reported above were conducted with samples mounted vertically, and a smoldering wave was initiated at the top or the bottom of the sample. For the cylindrical cellulosic materials tested, the results were not qualitatively different from the case of horizontal smoldering*. Upward smoldering propagated with a steady speed and was not accelerating as for the case of flaming combustion [2.2 and 2.4]. Furthermore, the change in speed and in the pyrolysis and char-oxidation lengths were not substantial (when compared to the case of flaming). This is illustrated in Table 2.5.2 for a cotton yarn and an α-cellulose cylinder. The length of the two zones were determined visually and not from the temperature profile as done in section 2.4.2. The region of partially discolored virgin material is taken as the pyrolysis zone and the region exhibiting char and/or glow is taken as the char-oxidation zone. The speed for vertically upward smoldering is only up to 50% higher than that of vertically downward; the corresponding increase for the case of flaming is one order of magnitude [2.2].

The weak dependence on the orientation in the gravity field suggests that the contribution of convection to the heat transfer to the virgin material is small. Accordingly, this mode of heat transfer was not included in the model proposed in chapter III. This result also permitted flexibility in the choice of sample orientation in the experiments conducted in this study.

---

* Similar conclusions were obtained for other materials, see Appendix 2.1

Table 2.5.2

Effects of Sample Orientation in the Gravity Field

Material	dia. cm	dia. x density g/cm^2	Smoldering Vertically up V cm/min	ℓp cm	ℓc cm	Smoldering Horizontally V cm/min	ℓp cm	ℓc cm	Smoldering Vertically down V cm/min	ℓp cm	ℓc cm
α-cellulose (Sulfa Flox®)	0.6	0.485	0.18*	0.7*	0.2*	0.13	0.1	0.4	0.11	0.1	0.4
Cotton Yarn	0.86	0.052	1.4	0.4	0.5	1.2	0.2	0.7	Sample cannot be supported in this orientation.		

V = Smoldering speed
ℓp = Pyrolysis zone length
ℓ = Char-oxidation zone length

* Steady smoldering may not have been reached within the tested length (∿ 4 cm). It was difficult to compact α-cellulose into longer cylinders to verify if steady smoldering was reached.

This study focused mainly on the smoldering of cellulosic materials because of their commercial importance. It is interesting to determine whether other synthetic or natural polymers smolder. Experiments were conducted for this purpose. See Appendix 2.1.

Under otherwise identical conditions, smoldering was observed for char-forming* polymers (such as wool and polyurethane) and was not observed for non-char forming polymers (such as nylon, polyester and polystyrene). This suggests that char formation is a necessary condition prior to smoldering. Accordingly, the formation of char was included in the smoldering mechanism proposed in this thesis.

Apparently, char has the "right" properties to react with oxygen and provide sufficient heat to sustain smoldering. One can speculate that these properties include the large internal surface area (because char is porous) and the high thermal diffusivity of the char. These properties ensure, respectively, oxygen availability and high temperatures within the char. This permits char-oxygen reactions throughout its interior, thus generating large quantities of heat.

A systematic check of the claim that char is necessary for smoldering is difficult, because of lack of knowledge on the pyrolysis and the smoldering behaviors of many polymers. It should be noted however, that to date, a non-flaming self-driven combustion process, without the formation of a char, has not been observed by the author.

---

* Note that the char-forming tendency of any polymer depends on the temperature-time history during its pyrolysis.

Much of the findings obtained in this study on cellulosic materials may be applicable to other polymers, in particular the proposed mechanism of smoldering and the analysis of char-oxygen reactions presented in chapter III. The new features that one may have to consider for non-cellulosic polymers are mainly their pyrolysis behavior. Pyrolysis differ significantly with polymers and can affect the characteristics of the resulting char, and consequently, the smoldering behavior is changed. For example, in the case of polyurethane and wool, the occurrence of melting during pyrolysis might block the pores of the char, thus, preventing the arrival of oxygen to its internal surface. This would reduce the energy generated by char oxygen reactions and might prevent the sustainment of smoldering. Such behavior has been reported by Ohlemiller et al. [23] for the case of smoldering in polyurethane.

2.7 EXPERIMENTAL RESULTS

The experimental phase of this investigation demonstrated the following:

- A region of steady-smoldering, an extinguishment limit and a flaming limit are observed depending on the environment (namely the oxygen partial pressure and mole fraction).
- In the region of steady-smoldering it is found that:
  1 - the speed increases strongly with oxygen mole fraction and weakly with its partial pressure.
  2 - the maximum temperature in the smoldering zone increases weakly with oxygen mole fraction and negligibly with its partial pressure.
  3 - for a specified fuel, one temperature-speed relationship is obtained for any environment.
  4 - the reaction zone length for various environmental parameters was of the size of the fuel element diameter ($\pm$ 30%).
  5 - the amount of char residue, left after the smoldering wave has spread over an element, varied significantly with environmental parameters.
  6 - the speed is inversely related to the product of density x diameter.
  7 - the temperature increase (though weakly) with the product of density x diameters.
  8 - the effects of sample orientation in the gravity field on the speed is small (when compared to its effects in the case of flaming).

- If the region exhibiting glow is separated from the region exhibiting thermal decomposition, glowing continues to burn-out while pyrolysis stops.

- The induction times, from the initiation of smoldering to a transition to flaming or to extinguishment, varied significantly for different environmental parameters.

- Smoldering was observed for char-forming polymers (such as cellulose, wool and polyurethane) and not for non-char forming polymers (such as nylon and polyester).

Chapter III

THEORETICAL ANALYSES AND COMPARISONS WITH EXPERIMENTS

The purpose of this chapter is two-fold: firstly, to develop a theoretical model of smoldering combustion, and secondly, to verify its validity by comparing its predictions with experimental results.

Intuitively, one expects smoldering to occur as follows. Upon heating, cellulose decomposes by various concurrent and sequential reactions yielding a multitude of gaseous, liquid and solid products. Some of these products may react with oxygen or with themselves thus liberating light (a glow, not a flame) and heat. The heat feeds back into the virgin material to sustain pyrolysis*. Clearly, accounting for all these reactions is a formidable task.

In this study, it is proposed to test whether a simplified model can interpret the main features of the experimental results, presented in the previous chapter. This model postulates an overall pyrolysis mechanism leading to the formation of char and volatiles**, and the subsequent char-oxidation yielding the energy needed to sustain smoldering.

To predict the smoldering behavior, the analysis treats pyrolysis and char-oxidation in two zones separated by an interface*** with suitable

---

* Should the energy feedback be insufficient to sustain the process, extinguishment occurs. Should the composition and the temperature of the mixture in the vicinity of the smoldering material become favorable, a transition to flaming occurs.

** Clearly, liquid tars may also be formed, but here they are lumped with volatiles.

*** As reported in Chapter II, experimental observations suggest the existence of a pyrolysis zone and a char-oxidation zone that are more or less separable.

matching requirements as described below:

(1) The temperature and speed of a steadily propagating pyrolysis zone were determined as functions of the heat flux specified at the interface, taking into account solid-phase conductive heat transfer and a reasonable, overall, scheme of cellulose degradation.

(2) The heat flux generated by char-oxidation was determined as a function of environmental parameters (namely, oxygen partial pressures and mole fractions), taking into account oxygen diffusion through a free-convective boundary layer around the char zone, and a reasonable, overall, surface reaction.

(3) The steady smoldering speed and temperature, and the transition to extinguishment were determined as functions of the environmental parameters by matching at the interface the heat flux required for pyrolysis (from (1)) with that generated by char-oxidation (from (2)), allowing for reasonable heat losses.

To verify the predicted smoldering behavior, one must know the kinetic parameters of cellulose pyrolysis and char-oxidation appropriate for this study. These kinetic parameters were determined by critical matching of theoretical and experimental results as described below:

(a) the pyrolysis study predicted a unique relationship between the temperature and the speed at any heat flux specified at the interface and for specific kinetic parameters. This was verified by measurements at various environmental parameters (i.e., at various heat fluxes as can be deduced from (2) and (3)). The pyrolysis kinetics appropriate for this study were

determined by matching the measured temperature-speed relationship with that predicted on the basis of specific kinetic parameters.

(b) An extinguishment limit was predicted and observed for critical combinations of environmental parameters. The char-oxidation kinetics appropriate for this study were determined by matching the observed extinguishment limit with that predicted on the basis of specific kinetic parameters, combined with the pyrolysis kinetics determined in (a).

Using the kinetics determined in (a) and (b), a set of dependencies is predicted and is found to agree with experimental results not used in the matching. These are the dependencies of the steady smoldering speed and temperature on the environmental parameters.

The validity of the proposed mechanism of smoldering is supported by agreement with experiments in three ways:

(1) The qualitative agreement on a temperature-speed relationship that is independent of the environmental parameters.

(2) The qualitative agreement on the existence of an extinguishment limit at well defined combinations of the environmental parameters.

(3) The agreement on the effects of the environmental parameters on the steady smoldering speed and temperature.

This chapter consists of three sections: firstly, the pyrolysis study, secondly, the char-oxidation study and thirdly, the predicted smoldering behavior. Comparisons with experiments are given in each section where found appropriate.

3.1 PYROLYSIS STUDY

The purpose of this pyrolysis study is to determine the characteristics of a steadily propagating pyrolysis zone under the influence of an imposed external heat flux. By matching theoretical predictions with experimental results, one can determine the pyrolysis kinetic parameters appropriate for this study. The results from this pyrolysis study can then be coupled with the char-oxidation study to determine the smoldering behavior.

This section presents, firstly, the rationale behind the choice of the overall mechanism of cellulose pyrolysis used in this study; secondly, a mathematical model of a semi-infinite slab pyrolysing according to the mechanism chosen above; thirdly, an approximate closed-form solution of this model; and fourthly, a comparison of theory and experiment to verify the model and to predict the kinetic parameters appropriate for this study.

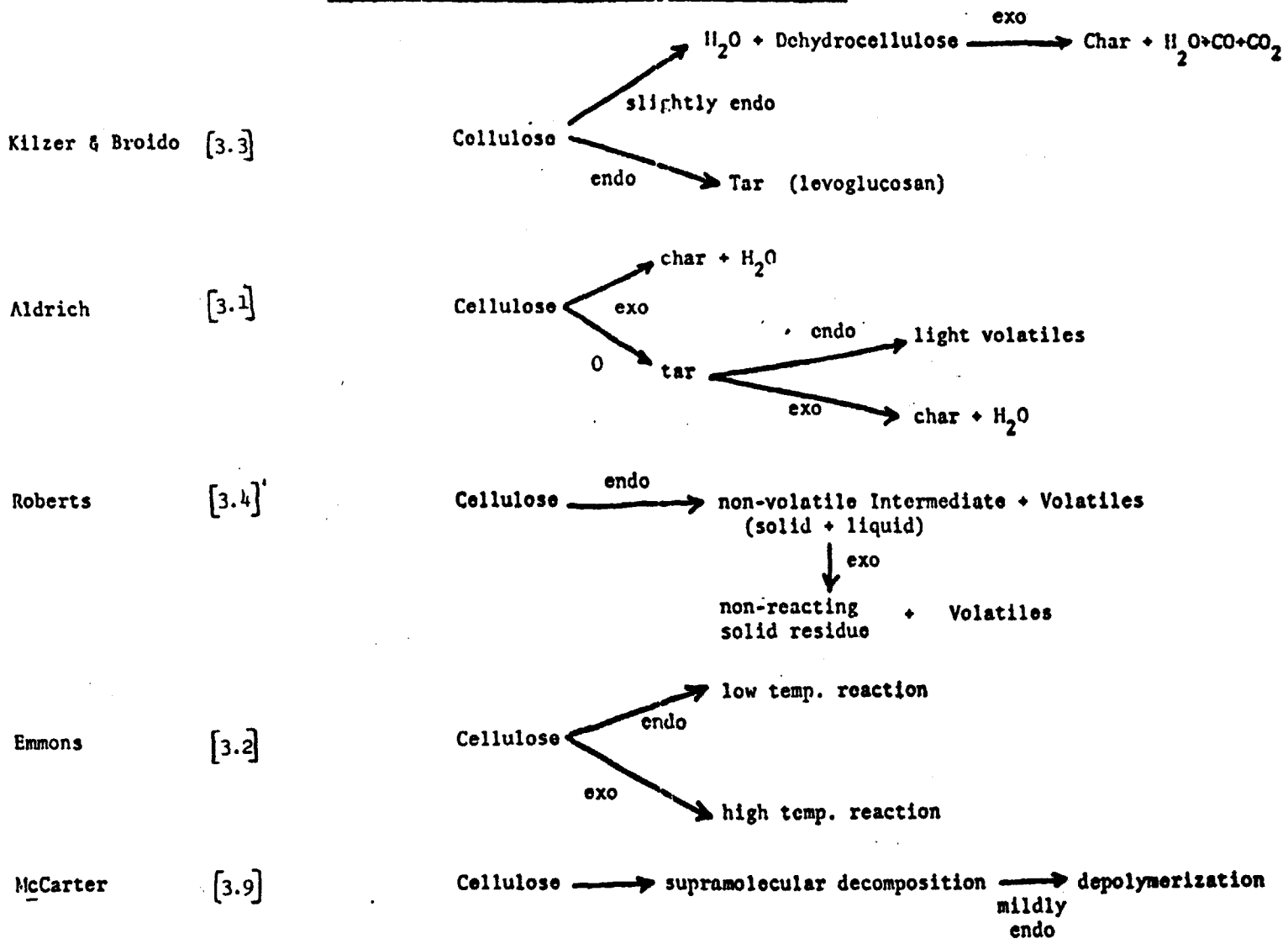
3.1.1 Overall Mechanism of Cellulose Pyrolysis

A review of the literature of cellulose pyrolysis [3.1 - 3.10] identified many postulated mechanisms of concurrent and consecutive reactions, as illustrated in Fig. 3.1.1 While there is considerable disagreement on the detailed reactions in each proposed scheme, two overall features of cellulose pyrolysis are well agreed upon. Firstly, the pyrolysis products include char and volatiles*. And secondly, char and volatile formation are favored (proportionately) at low and high heating rates, respectively.

---

* Clearly, liquid tars may also be found, but here they are lumped with volatiles.

FIG. 3.1.1 POSTULATED MECHANISMS OF CELLULOSE PYROLYSIS



Aldrich [3.1] and Emmons [3.2] showed that their pyrolysis data can be described quite well by an overall model incorporating only the two aforementioned features. This model postulates two concurrent reactions, a low activation energy one and a high activation energy one. Aldrich specified that the former reaction is char-forming, while the latter is volatile-forming. Emmons did not speculate on the composition of the products of pyrolysis, being only interested in the rate of virgin cellulose degradation.

It seemed reasonable to adopt such an overall (two reactions) model to study the characteristics of a pyrolysis zone under smoldering conditions. The choice of any more elaborate pyrolysis model offers no advantages for the purpose of this study and its validity might be more subject to criticism* than that of the simplest overall model.

By adopting this model, it is assumed in this study that oxygen does not affect pyrolysis**. It is later (in section 3.2) assumed that oxygen plays a role in the char-oxidation zone. The validity of such assumptions will be discussed further in section 3.1.4.

Despite the simplicity of the two-reaction model, the kinetic parameters reported by Aldrich and Emmons differ significantly as illustrated in Table 3.1.1. The overall specific reaction rate, calculated using these kinetic parameters in the range investigated, is on the average one order of magnitude higher for Emmons' than for Aldrich's as illustrated in Fig. 3.1.2. Clearly, these two pyrolysis studies

* By the cellulose chemists.

** Broido [3.6] reported that such an assumption is good at high heating rate, but become erroneous at low heating rate . He speculated that at the high heating rate , the larger mass of volatiles flowing out of the material might prevent oxygen from reaching the surface. Alternative explanations will be explored in section 3.1.4.

TABLE 3.1.1

Comparison of the Kinetic Parameters

Reported for the Two-Reaction Pyrolysis Model

SOURCE	Aldrich [3.1]	Emmons [3.2]
ACTIVATION ENERGY, K cal/mole		
Step 1	26.5	26
Step 2	31	54
FREQUENCY FACTOR, sec^{-1}		
Step 1	$1x10^6$	$5.9x10^6$
Step 2	$5x10^7$	$1.9x10^{16}$
HEAT OF PYROLYSIS, cal/g		
Step 1	994 exo	88 endo
Step 2	0	440 exo
REACTION ORDER		
Step 1	1	1
Step 2	1	1
TRANSITION TEMPERATURE*, °K	580	646

* Temperature at which the two reaction rates are equal.

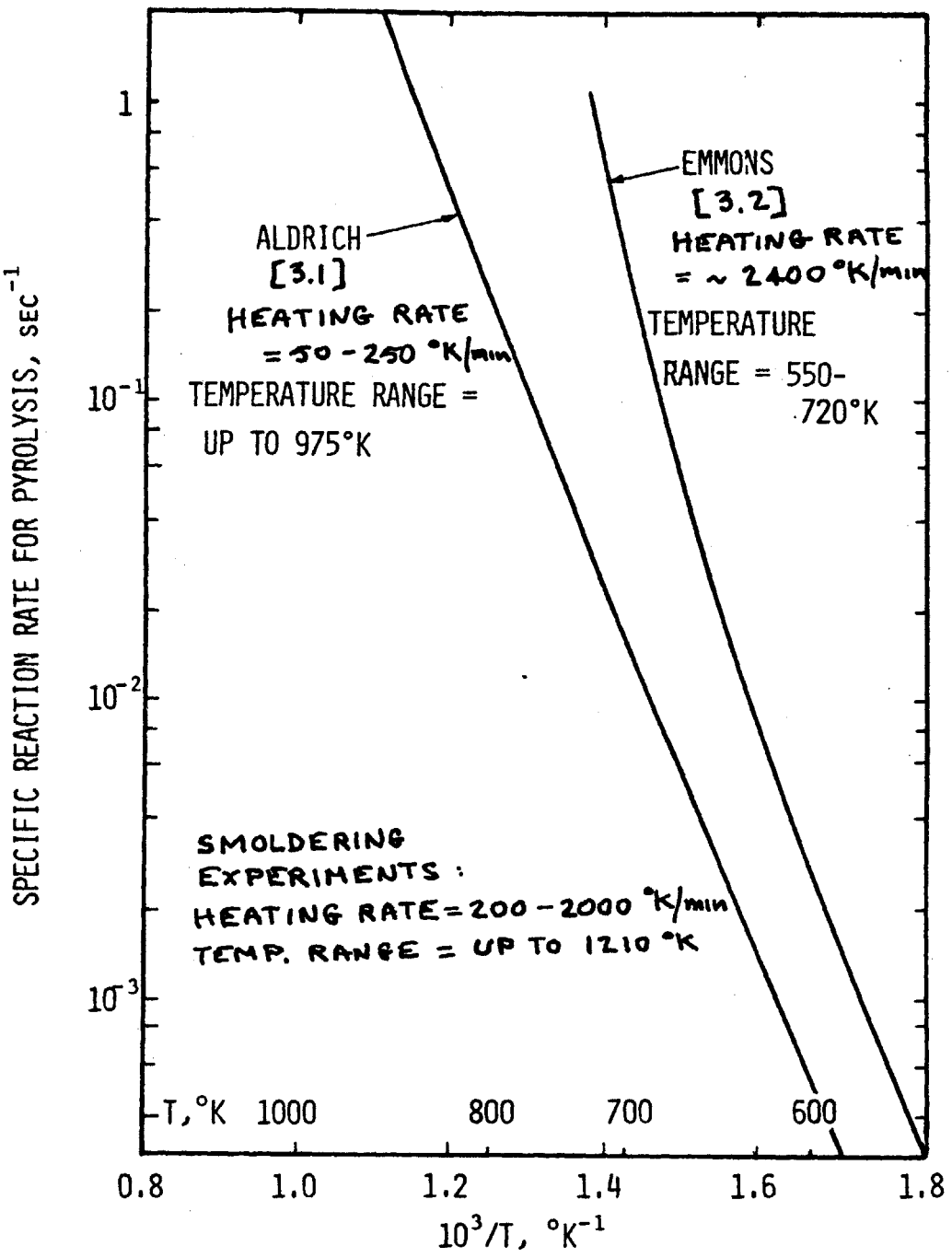


FIGURE 3.1.2 Overall Specific Reaction Rate for Cellulose Pyrolysis versus Temperature for Two Sets of Kinetic Parameters. Overall specific reaction rate = $k_c + k_g$, as defined by equations (3.1.5) and (3.1.6).

were conducted under different conditions, thus leading to the determination of different kinetic parameters.

The pyrolysis studies of these two investigators can be summarized briefly as follows. Aldrich measured the weight loss history and the temperature history, at various depths, in finite-thickness cylinders of α-cellulose held in a Nitrogen environment and exposed to infra-red radiation. Emmons measured the surface-density and the temperature histories of thin filter-paper sheets, held in free air, also exposed to infra-red radiation. They both determined the kinetic parameters by matching their experimental results with appropriate pyrolysis models that assumed two concurrent first-order reactions with Arrhenius kinetics.

In a pyrolysis study, the critical experimental conditions that influence the rate of cellulose decomposition are as follows:

(1) The heating rate and the temperature range determine the temperature-time histories and consequently the path followed by the reactions.

(2) The thickness of the material determines the extent of secondary pyrolysis reactions (i.e., between the gaseous products of pyrolysis and the char [3.3]).

(3) The gases in the environment in which pyrolysis occurs might catalyze pyrolysis [3.6] or might react with the products of pyrolysis, thus, generating heat that would enhance pyrolysis. (This effect will be studied further in section 3.2).

(4) The impurities in the samples used, such as organic additives and ash, can act as catalysts.

Some of these critical conditions varied significantly for the experiments of Aldrich and Emmons as illustrated in Table 3.1.2. It seems that the higher heating rates and the presence of oxygen* favored the high activation energy reaction as reflected in Emmons' calculations of the kinetic parameters.

Table 3.1.2 compares also the conditions of the present study with Aldrich's and Emmons'. Note that in the present study, the test samples are semi-infinite (while Aldrich's are of finite thickness and Emmons' are thermally thin†), the heating rates vary significantly (covering the range of Aldrich and Emmons), the surface temperature reaches high levels (as for the case of Aldrich), and the environment contains oxygen (as for the case of Emmons). On the basis of these comparisons, it is not a priori obvious which of the two sets of kinetic parameters is appropriate for the present study.

Thus, a model simulating the conditions of the present study is developed, accounting for conduction heat transfer and pyrolysis by an overall two-reaction scheme (similar to Aldrich's and Emmons'). The kinetic parameters appropriate for this study are determined by matching the model predictions with experimental results as presented in section 3.1.4. The mathematical formulation of this model is presented in the following section.

---

* Which may react exothermically with the product of pyrolysis.

† Thermally thin samples have little subsurface temperature gradients.

TABLE 3.1.2

Comparison of the Experimental Conditions of the

Present Study and those of Aldrich [3.1] and Emmons [3.2]

Item	Aldrich	Emmons	This Study
Sample	Finite thickness	Thermally thin (little subsurface temperature gradients)	Semi-infinite thickness
Heating rate	50 - 250° K/min	∿ 2400° K/min	200 - 2000° K/min
Temperature range	Maximum Surface Temperature = 975°K	550 - 720°K	Maximum Temperature = 1210°K
Environment	Nitrogen	Air	O_2/N_2 mixtures of varying compositions
Heat Flux	0.408 - 1.11 cal/cm^{2}s	0.67 - 1.05 cal/cm^{2}s	--

3.1.2 Mathematical Formulations

In this section, a mathematical model of condution heat transfer in a semi-infinite slab is formulated incorporating the pyrolysis scheme chosen in the previous section.

Consider the propagation of a pyrolysis zone with a constant speed V in a semi-infinite, stationary, slab under the effect of an external, specified heat flux imposed at one side of the pyrolysis zone. Presumably, this side is the interface between the pyrolysis zone and the char-oxidation zone, and the external heat flux is determined by char-oxidation reactions (as presented in section 3.2).

Upon heating, cellulose decomposed by two concurrent reactions forming char and volatiles according to the model discussed in the previous section. For simplicity, the momentum considerations governing the flow of the volatiles after their formation are not invoked. Assuming a one-dimensional problem, the flow of volatiles, char and heat is only in a direction perpendicular to the smoldering zone.

Additional simplifications are: equal local gas-phase and solid-phase temperatures (i.e., infinite heat transfer between the two phases); equal specific heats for virgin material, char and volatiles; negligible internal radiative and convective heat transfer; and uniform and time-invariant thermal conductivity.

A transfer of coordinates will move the virgin material into a stationary zone (at x = o), at the same speed V, as illustrated in Fig. 3.1.3. The equations governing the steady state of such a system are:

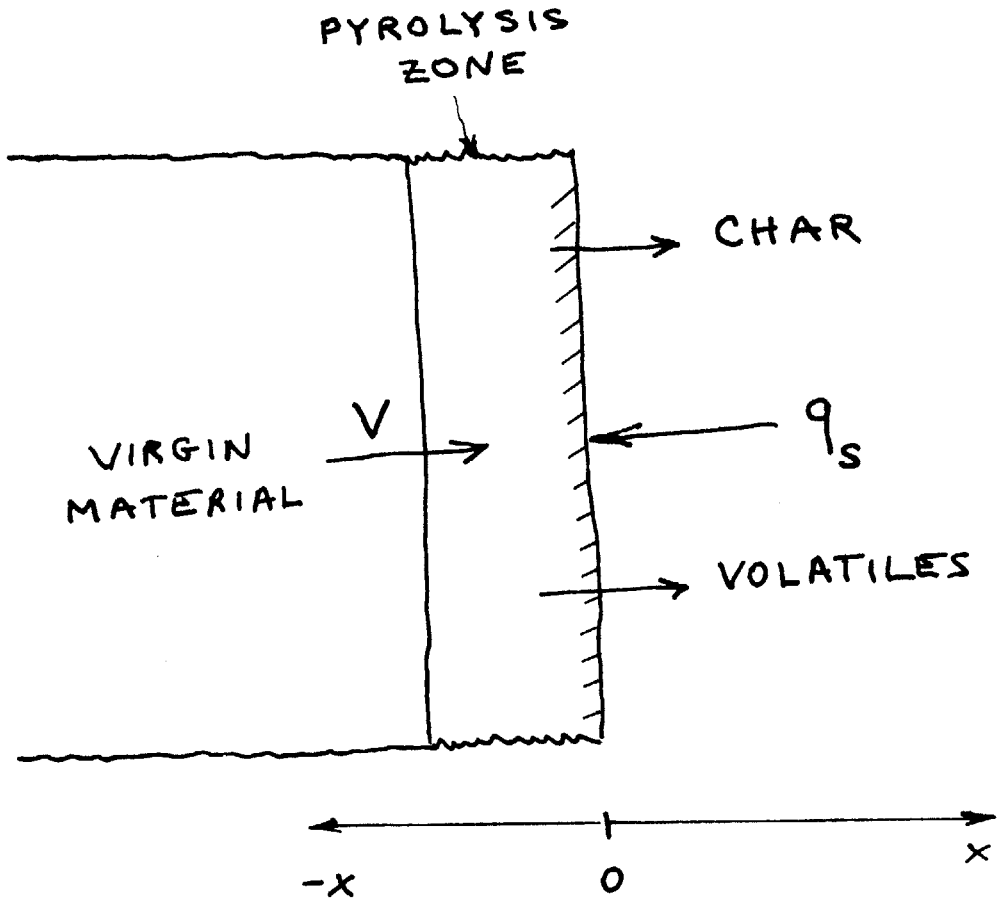


FIGURE 3.1.3 Physical Description of the Stationary Pyrolysis Zone. External Heat Flux (q_s) is Imposed at x = o. Virgin Material is Entering Zone and Char and Volatiles are Leaving it

Virgin Material Continuity

$$V\frac{d\rho_u}{dx} = -\rho_u\,(k_c + k_g) \tag{3.1.1}$$

Char Continuity

$$V\frac{d\rho_c}{dx} = \rho_u k_c \tag{3.1.2}$$

Volatile Continuity

$$\frac{d(\rho_g v_g)}{dx} = \rho_u k_g \tag{3.1.3}$$

Energy*

$$\rho_\infty c\, V\frac{dT}{dx} = \lambda\frac{d^2T}{dx^2} + \rho_u(H_c k_c + H_g k_g) \tag{3.1.4}$$

Rate

$$k_c = f_c \exp\left(-\frac{E_c}{RT}\right) \tag{3.1.5}$$

$$k_g = f_g \exp\left(-\frac{E_g}{RT}\right) \tag{3.1.6}$$

---

*Performing a mass balance between any position x and $x \to -\infty$, it may be shown that:

$$\rho_g v_g = \rho_\infty V - (\rho_u + \rho_c)\, V$$

and, for equal specific heats for all species, it follows that:

$$\rho_\infty c V\frac{dT}{dx} = (\rho_u + \rho_c)cV\frac{dT}{dx} + \rho_g v_g\, c\,\frac{dT}{dx}$$

Thus, the convective term in the energy equation accounts for the convection of virgin cellulose, char and volatiles.

With boundary conditions:

$$\text{at } x \to -\infty: \quad \rho_u \to \rho_\infty \tag{3.1.7}$$

$$\rho_c \to 0 \tag{3.1.8}$$

$$T \to T_\infty \tag{3.1.9}$$

$$\text{at } x = 0: \quad \frac{dT}{dx} = \frac{q_s}{\lambda} \tag{3.1.10}$$

$$\frac{\rho_u}{\rho_\infty} = \beta << 1 \tag{3.1.11}$$

Where:

V = Speed of propagation of pyrolysis zone

ρ = Mass density

x = Coordinate in direction of propagation

k_i = Specific rate of $i^{\underline{th}}$ reaction

f_i = Frequency factor of $i^{\underline{th}}$ reaction

E_i = Activation energy of $i^{\underline{th}}$ reaction

R = Universal gas constant

v_g = Velocity of the volatiles with respect to the pyrolysis zone

λ = Thermal conductivity

H = Heat of reaction

c = Specific heat

q_s = Heat flux at interface of pyrolysis zone

Subscripts:

u = Virgin material

c = Char

g = Gaseous volatiles

s = Conditions at $x = o$

∞ = Conditions at $x = -\infty$

Dimensionless variables:

Let:

$$\left.\begin{aligned} \rho_u' &= \rho_u/\rho_\infty & E_i' &= \frac{E_i}{RT_\infty} \\ \rho_c' &= \rho_c/\rho_\infty & f' &= f_g/f_c \\ T' &= T/T_\infty & \kappa &= \frac{\lambda f_c}{\rho_\infty c\, V^2} \\ x' &= \frac{\rho_\infty c\, V}{\lambda}\, x & & \\ q_s' &= \frac{q_s}{\rho_\infty c\, T_\infty V} & H_i' &= H_i/(c\, T_\infty) \end{aligned}\right\} \qquad (3.1.12)$$

Substituting these dimensionless variables into Equations (3.1.1) - (3.1.11), it yields:

$$\frac{d\rho_u'}{dx'} = -\kappa\rho_u' \left(\exp\left(-\frac{E_c'}{T'}\right) + f' \exp\left(-\frac{E_g'}{T'}\right)\right) \qquad (3.1.1a)$$

$$\frac{d\rho_c'}{dx'} = \kappa\rho_u' \exp\left(-\frac{E_c'}{T'}\right) \qquad (3.1.2a)$$

$$\frac{d^2T'}{dx'^2} = \frac{dT'}{dx'} - \kappa\rho_u' \left\{ H_c' \exp\left(-\frac{E_c'}{T'}\right) + f'H_g' \exp\left(-\frac{E_g'}{T'}\right)\right\} \qquad (3.1.4a)$$

With boundary conditions:

at $x' \to -\infty$: $\rho_u' \to 1$ (3.1.7a)

$\rho_c' \to 0$ (3.1.8a)

$T' \to 1$ (3.1.9a)

at $x = 0$ $\frac{dT'}{dx'} = q_s'$ (3.1.10a)

$\rho_u' = \beta << 1$ (3.1.11a)

Note that the last boundary condition eq. (3.1.11a) requires most of the virgin material to be consumed at the location of the front. This is the smolder-spreading condition that determines the eigenvalue of the system. (The dependence of the eigenvalue on the choice of β will be discussed in the next section.)

In mathematical parlance, the system of eqs, (3.1.1a), (3.1.2a) and

(3.1.4a) is fourth order, subject to five boundary conditions. Thus, it can be solved for only specific values of the floating parameter κ, i.e., it is an eigenvalue problem. Note that inverse κ is the square of the ratio of the pyrolysis speed to a characteristic speed $\left(\sqrt{\frac{\lambda}{\rho c}\, f_c}\right)$ determined by the system properties governing conduction and pyrolysis. Thus, the process possesses the wave-character of propagating at characteristic speeds determined by the medium of propagation.

This fourth order system of non-linear ordinary differential equations was solved numerically by Garris [3.11]. His solutions will be used to justify two approximations that simplified the system greatly and permitted a closed-form expression for the eigenvalue without solving the complete system. The closed-form expression gives insight in the character of the solution, not possible without extensive numerical calculations.

3.1.3 Closed-form, Approximate Eigenvalue

This section presents an approximate closed-form expression for the eigenvalue of the problem presented in the previous section. The agreement between the exact and the approximate eigenvalues is very good. Thus, the closed-form solution provides a quick indication of the effects of kinetic parameters and thermophysical properties on the smoldering speed.

The eigenvalue condition requires that the virgin material be consumed at the position of the pyrolysis front, i.e.,

$$\frac{\rho_u}{\rho_\infty} = \beta << 1 \quad \text{at } x = 0 \tag{3.1.11}$$

If the temperature profile in the slab is known, one can determine the eigenvalue by integrating the virgin material continuity equation (3.1.1) subject to boundary condition, eq. (3.1.7), and to the eigenvalue condition, eq. (3.1.11).

Various techniques, such as Fourier transform, Laplace transform and separation of variables, have been tried without success to obtain the temperature profile from the energy equation (3.1.4a) subject to the boundary conditions (3.1.9a) and (3.1.10a). These techniques failed because of the presence of the non-linear reaction terms. However, the numerical results of Garris indicate that the reaction terms can be neglected in eq. (3.1.4a)* without significant error [3.11]. These results are illustrated in figures 3.1.4 and 3.1.5 which give, respectively, the pyrolysis wave speed and temperature (at x = o) as a function of the heat flux for various reasonable thermicities. Note that a non-zero thermicity for the low activation energy reaction has a negligible affect and for the high activation energy reaction, it increases** the speed by up to only 25% and the temperature by ~ 10%. These effects are small given the large uncertainties in the material kinetics and thermophysical properties. Thus, it is justifiable to neglect the thermicity of the pyrolysis reactions, and eq. (3.1.4a) is reduced to:

$$\frac{d^2T'}{dx'^2} = \frac{dT'}{dx'} \qquad (3.1.13)$$

which can be solved subject to the boundary conditions (3.1.9a) and (3.1.10a) to give the following temperature profile:

$$T'(x') = 1 + q'_s \quad \exp(x') \qquad -\infty < x' \leq 0 \qquad (3.1.14)$$

---

* This means that the energy source or sink associated with the pyrolysis reaction is negligible compared to the energy rates of convection and conduction. The reacting terms are still important in the species continuity equations, however.

** Clearly, an exothermic reaction causes an increase in speed and temperature while an endothermic reaction would cause a decrease. Further discussion of the effects of thermocity can be found in reference 3.11.

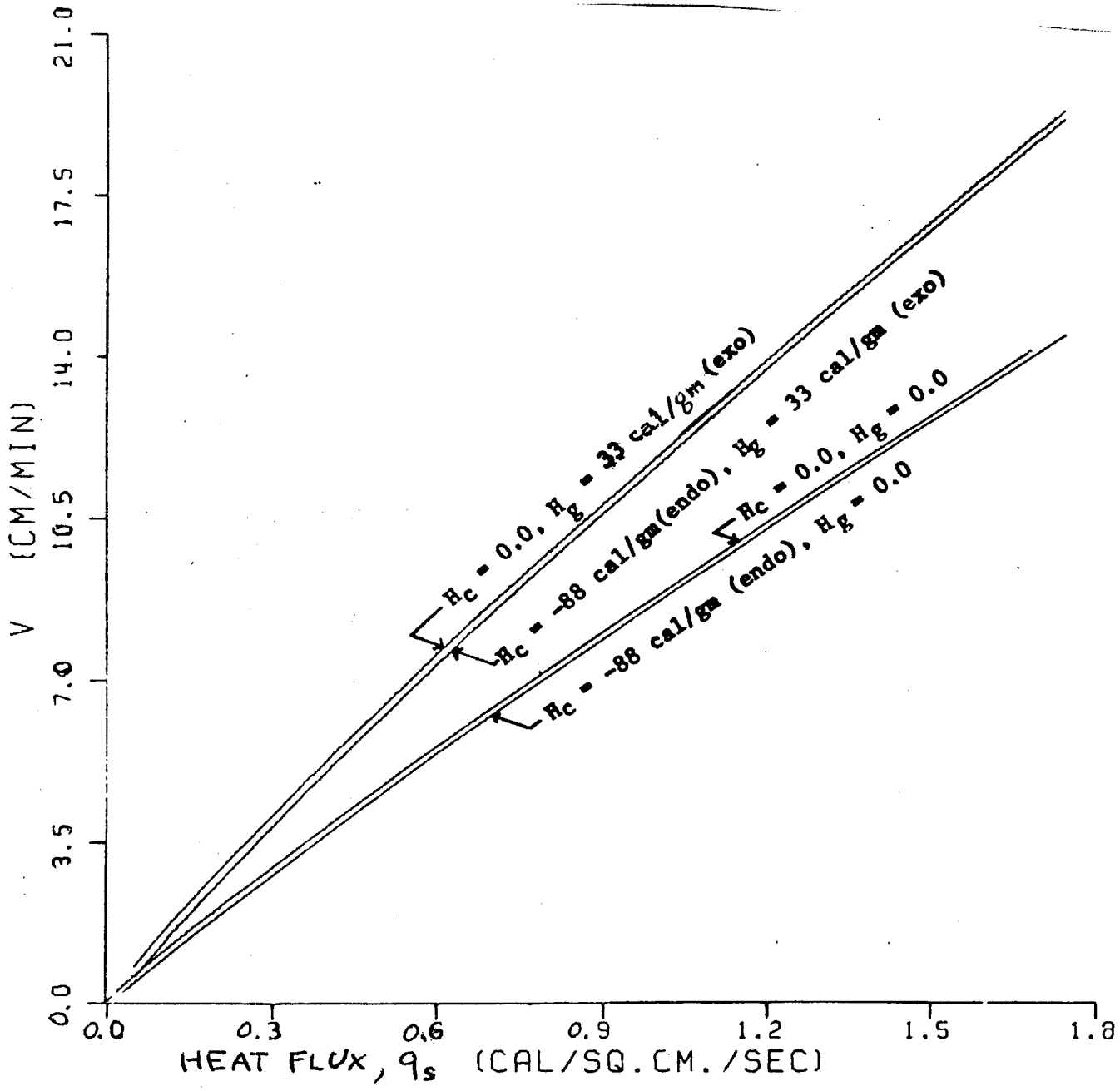


FIGURE 3.1.4 Steady Smoldering Speed, V, versus Imposed Heat Flux as a Function of the Thermicity of the Pyrolysis Reactions [3.11]

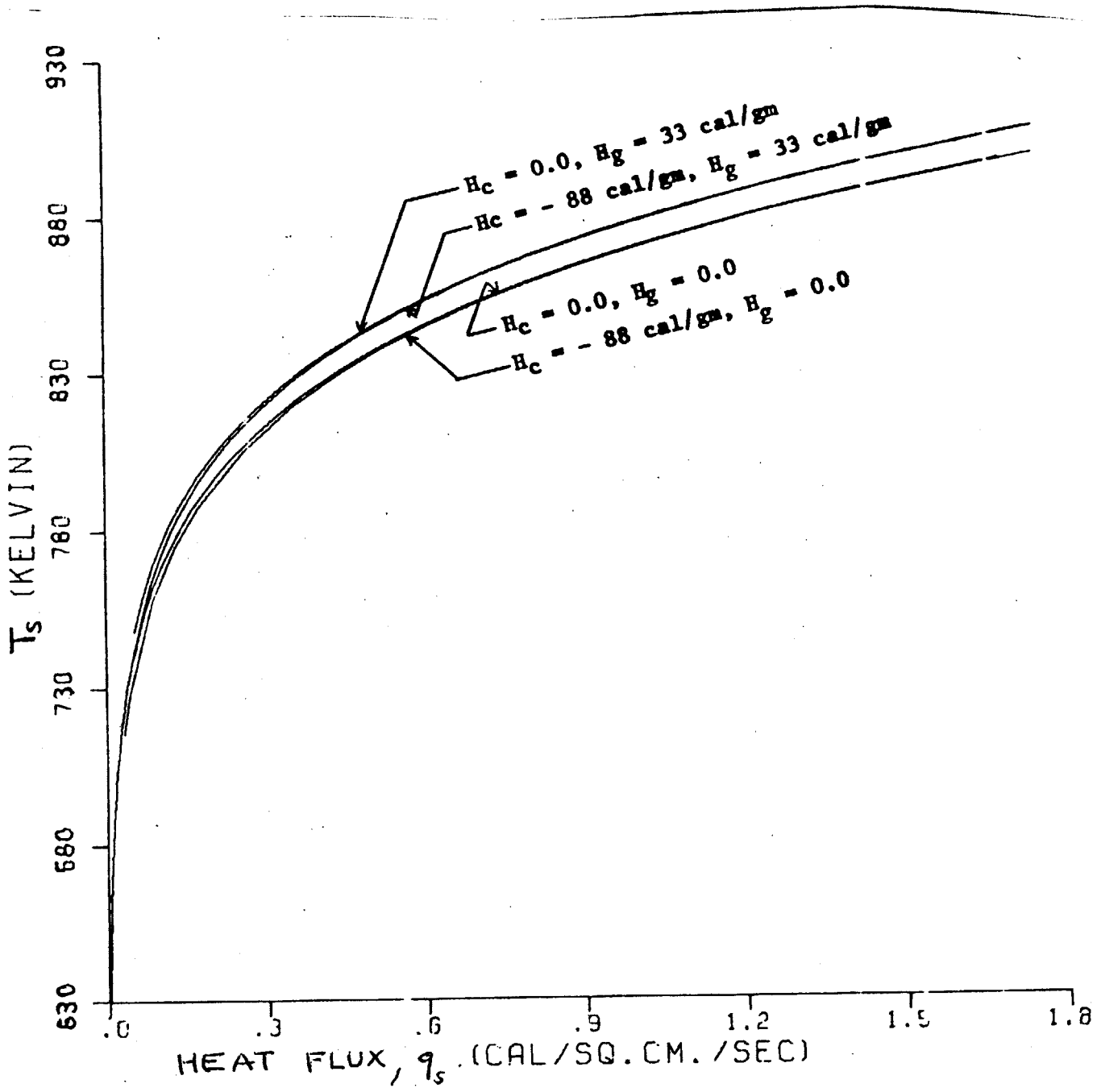


FIGURE 3.1.5 Interface Temperature versus Imposed Heat Flux as a Function of the Thermicity of the Pyrolysis Reactions [3.11].

Using this temperature profile, the eigenvalue is obtained by integrating (3.1.1a) with respect to temperature subject to the boundary conditions (3.1.7a) and (3.1.11a):

$$\int_1^{\beta} \frac{d\rho_u'}{\rho_u'} = \int_1^{T'(o)} - \frac{\kappa \left(\exp\left(-\frac{E_c'}{T'}\right) + f' \exp\left(-\frac{E_g'}{T'}\right) \right) dT'}{\frac{dT'}{dx'}} \qquad (3.1.15)$$

The temperature gradient is obtained from eq. (3.1.14) as follows:

$$\frac{dT'}{dx'}(x') = q_s' \exp(x') = T'(x') - 1 \qquad (3.1.16)$$

Integration of the right hand side of eq. (3.1.15) can be performed in closed-form if we assume that in the region of interest to pyrolysis:

$$\frac{dT'}{dx'}(x') \simeq T'(x') \qquad (3.1.17)$$

i.e., $T'(x') \gg 1$

This is reasonable because, as $T(x) \to T_\infty$, the contribution of the reaction terms becomes negligible, i.e., significant pyrolysis occurs only when $T(x) \gg T_\infty$. This is well borne out by the numerical results of Garris [3.11].

The resulting eigenvalue is:

$$\kappa = \frac{\ln\beta}{Ei\left(-\frac{E_c'}{T_s'}\right) + f' Ei\left(-\frac{E_g'}{T_s'}\right) - Ei\left(-E_c'\right) - f' Ei\left(-E_g'\right)} \qquad (3.1.18)$$

with $T_s' = 1 + q_s'$ = surface dimensionless temperature

or in dimensional form:

$$V = \left\{ \frac{\dot{\lambda}}{\rho_\infty c} \frac{f_c}{\ell n \beta} \left[Ei\left(-\frac{E_c}{RT_s}\right) + \frac{f_g}{f_c} Ei\left(-\frac{E_g}{RT_s}\right) - Ei\left(-\frac{E_c}{RT_\infty}\right) - \frac{f_g}{f_c} Ei\left(-\frac{E_g}{RT_\infty}\right) \right] \right\}^{1/2} \qquad (3.1.18a)$$

with $T_s = T_\infty + \frac{q_s}{\rho_\infty c V}$ = surface temperature

where Ei(x) is the exponential integral function defined as:

$$Ei(x) = \int_{-x}^{\infty} \frac{\exp(-t)}{t}\, dt, \qquad \text{for } x < 0, \qquad (3.1.19)$$

and illustrated in Figure 3.1.6 for a range of values of interest.

Figure 3.1.7 compares approximate, Eq. (3.1.18a), and exact smoldering speeds as a function of the external heat flux for the kinetics of Emmons.* The agreement is very good (with the approximate speeds ~10% lower than the exact ones). The approximate solution is also plotted for the kinetics of Aldrich. Note that the pyrolysis speed is almost linearly dependent on the heat flux.

A similar comparison for the surface temperature versus external heat flux is given in Figure 3.1.8, showing also good agreement. The approximate solution is about 7% higher than the exact one for heat fluxes of interest. These heat fluxes correspond to the measured smoldering speeds according to Fig. 3.1.7.

---

* The thermophysical properties employed in these calculations are given in Appendix 3.6. The computer program used to evaluate eq. (3.1.18a) is given in Appendix 3.5.

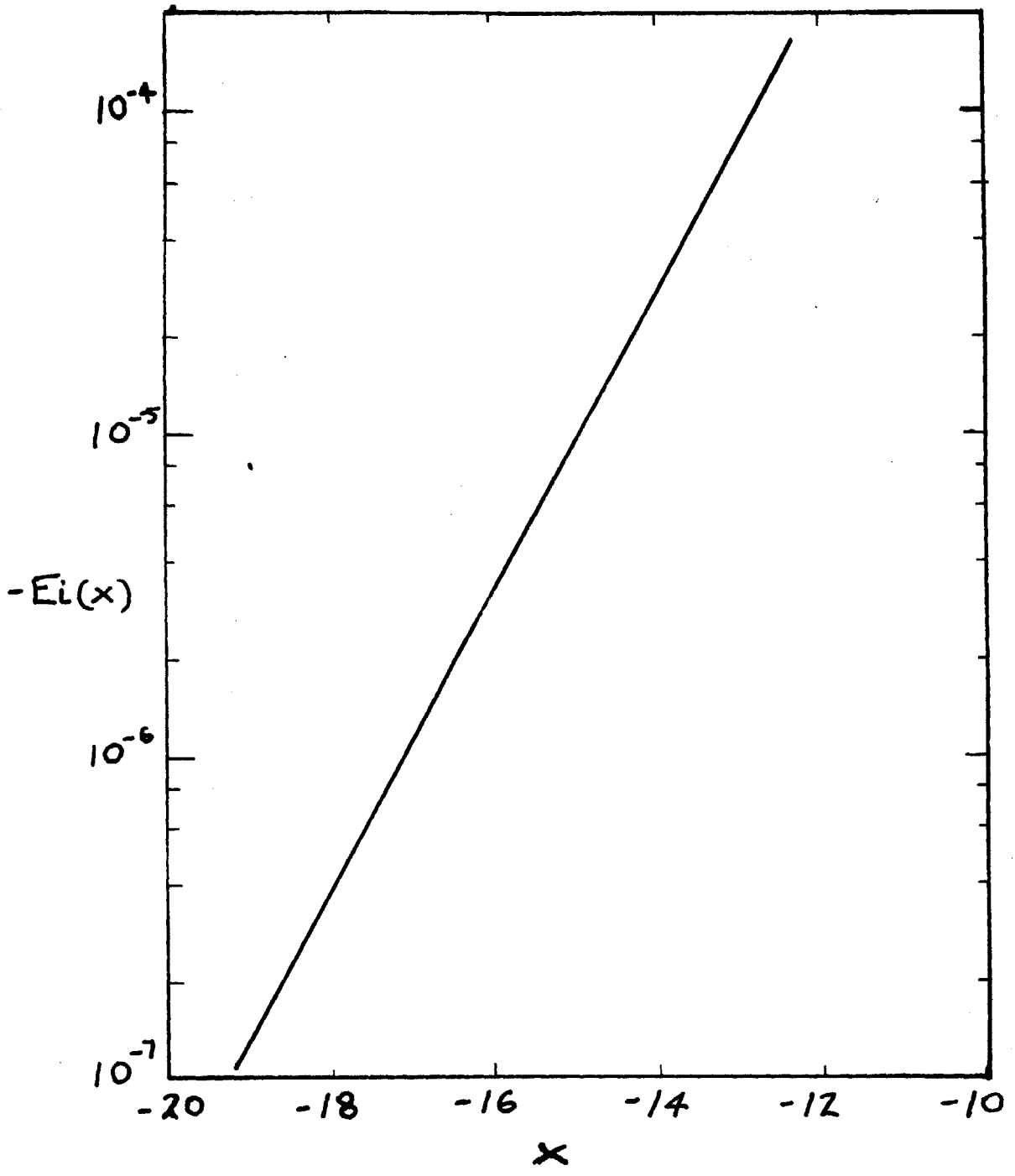


FIGURE 3.1.6 Exponential Integral Function, Ei(x), for a Range of Values of Interest

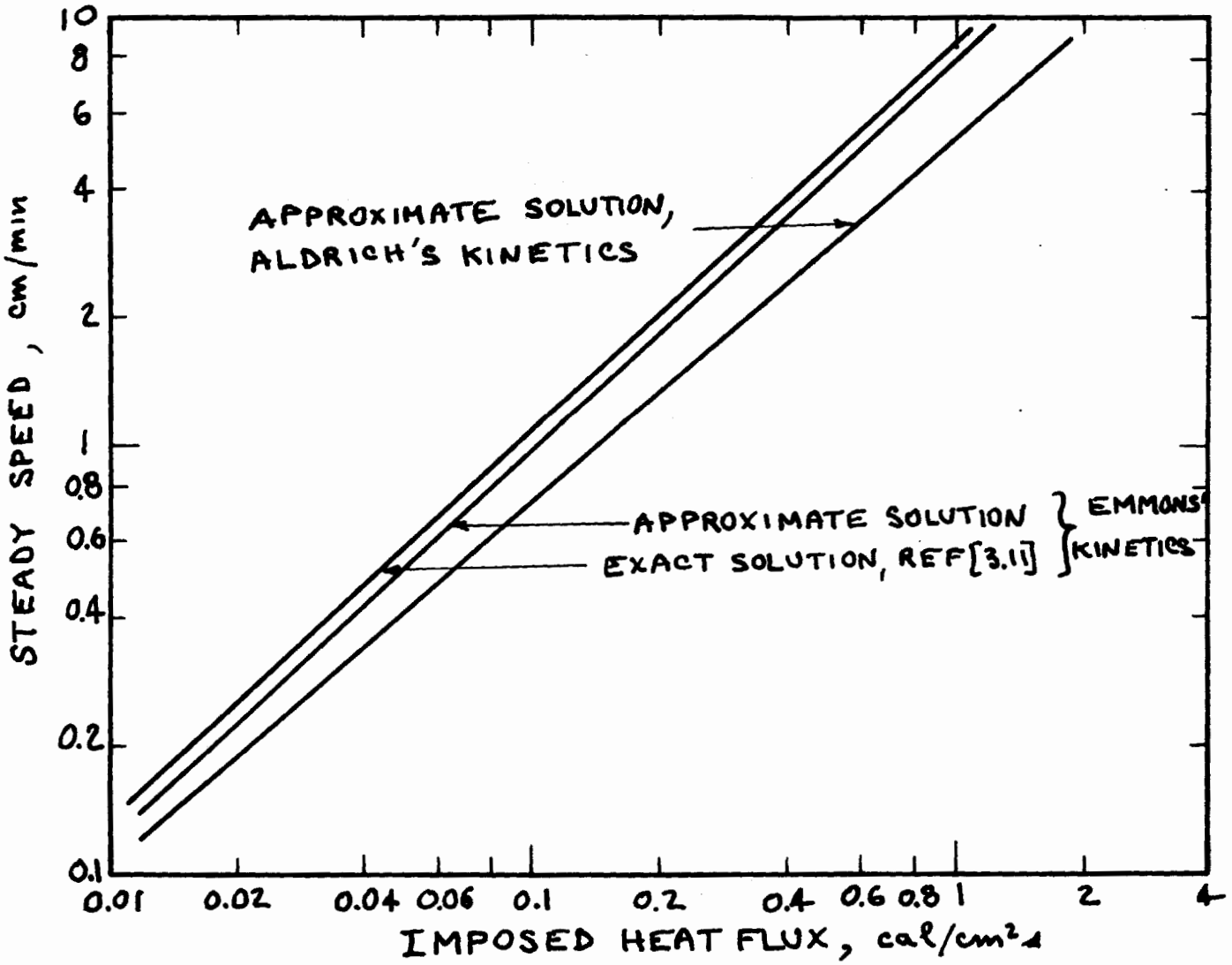


FIGURE 3.1.7 Approximate and Exact Pyrolysis Speed versus Imposed Heat Flux

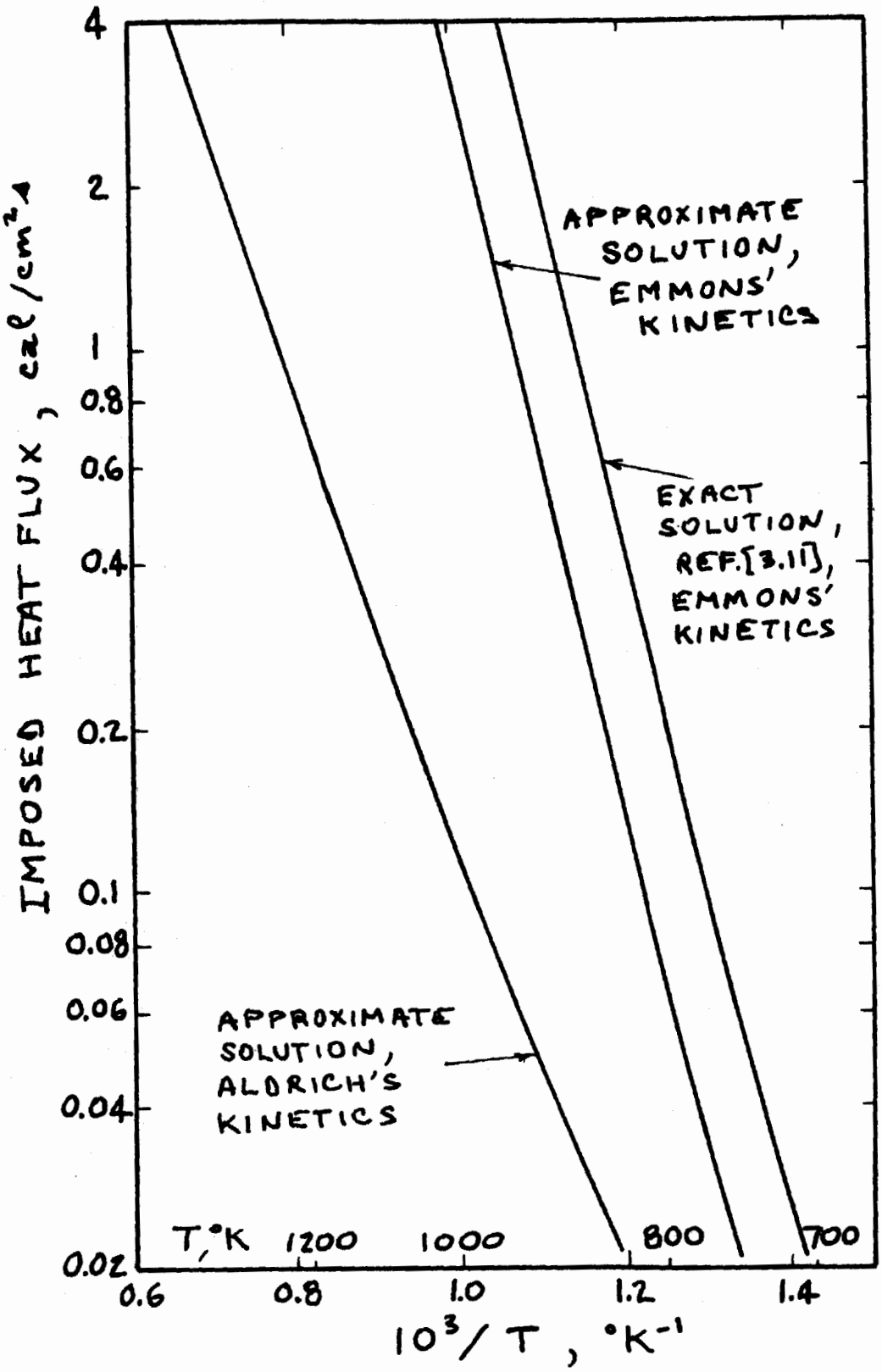


FIGURE 3.1.8 Approximate and Exact Interface Temperature versus Imposed Heat Flux

The surface temperature is related to the speed and the heat flux as follows (from the temperature profile, eq. (3.1.14)):

$$T_s = T_\infty + \frac{q_s}{\rho_\infty c V} \tag{3.1.20}$$

This can be also obtained by an energy balance over a control volume enclosing the pyrolysis zone and virgin material still unaffected by the wave. Thus, at any specified heat flux, the prediction of a lower speed by the approximate method (vis-a-vis the exact method) is consistent with a prediction of a higher surface temperature, because of energy conservation according to eq. (3.1.20).

It is also of note that Emmons' fast kinetics predict a lower temperature and a higher speed than Aldrich's slow kinetics, for any specified heat flux. This is plausible, because the decomposition of virgin cellulose into char and volatiles can be completed at a lower temperature when the kinetics are fast. Furthermore, energy conservation requires a faster speed with a lower temperature, as discussed in the previous paragraph.

The significant differences between the predictions on the basis of the kinetic parameters of Aldrich and Emmons make it imperative to determine what kinetic parameters are appropriate for this study. This is presented in the following section. Note further, that for a specific set of kinetics the differences between approximate and exact predictions are much smaller than the uncertainties due to unknown kinetics. This increases the utility of the approximate solution.

This approximate solution, eq. (3.1.18a), is useful in determining by inspection the effects of the kinetic and thermophysical parameters on the pyrolysis wave speed. Note that the right hand side of this equation is an implicit function of the speed through its dependence on the temperature. Thus, numerical calculations of this equation are needed to determine these effects quantitatively. However, by inspection of equation (3.1.18a) it is obvious (at least qualitatively) that:

(1) an increase in thermal conductivity will increase the speed, because of increase in heat transfer to the virgin material (namely, conduction in the solid phase).

(2) an increase in heat capacitance (ρc) will decrease the speed*, because the temperature rise will be slower and thus pyrolysis is retarded.

(3) an increase in the activation energy will decrease the speed, because pyrolysis is retarded. The converse is true for the effect of the frequency factor.

(4) in a multi-reaction pyrolysis scheme, the relative importance of any specific reaction on the wave speed can be simply determined by calculating its relative contribution in eq. (3.1.18a). Consequently, the natural criterion determining the relative importance of any two reactions (n and m) becomes the following ratio:

$$\frac{f_n \, Ei(- E_n/RT)}{f_m \, Ei(- E_m/RT)} \qquad (3.1.21)$$

* Note that for cellulosic samples of varying diameters (d), the measured speed was inversely related to the product (ρ c d), as reported in Chapter 2 (assuming that the specific heat (c) is a constant for cellulose). To compare this result with prediction (2), the effect of the diameter must be investigated as can be done by the model developed in the next section.

Finally, because the pyrolysis speed is inversely related to the half power of $\ell n\beta$, according to eq. (3.1.18a), its dependence on β is weak. This is also verified by the numerical calculations of Garris [3.11], which show that for variations in β from 10^{-5} to 10^{-11}, the speed decreases by less than 5%, approaching an asymptote as $\beta \to o$.

3.1.4 Comparison of Theory and Experiment

The purpose of this section is two-fold: firstly, to verify the validity of the pyrolysis model developed and solved in the previous sections, and secondly, to determine the kinetic parameters appropriate for this study.

In the previous section, the solution of the pyrolysis study, given by eq. (3.1.18a), determined the dependence of the pyrolysis wave speed and interface temperature on the imposed heat flux and the kinetic and thermophysical parameters of the system. Verification of these dependences are very difficult, however, because of the difficulty in measuring the heat flux at the pyrolysis zone and in varying (at will) the aforementioned parameters. Yet, for a specified set of these parameters, the solution indicates a unique relationship between the temperature and the speed, despite the unknown heat flux. In this study, changing the environmental conditions changes the char-oxidation rate (as described in the next section) and consequently changes the heat flux into the virgin material. Under these conditions, variations in the pyrolysis kinetic parameter are assumed negligible. Thus, one can test the predicted unique temperature-speed relationship with measurements under different environmental conditions.

It should be noted that in reality the zones of pyrolysis and char-oxidation are not separate as assumed in our model*. Visual observations can correlate the temperature-time profile with the

---

* In fact, char may react with oxygen as soon as it is formed, in which case the two zones become identical. However, significant char-oxidation is expected when the material becomes porous, i.e., after it has somewhat pyrolyzed. Therefore, one might still distinguish between the two zones.

onset of events such as pyrolysis*, charring and glowing as illustrated in Figure 2.3.2, but, the interface temperature is difficult to determine from such observations. It is of note that the temperature profile exhibits two inflection points, presumably denoting the onset and the end of significant exothermic reactions, respectively. Presumably, the interface temperature must be somewhere between the first inflection point and the maximum temperature.

Accordingly, these two temperatures are illustrated as a function of speed in Figure 3.1.9 for runs in different environmental conditions (including He - O_2 mixtures). The approximate solution (eq. (3.1.18a)) based on the kinetics of Aldrich and Emmons and the exact solution (from the numerical work of Garris [3.11]) with Emmons' kinetics are also illustrated.

The experimental uncertainty is about 6% for the speed and the maximum temperature, as determined in section 2.2. The uncertainty in the inflection point is even higher because the small curvature in in the temperature profile makes it difficult to estimate such a point. Within this uncertainty, the data form a unique relationship between each temperature** and speed, regardless of the oxygen mole fraction or the oxygen partial pressure, or the inert diluent in the environment whether Nitrogen or Helium. (The combination of oxygen mole fraction and partial pressure determine only where each run falls on the unique relationship). This verifies the prediction of the pyrolysis model.

The interface temperature is expected to be somewhere between

---

* as indicated by the outflow of greyish gases

** i.e., the maximum and the inflection point temperatures

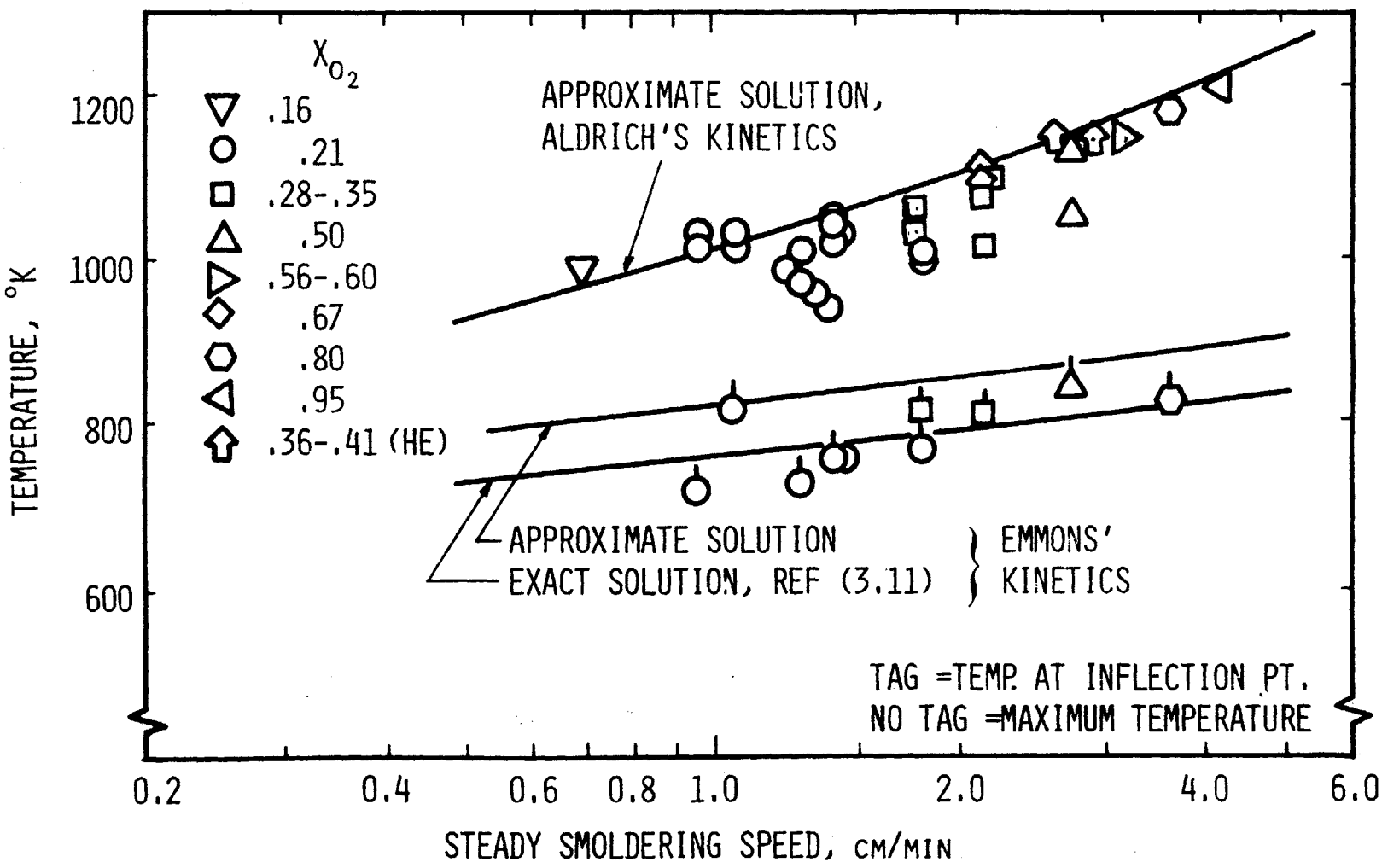


FIGURE 3.1.9 Comparison of Theory and Experiment for the Steady Smoldering Temperature-Speed Relationship. Theory gives Approximate and Exact Solutions. Horizontal Cellulosic Samples were tested in Various Oxygen Mole Fractions (X_{O_2}) and Partial Pressures (P_{O_2})

the maximum temperature and that at the inflection point. Thus, it seems that the exact solution using the kinetics of Aldrich would represent best our data. This solution is not illustrated in Fig. 3.1.9 because it was not obtained by Garris [3.11]. However, it is expected to fall below the approximate solution, as is the case for Emmons' kinetics.

It is of note that the approximate solution can also be used to generate the kinetics that fit best the experimental data of this study if the location of the interface temperature were known. Because of this uncertainty, no attempt is made to generate these kinetic parameters, however.

The overall pyrolysis scheme used in this study assumed no dependence on the oxygen in the environment of the sample. The experimental data illustrated in Figure 3.1.9 appear to verify this assumption, as discussed earlier. This result suggests that the environmental oxygen does not catalyze the pyrolysis reactions as reported by many investigators [3.6], but reacts with the products of pyrolysis thus providing heat that enhances pyrolysis.

3.1.5 Conclusion of the Pyrolysis Study:

The following conclusions can be drawn from the pyrolysis study:

1. An overall two-reaction scheme is useful in describing cellulose pyrolysis. The two reactions are concurrent and the low activation energy one leads to char formation, while the high activation energy one leads to volatiles formation.

2. A model of conduction heat transfer in a semi-infinite slab undergoing pyrolysis yielded a closed-form solution of the pyrolysis speed as a function of the imposed heat heat flux or the surface temperature and the kinetic and thermophysical parameters of the system. This solution is very useful for design purposes in order to reduce the smoldering speed. It predicts that the speed will increase with:
   - an increase in thermal conductivity
   - a decrease in heat capacitance
   - faster kinetics for the pyrolysis reaction
3. Comparison of the predicted and measured temperature-speed relationship suggests that the kinetic parameters given by Aldrich are adequate for use in this study.

3.2 CHAR-OXIDATION

As presented in the introduction to this chapter, the smoldering behavior is predicted by heating pyrolysis and char-oxidation in two zones separated by an interface, with suitable matching requirements. In the previous section, the characteristics of a steadily propagating pyrolysis wave were determined for specified, external heat fluxes. Presumably, these heat fluxes are provided by the exothermic reactions occurring during smoldering. These reactions include:

(a) Cellulose pyrolysis

(b) Char reactions with volatiles formed by pyrolysis

(c) Char-oxidation reactions

(d) Gas-phase reactions (without appearance of a flame)

(e) Char reactions with the products of these gas-phase reactions

It is difficult to determine the energy contributed by each of these reactions because of lack of basic kinetic data, except for the char-oxidation reaction. Thus, it is proposed to test whether char-oxidation alone can provide the heat flux needed to sustain smoldering.

In this section, an overall "apparent"* Arrhenius expression is chosen from the literature for char-oxygen reations. The energy generated is calculated for various oxygen partial pressures and mole fractions, taking into account both kinetics and diffusion considerations, An energy balance is performed matching the heat flux required for pyrolysis with that generated by char-oxidation, allowing for reasonable losses. This predicts steady smoldering solutions and an extinguishment limit depending on the environmental parameters. These predictions are in

---

* This expression is called "apparent" because it is based on the external area of the porous char not on its true area including that of the internal pores.

qualitative agreement with experiments. The "apparent" kinetic parameters appropriate for the present study are determined by matching the observed extinguishment limit with that predicted on the basis of specific kinetic parameters. These kinetic parameters are later used in the following section to predict the steady smoldering behavior.

3.2.1 Overall Kinetics of Char-Oxidation

The chemical composition of the char obtained under the smoldering experiments in this study is unknown and is expected to vary because of possible variations in cellulose pyrolysis. It is generally known, however, that such char is mainly carbon. For example, Robert [3.5] reported the following composition for char obtained from wood: $C\,H_{0.2}O_{0.02}$ Thus, for want of better information, it is assumed that the kinetics of the char in this study are the same as those reported for carbon and pulverized fuels*.

A review of the literature of carbon and pulverized fuel oxidation studies [3.12 - 3.19] identified various postulated mechanisms of sequential and concurrent kinetic steps. These steps include adsorption of the oxygen, its surface migration to an active site, its chemical combination with a carbon atom at that site and desorption of the product. Additional complicating kinetic steps are introduced if the oxygen dissociates, if multiple products are formed (as, for instance, carbon dioxide and carbon monoxide), if these products subsequently react with the char, if an inert diluent in the reactant gas competes for active sites (as might nitrogen in air), and if there is more than one type of active site [3.14].

Despite the afore-mentioned complications, overall Arrhenius expressions for the reaction rate as a function of the temperature and the oxygen concentration at the carbon surface were found to

---

* Examples of pulverized fuels are: coal, soot, charcoal, coke, anthracite [3.12].

correlate well with the experimental data [3.16]. Scala [3.13] and Maahs [3.14] suggested that the data available in the literature for temperature below 1320° K* can be bracketed by two overall Arrhenius expressions:

$$r_{lower} = 2.18 \times 10^4 P_{O_2,s}^{1/2} \exp(-\frac{42300}{RT_s}) \quad (3.2.1)$$

and

$$r_{upper} = 3.29 \times 10^8 P_{O_2,s}^{1/2} \exp(-\frac{44000}{RT_s}) \quad (3.2.2)$$

where:

r = gram of carbon/s-cm^2 of external surface area

P_{O_2} = partial pressure of xoygen, atm

T = surface temperature, °K

R = universal gas constant

and the subscript s denotes surface conditions.

It is of note that these two sets of data differ by four orders of magnitude, probably because of variations in the properties of the carbon tested and in experimental conditions. Clearly, they are an oversimplification of the complex processes occuring in carbon combustion. Furthermore, as discussed by Mulcahy and Smith [3.12], these reported activation energies, frequency factors and reaction orders are "apparent" and not "true" kinetic parameters because no account is made for the "true" surface area of porous carbon nor for oxygen diffusion through the pores of the carbon.

---

* The highest temperature measured in this study is 1210°K.

A simplified analysis for heterogenous reaction of a porous surface is given in Appendix 3.1. It shows that to determine the reaction rate, one needs to know the "true" kinetics and the diffusion characteristics in the pores (i.e., the number of pores, their geometries and sizes, and the diffusion coefficient). These are two formidable tasks! For the conditions of this study, the true kinetics are unknown, and the porosity varies from one experiment to another and with time in each experiment (because of variations in the extent of cellulose pyrolysis and char reaction, both governed by the environmental parameters of each experiment). While, it might be interesting to study such a complicated process, its inclusion in the study of smoldering at this stage is not warranted. Instead, the reaction rate is calculated on the basis of the "external" area of a solid surface and not the "true" area of a porous surface. This is consistent with using "apparent" kinetic data for porous carbon that are reported on the basis of the "external" area of a solid surface. In fact, the use of these "apparent" kinetics accounts somewhat for the effect of actual porosity of the char that we neglect in the analysis.

3.2.2 Reaction Rate Accounting for Kinetics and Diffusion Considerations

Consider a non-porous surface reacting with oxygen. The reaction rate at the surface is governed by the temperature and the oxygen concentration at the surface according to eq. (3.2.1) as presented in the previous section.* The oxygen concentration at the surface is determined by the balance of oxygen arrival and oxygen consumption at the surface. Thus, to determine the reaction rate at any temperature, one must couple oxygen mass transfer and kinetic considerations as done below.

The free-convective flow field around the steady-smoldering of a cylindrical element is illustrated in Fig. 3.2.1. The boundary layer and the plume are visible because of the smoke generated. The streamlines indicate the entrained flow of ambient gas. Clearly, ambient oxygen must diffuse through the boundary layer to reach the reacting surface. The diffusion time is about five times longer than the free-convection time*,** so that diffusion controls the rate of oxygen arrival to the surface.

To determine the rate of oxygen arrival to the surface, one could solve the species diffusion equations in a natural convective boundary layer. However, it is not a priori known if mass transfer considerations play any role in smoldering (because of the low temperatures involved, the process could be in a kinetics-limited regime.) Thus, one should determine that the role of diffusion is important before the elaborate task of solving the diffusion equations.

---

* Presumably only the kinetic parameters will vary with different situations

** See Appendix 3.2

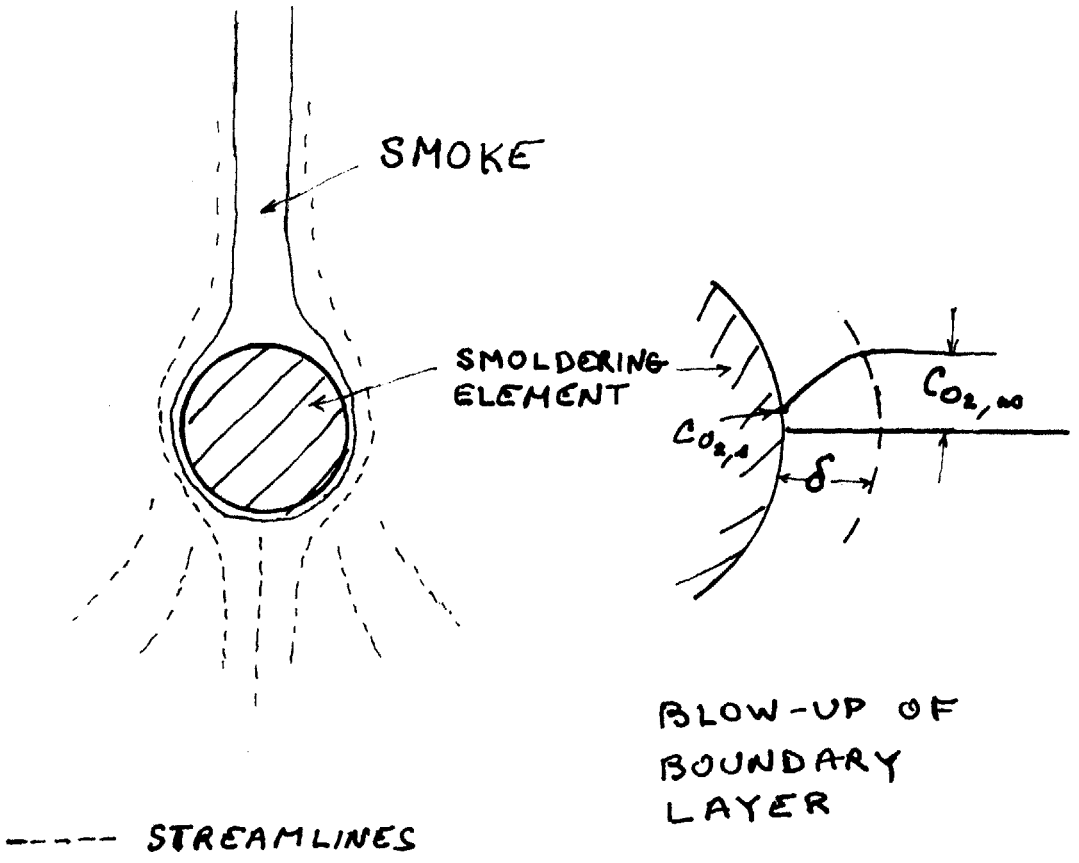


FIG. 3.2.1 FLOWFIELD AROUND SMOLDERING ELMENT

To accomplish this, an approximate expression for the rate of oxygen diffusion through the boundary layer is derived. As illustrated in Fig. 3.2.1, the oxygen concentration at the outer end of the species boundary layer is equal to the ambient concentration. The oxygen concentration at the surface is unknown and will be determined by balancing the rate of oxygen arrival and oxygen consumption at the surface.

The oxygen diffusion flux to the surface (J_{o_2}) is given by Fick's Law as follows:

$$J_{o_2} = D \cdot \nabla C_{o_2} \tag{3.2.3}$$

Where:

D = diffusivity

C_{o_2} = Concentration of oxygen

Here, the film theory approximation is introduced. It assumes that the reaction surface is covered by a relatively stagnant film of constant properties* through which oxygen and the smoldering products diffuse countercurrently, and the total effect of which is equivalent to that of the actual film. The thickness of this film (δ) is determined by the fluid mechanical considerations as presented later in this section. Neglecting the effects of counter-diffusion of the smoldering products (see Appendix 3.3), an approximate expression for the oxygen flux becomes:

$$J_{o_2} \simeq \frac{D\,(C_{o_{2,\infty}} - C_{o_{2,s}})}{\delta} \tag{3.2.4}$$

where δ = the film thickness or boundary layer.

---

* At the arithmetic mean temperature between the surface and ambient temperature.

and the subscripts ∞ and s denote ambient and surface conditions, respectively.

A semi-empirical expression for the diffusivity (cm^2/s) between two gases is given by Gilliland as follows [3.20]:

$$D = 4.30 \times 10^{-3} \frac{T^{3/2}}{P\,(V_a^{1/3} + V_b^{1/3})^2} \sqrt{\frac{1}{M_a} + \frac{1}{M_b}} \qquad (3.2.5)$$

Where T = Temperature, °K

P = Pressure, atm

V = Atomic volume

M = Molecular weight

and the subscripts a and b denote the two gases.

Assuming a perfect gas and replacing eq. (3.2.5) in eq. (3.2.4) yields the oxygen flux as follows:

$$J_{O_2} = \frac{A\sqrt{T_s + T_\infty}}{P\delta} (P_{O_{2,\infty}} - P_{O_{2,s}}) = \frac{A\sqrt{T_s + T_\infty}}{\delta} (X_{O_{2,\infty}} - X_{O_{2,s}}) \qquad (3.2.6)$$

Where X_{O_2} = mole fraction of oxygen

A = A physical constant introduced to describe the binary diffusion of oxygen through nitrogen, see Appendix 3.3

From the previous section, the rate of char reaction is:

$$r = f_e P_{O_{2,s}}^{1/2} \exp\left(-\frac{E_e}{RT_s}\right) \qquad (3.2.7)$$

where the subscript e denotes exothermic reaction.

For a steady state, the oxygen partial pressure at the surface is found by equating the rate of oxygen arrival, eq. (3.2.6), with the rate of its consumption (i.e., the rate of char reaction, eq. (3.2.7),

times some stoichiometric coefficient ϕ). This yields:

$$P_{O_{2,s}} = f(\xi)\, P_{O_{2,\infty}} \tag{3.2.8}$$

$$\text{where} \quad \xi = \frac{f_e \exp(-\frac{E_e}{RT_s}) P_{O_{2,\infty}}^{1/2}}{A\sqrt{T_s + T_\infty}\, X_{O_{2,\infty}}/\phi\delta} \tag{3.2.9}$$

$$\text{and} \quad f(\xi) = 1 + \frac{\xi^2}{2} - \sqrt{\left(1 + \frac{\xi^2}{2}\right)^2 - 1} \tag{3.2.10}$$

It should be noted that the parameter ξ is the ratio of the diffusion to chemical times, or alternatively, the ratio of the diffusion and chemical resistances, R_{diff}/R_{chem}, where

$$R_{diff} = \frac{\phi P \delta}{A\sqrt{T_s + T_\infty}} \tag{3.2.11}$$

and

$$R_{chem} = \frac{P_{O_{2,\infty}}^{1/2}}{f_e \exp(-E_e/RT_s)} \tag{3.2.12}$$

In the limit, as $\xi \to$ zero (see Fig. 3.2.2a)

$$P_{O_{2,s}} \equiv P_{O_{2,\infty}} \tag{3.2.13}$$

and the reaction rate is given by:

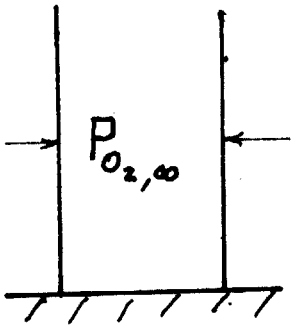
$$r = f_e \exp(-\frac{E_e}{RT_s})\, P_{O_{2,\infty}}^{1/2} \tag{3.2.14}$$

This is the case of slow kinetics and is called the kinetics-limited regime.

(a) KINETICS-LIMITED REGIME

$\xi \ll 1$

$P_{O_2,A} \equiv P_{O_2,\infty}$



(b) DIFFUSION-LIMITED REGIME

$\xi \gg 1$

$P_{O_2,A} \longrightarrow 0$

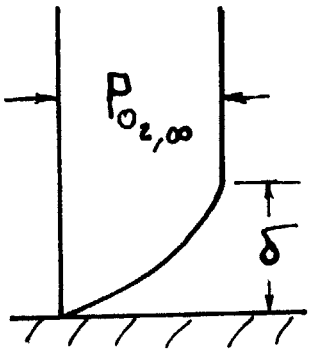


FIG. 3.2.2

As $\xi \rightarrow$ infinity (see Fig. 3.2.2b):

$$P_{O_{2,s}} \rightarrow 0$$

and the reaction rate is determined by the flux of oxygen to the surface:

$$r = \frac{A\sqrt{T_s + T_\infty}}{\delta\phi} X_{O_{2,\infty}} \qquad (3.2.15)$$

This limit means infinitely fast kinetics and is called the diffusion-limited regime.

Note that the dependence of the reaction rate on the environmental parameters (i.e., the oxygen partial pressure and mole fraction) is different in the two regimes. This result is used in this study to determine the relative role of kinetics and diffusion in smoldering.

Boundary Layer Thickness

Estimates for the boundary layer thickness, δ, were obtained from the data presented by McAdams [3.21] for natural convection around an infinitely long cylinder. For the Grashof number range of this study (5-6000), the following relationship was used:

$$N_u \equiv \frac{d}{\delta} = 1.23\ (Gr\ Pr)^{0.15} \qquad (3.2.16)$$

for $1 < Gr < 5000$.

where Nu = Nusselt number $\equiv hd/k$

Gr = Grashof number $\equiv d^3\rho^2 g\beta(T_s - T_\infty)/\mu^2$

Pr = Prandtl number $\equiv c\mu/k$

d = Diameter of smoldering element

h = heat transfer coefficient

k = thermal conductivity

ρ = density

g = gravity constant

β = coefficient of thermal expansion

μ = viscosity

c = specific heat

and all the properties are calculated at an average temperature between the surface and ambient temperatures.

By assuming unit Lewis number (i.e., Prandtl number = Schmidt number), the mass and thermal boundary layers are assumed to be the same. Details on the justification behind the choice of eq. (3.2.16) are given in Appendix 3.4.

3.2.3 Energy Balance

In the previous section, taking into consideration kinetics and diffusion, the reaction rate was determined, and is given by eqs. (3.2.7) to (3.2.10). The energy generated (q in cal/cm^2-s)is then given by:

$$q = r \times Q \qquad (3.2.17)$$

where:

Q = heat of combustion, cal/g of char

Assuming a heat of combustion of 7700 cal/g of char [3.21]*, the energy generated† is illustrated in Fig. 3.2.3 as a function of temperature for a specified environment (X_{O_2} = 0.21 and P_{O_2} = 15.7 cm Hg; namely, standard atmospheric conditions). Note that in the low temperature range, the energy generated merges with the prediction for the kinetics-limited regime (according to eqs. (3.2.14)and (3.2.17)) and in the high temperature range, it merges with that of the diffusion-limited regime (according to eqs. (3.2.15) and (3.2.17)). The transition from one regime to another is abrupt, (i.e., within a temperature interval of only about 200°K), and the energy generated in the mixed regime is only slightly different from that generated in the two other regimes. The dependence on temperature is strong and weak for the kinetics and the diffusion-limited regimes, respectively.

Part of this generated energy is lost to the surroundings by radiation and free convection, and part is transferred by forward

---

* This assumes carbon-oxidation to carbon dioxide, which is substantiated by the measurements of Parker and Hottel [3.16] taken for temperature and air flow covering those of this study. (Note that the air flow in this study is due to free convection).

† The kinetic parameters used in this calculation are given in Appendix 3.6

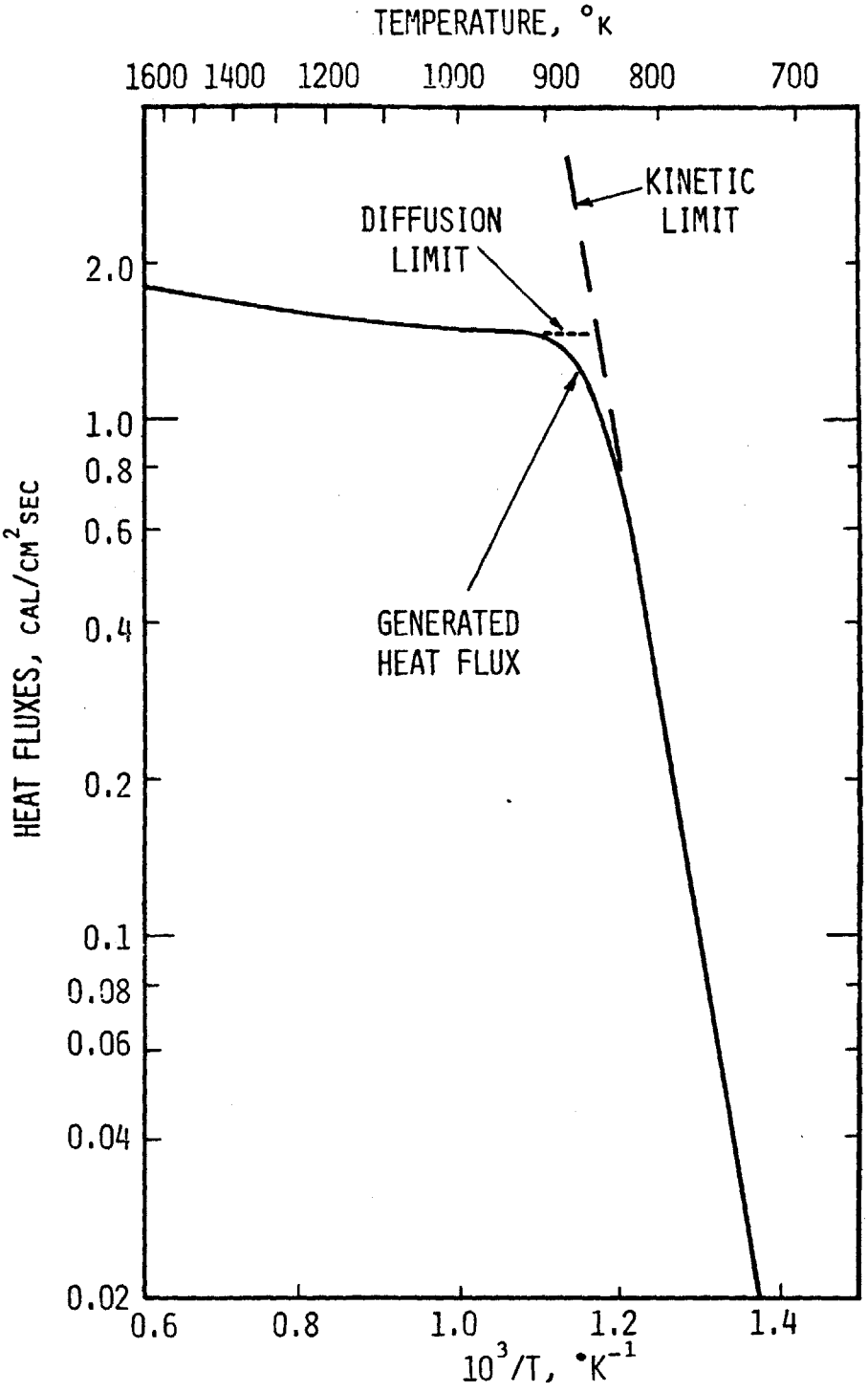


FIGURE 3.2.3 Heat Flux Generated by Char-Oxidation Reaction versus Temperature for Ambient Oxygen Mole Fraction = 0.21 and Partial Pressure = 15.7 cm Hg

conduction to the pyrolysis zone and by backward conduction to the semi-burnt char and ash, as illustrated in Fig. 3.2.4. To make a balance of these energy rates, it was necessary to make the following assumptions:

(1) The reaction zone length is equal to the yarn diameter. This is plausible from inspection of Fig. 2.4.8 which gives the measured reaction zone length (as defined in section 2.4.2) for the various conditions tested. Note that this length varies only by about $\pm$ 30% from the yarn diameter.

(2) The temperature is uniform in the char-oxidation zone. This assumption can be relaxed by solving the heat diffusion equation in the char zone, as was done for the case of pyrolysis. This is more difficult, however, because the non-linear terms of reaction and radiative transfer may not be assumed negligible in this zone as was done in the pyrolysis zone.

(3) The energy rates of conduction to the cellulose and to the char are qual (for want of any better estimates). Clearly, it is difficult to estimate the fraction conducted to the char because its porosity is not known and varies for each environmental condition. However, the assumption seems plausible because the factors determing the two conductive heat transfer rates are such that they might just be equal. Namely, the temperature gradients at both sides are about the same for most of experiments, see Fig. 2.3.2; the thermal conductivity of the char is much higher than that of cellulose while its porosity is much lower. (Note

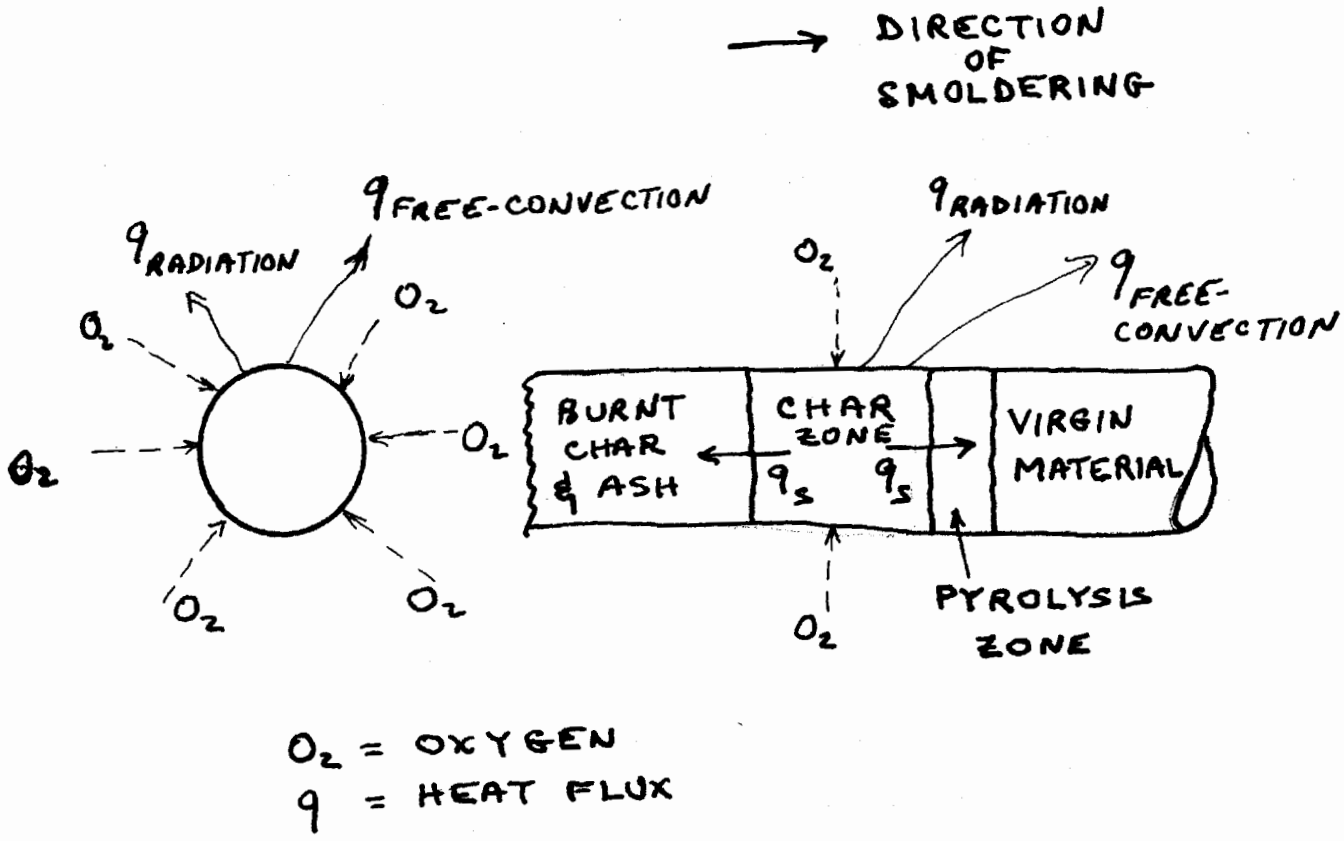


FIGURE 3.2.4 Schematic for the Energy Balance over the Smoldering Element

that: porosity = 1 - solidity, and the solidity determines the area for conductive heat transfer).

Using these assumptions, the heat losses are subtracted from the energy generated by char-oxidation to yield the feedback heat flux (q_s) according to the following equation:

$$q_s \pi \frac{d^2}{4} = \frac{1}{2} \left\{ \pi d^2 \left[q - \varepsilon \sigma T_s^4 - h(T_s - T_\infty) \right] \right\} \qquad (3.2.18)$$

where q = energy generated given by eq. (3.2.17)

ε = char emissivity, taken to be 0.9 [3.23]

σ = Stefan-Boltzmann constant

h = free-convection coefficient given by eq. (3.2.16)

d = smoldering element diameter

Note that heat is generated at and lost (by radiation and convection) from the circumferential area of the smoldering element. However, heat is conducted to the virgin material through the cross-sectional area (see Fig. 2.3.4). The factor of half in eq. (3.2.18) accounts for the conductive losses to the burnt char and ash (see assumption (3)). The properties used in eq. (3.2.18) are listed in Appendix 3.6.

The generated heat flux (eq. (3.2.17)) and the feedback heat flux into the surface (eq. (3.2.18)) are calculated* as functions of temperature for various environmental parameters. An example of these two heat fluxes is illustrated in Fig. 3.2.5 for $X_{o_2} = 0.21$ and $P_{o_2} = 15.7$ cm Hg, see

---

* As listing of the Computer Program used for these calculations is given in Appendix 3.5.

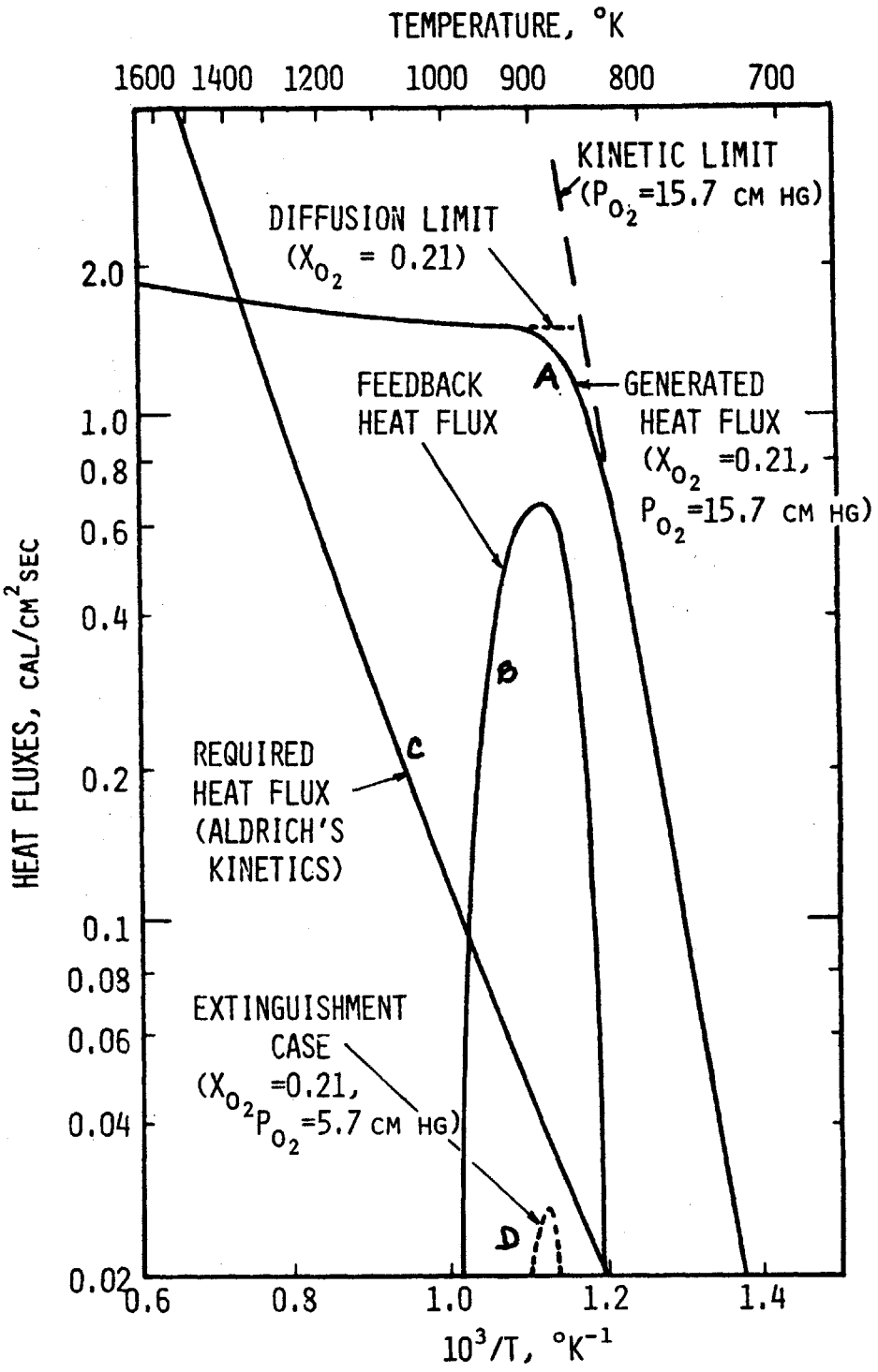


FIGURE 3.2.5 Balance of Heat Fluxes versus Temperature

curve A and B. The heat flux required for pyrolysis as determined in section 3.1 (and illustrated in Fig. 3.1.8) is also plotted in Fig. 3.2.5 (curve C). Clearly, the intersection point between required heat flux and feedback heat flux into the surface determines the solution of the system. Note that in general two intersections are possible: one at low temperature and one at high temperature. The character of these solutions is discussed below:

(1) The solution at low temperature is unstable. By inspection of Fig. 3.2.5, one observes that at this point of intersection, if the temperature is perturbed the system will move in the direction of perturbation. For example, if the temperature is decreased slightly, the heat flux generated will be lower than that required. Thus, the temperature will decrease further, leading eventually to a decay of the reaction. However, if the temperature is increased slightly, the system will move to the second point of intersection (at higher temperature) where the solution is stable. The first intersection point seems to specify an "initiation temperature" to which a material has to be raised so that smoldering occurs, a concept similar to the "ignition temperature" in flaming combustion.

(2) The solution at high temperature is stable as can be shown by the converse of the above arguments.

(3) The point of tangency between curves B and C determines a natural extinguishment limit. Because the curve of energy

generated (Λ) is determined at each combination of oxygen partial pressure and mole fraction, the point of tangency will occur at critical values of these combinations, for a constant C curve. At other than these critical values, the result is (a) two intersections yielding a steady smoldering solution as discussed above, or (b) the feedback heat flux will be lower than that required at any temperature, yielding extinguishment (see curve D).

A comparison of these predictions with experimental results is presented in the following section.

3.2.4 Comparison of Theory and Experiment

The purpose of this section is two-fold: firstly, to verify the validity of the char-oxidation model developed in the previous sections, and secondly, to determine the overall kinetic parameters appropriate for this study.

Because of the coupling between the char-oxidation zone and the pyrolysis zone, the char reaction rate calculated in the previous section can not be measured directly under smoldering conditions*. Thus, one must resort to testing the model's other predictions with experimental results. Because of the uncertainty in the kinetic parameters, a qualitative agreement between theory and experiment will be adequate. Then, by matching theory and experiments, the appropriate overall kinetic parameters are determined.

---

* Clearly, if a rate of mass loss is measured, one cannot differentiate whether it is due to char-oxidation or to pyrolysis.

The main predictions of the model are the following:

1. The existence of an "initiation" temperature where run-away exothermic reactions occur.
2. The characteristics of steady smoldering, namely, the speed temperature and heat flux at the front.
3. The existence of an extinguishment limit.
4. The dependence of (1), (2) and (3) on fuel and environmental characteristics.

To verify experimentally the existence of an "initiation" temperature and to measure it are formidable tasks*. Thus, it was not attempted in this study. Furthermore, because the extinguishment limit occurs at lower ratios of the diffusion to chemical times than steady smoldering, it is expected that the results of the former are more sensitive to the choice of the kinetic parameters than the results of the latter**. Thus, the extinguishment results are chosen to verify the char-oxidation model and to determine the overall kinetic parameters appropriate for this study. Then, these results are used (in the following section) in conjunction with those obtained in the pyrolydis study to predict the characteristics of steady smoldering. Finally, the measurements at steady smoldering are used to verify the overall validity of the model.

---

* In Fig. 3.2.5, this temperature is found to be 830°K. Kinbara [1.9] has measured smoldering initiation temperatures (in an oven) of $\sim$ 680°K and 730°K for standard atmospheric conditions and two cellulosic fuel elements. The large difference between the three temperatures may be due to difference in the fuel characteristics.

** The ratio of the diffusion to chemical times (i.e., the parameter ξ as defined by eq. (3.2.9) in section 3.2.2) for the predicted extinguishment limits is found to be a constant of about three. This indicates that at this limit kinetic and diffusion considerations are of the same order. (The constancy of ξ at extinguishment is not understood.) For the range of steady smoldering in this study, ξ varies from 3 to 2000.

This approach avoids curve-fitting the steady smoldering results by arbitrary choice of the kinetic parameters.

By performing the energy balance presented in the previous section, the critical combinations of oxygen mole fractions and partial pressures at the extinguishment limit,are determined, as illustrated in Fig. 2.4.1, section 2.4.1, for specific values of the kinetic parameters. Note that for faster kinetics (namely for larger frequency factor), the extinguishment limit is reached at lower oxygen partial pressure for any constant oxygen mole fraction, or vice versa. This is plausible because with faster kinetics, the energy generated is larger and less oxygen is needed to sustain smoldering. Fig. 2.4.1 maps also the experimental results for steady smoldering and the transitions to flaming or extinguishment. Note the qualitative agreement between theory and experiment for the dependence of the extinguishment limit on the environmental parameters. Namely, as one parameter increases, the other has to decrease to remain at the extinguishment limit.

To determine the appropriate kinetics, the extinguishment experimental data are matched with the theoretical predictions on the basis of specific kinetic parameters. Only the frequency factor was varied because the data in the literature showed a larger uncertainty in this parameter than in the activation energy*. Note that the value of $10^8 \pm 100\%$ sec.$^{-1}$ for the frequency factor (with an activation energy of 44 Kcal/mole) matches fairly well the experimental data. Further refinement of this matching is not attempted given the uncertainties in the heat losses and in the

---

* See the upper and lower kinetic bounds reported in the literature (eq. (3.2.1) and (3.2.2), section 3.2.1). For the temperature range of interest, the reported uncertainties in the frequency factor and in the activation energy lead to variations in the reaction rate of four orders of magnitude and a factor of three, respectively. Thus, the uncertainties in the reported frequency factor are more significant than those in the activation energy.

thermophysical properties of the fuel.

It is of note that the overall kinetic parameters determined by matching theory and experiment are "apparent" and not "true" kinetics, as discussed in section 3.2.1. They are "apparent" because they are calculated on the basis of the external area of a solid cylinder and not the internal area of the porous char under consideration. However, because theory and experiment are intentionally matched, the effect of porosity is included in the kinetic parameters determined above.

It is of note that the experimental results of Fig. 2.4.1 suggest that the transition to flaming is also governed by critical combinations of oxygen mole fractions and partial pressures. It is recommended that this observed trend be investigated further.

In conclusion, the qualitative agreement between the predicted and observed extinguishment limits suggest that the model is valid for the purposes of studying smoldering. Furthermore, by matching theory and experiment, the overall apparent kinetic parameters appropriate for this study can be determined.

3.3 SMOLDERING BEHAVIOR: THEORY AND EXPERIMENT

The energy balance described in the previous section, matching the heat flux at the interface between the pyrolysis zone and the char-oxidation zone (incorporating reasonable losses), is now performed on the basis of the overall kinetic parameters determined in sections 3.1.4 and 3.2.4. This determines the speed and the interface temperature as functions of the environmental parameters and allows direct comparison with experiment.

Comparison of theory and experiment for steady smoldering speed and temperature* as functions of oxygen mole fraction at its constant partial pressure, and vice versa, are given in Figs. 3.3.1 and 3.3.2. Note the good agreement between theory and experiment in determining extinguishment. This is not surprising because it was built-in to determine the appropriate overall kinetic parameters for char-oxidation, as presented in section 3.2.4. However, the general agreement between theory and experiment for the dependence of steady smoldering speeds and temperatures* on the environmental parameters is very remarkable. It indicates that the mechanism proposed in this thesis incorporates the essential features of smoldering.

The discussion presented below for the results of speed and temperature apply to both theory and experiment. Fig. 3.3.1 illustrates that

---

* For the theory, the interface temperature is used. For the experiments, it has been shown in section 3.1.4 that the appropriate temperature is somewhere between the maximum and the inflection point. For want of an exact estimate of the interface temperature, and because determining the maximum temperature is straight forward, the latter has been used in the comparisons with theory.

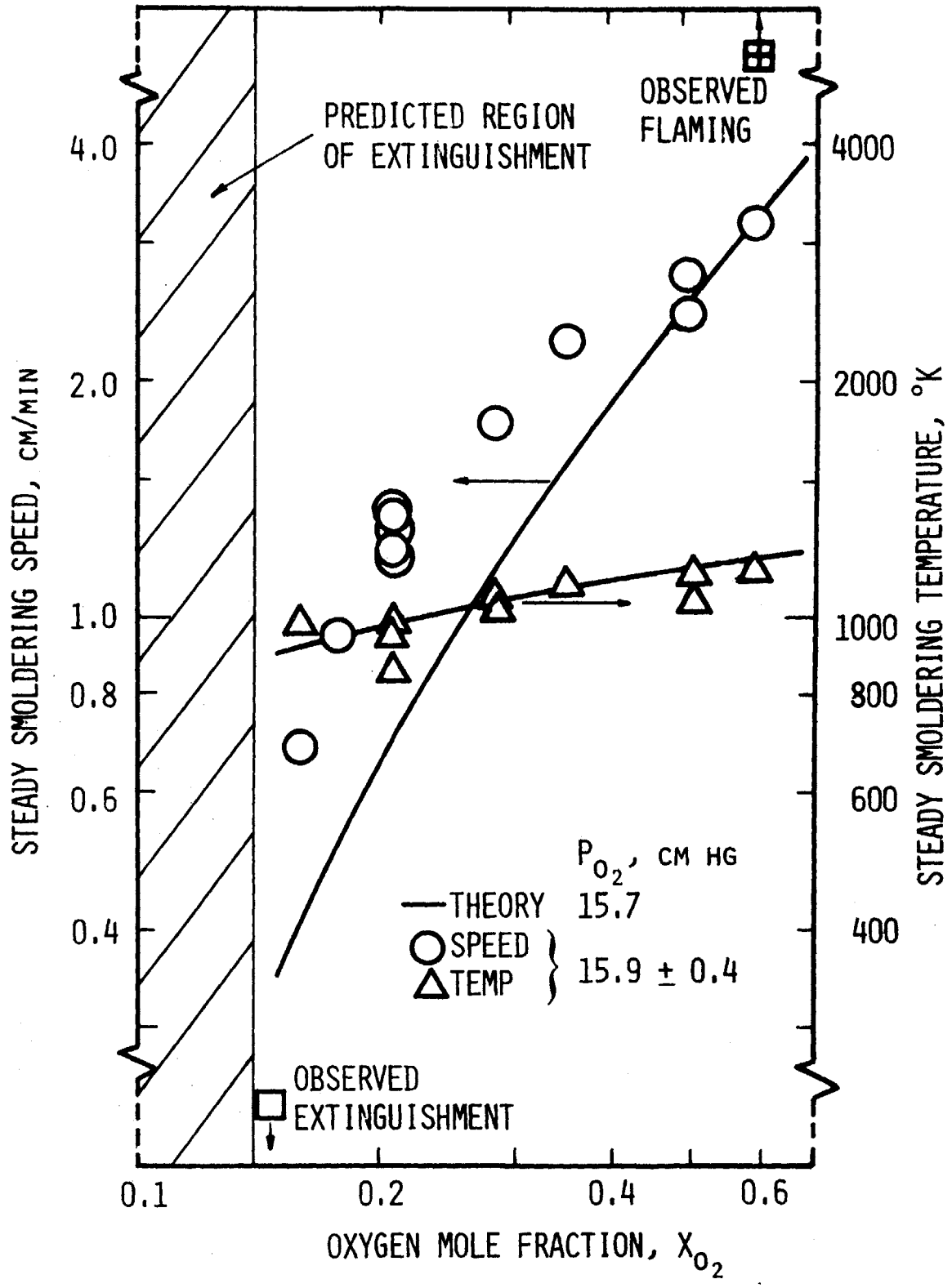


FIGURE 3.3.1 Comparison of Theory and Experiment for the Steady Smoldering Speed and Temperature versus Ambient Oxygen Mole Fraction at a Constant Oxygen Partial Pressure, Cellulosic Samples are Mounted Horizontally

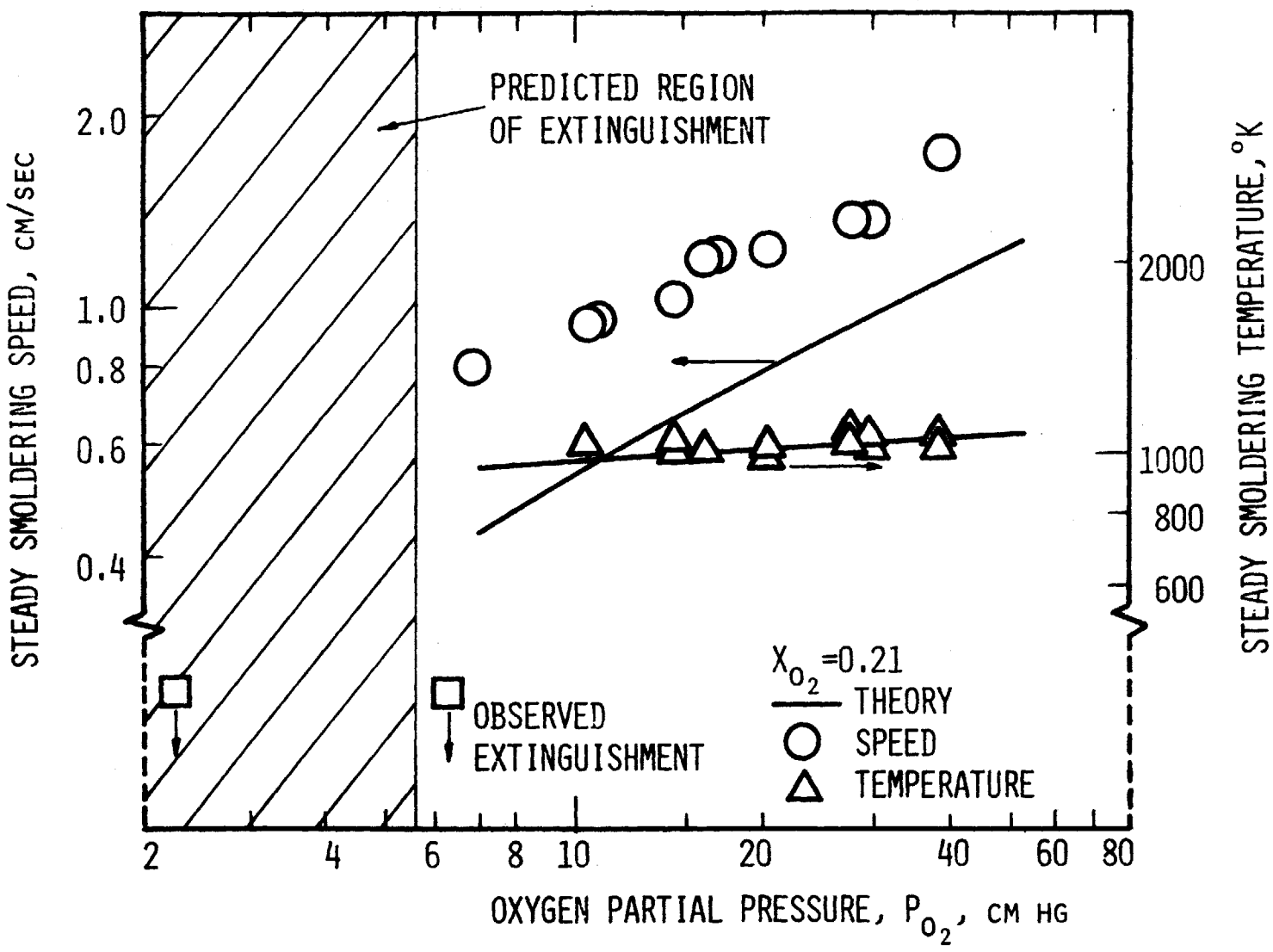


FIGURE 3.3.2 Comparison of Theory and Experiment for the Steady Smoldering Speed and Temperature versus Ambient Oxygen Partial Pressure at a Constant Oxygen Mole Fraction, Cellulosic Samples are Mounted Horizontally

the speed and the temperature are respectively strong and weak functions of the ambient oxygen mole fraction, when its partial pressure is held constant. Should diffusion be important one can interpret these results as follows. Increasing the mole fraction would increase the oxygen flux to the smoldering surface as indicated by equation (3.2.6) in section 3.2.2. This enhances the char-oxidation reaction and the feedback heat flux into the virgin material. An increase in this heat flux will result in a faster speed and a higher temperature as described in the pyrolysis study of section 3.1 (see Figs 3.1.7 and 3.1.8).

It is of note that an increase in the mole fraction of oxygen while holding its partial pressure constant, requires a decrease in the mixture pressure. This reduces the Grashof Number and increases the boundary layer thickness, as illustrated in Fig. 3.3.3. Thus, the oxygen concentration gradient at the surface is decreased, reducing the flux to the surface, according to equation (3.2.6). However, the dependence of the boundary layer thickness on the pressure (and in this case on the oxygen mole fraction) is weak, see eq. (3.2.16) and Appendix 3.4. Thus, the net effect of an increase in mole fraction is still an increase in oxygen flux to the surface despite the increase in boundary layer thickness.

However, when the oxygen mole fraction is held constant, the weak effect of the boundary layer thickness on the oxygen flux to the surface becomes noticeable. This is illustrated in Fig. 3.3.2, where the speed increases (though weakly) with increase in oxygen partial pressure, i.e., with decrease in boundary layer thickness or increase in the oxygen flux to the surface. Note that the corresponding increase in temperature is negligible.

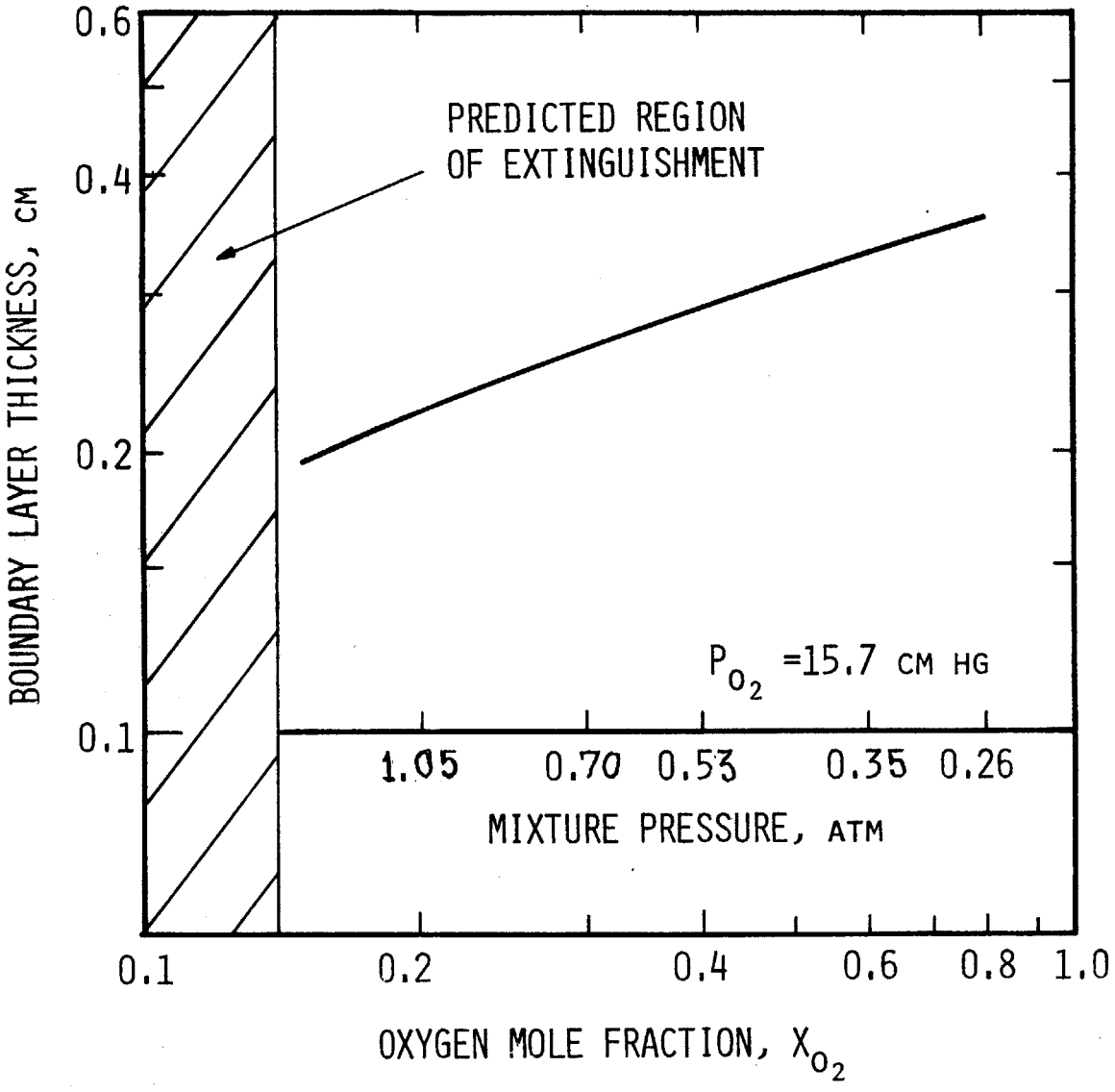


FIGURE 3.3.3 Calculated Boundary Layer Thickness versus Oxygen Mole Fraction or Mixture Pressure at a Constant Oxygen Partial Pressure, P_{O_2}

Thus, one can interpret the dependence of the steady smoldering speed and temperature on the oxygen mole fractionand partial pressure by examining the variations of the oxygen flux to the surface (eq. (3.2.6)) with these parameters. This suggests that oxygen diffusion plays an important role in smoldering. Thus, a large ratio for the diffusion to the kinetic time or resistance*, ξ (as defined by eq. (3.2.9), section 3.2.2) is expected. The values of ξ for the conditions of this study are calculated as function of oxygen mole fraction and partial pressures, as illustrated respectively in Figs. 3.3.4 and 3.3.5. These values vary from 6 to 3000 suggesting that the regime under study varies from mixed (where kinetics and diffusion are important) to diffusion-limited, being closer to the latter. However, one must note that there may be other smoldering cases**, where the char resulting from pyrolysis is not sufficiently reactive; then the slow kinetics may become more important than diffusion. In this connection, it is important to note that when an air flow is imposed on a smoldering element, smoldering becomes more vigorous as the air velocity increases. This result can be also interpreted by examining the oxygen flux to the smoldering element (eq. (3.2.6)). As the air velocity increases, the forced-convection boundary layer decreases, yielding a larger ocygen flux and a faster char-oxidation reaction. This result suggests further that diffusion plays an important role in smoldering.

---

* Because the two processes are in series, the slower one limits the overall rate. Thus, when $\xi \rightarrow$ zero, the reaction is kinetics-limited and when $\xi \rightarrow$ infinity, it is diffusion-limited, as discussed in section 3.2.2.

** For example, the smoldering of materials other than cellulose or cellulose with chemical additives that reduce the char reactivity.

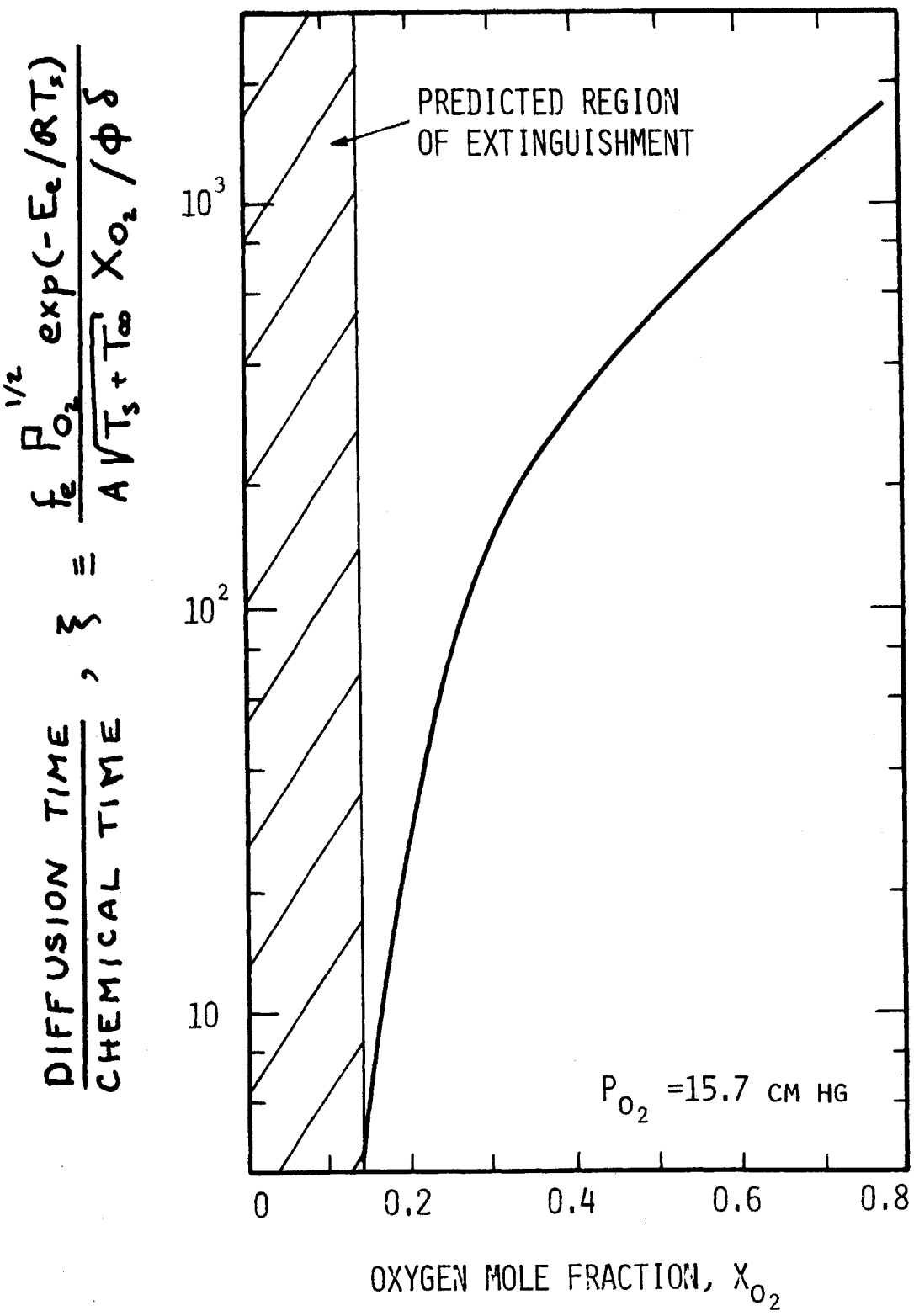


FIGURE 3.3.4 Predicted Ratio of Diffusion to Chemical Times versus Ambient Oxygen Mole Fraction at a Constant Oxygen Partial Pressure, P_{O_2}

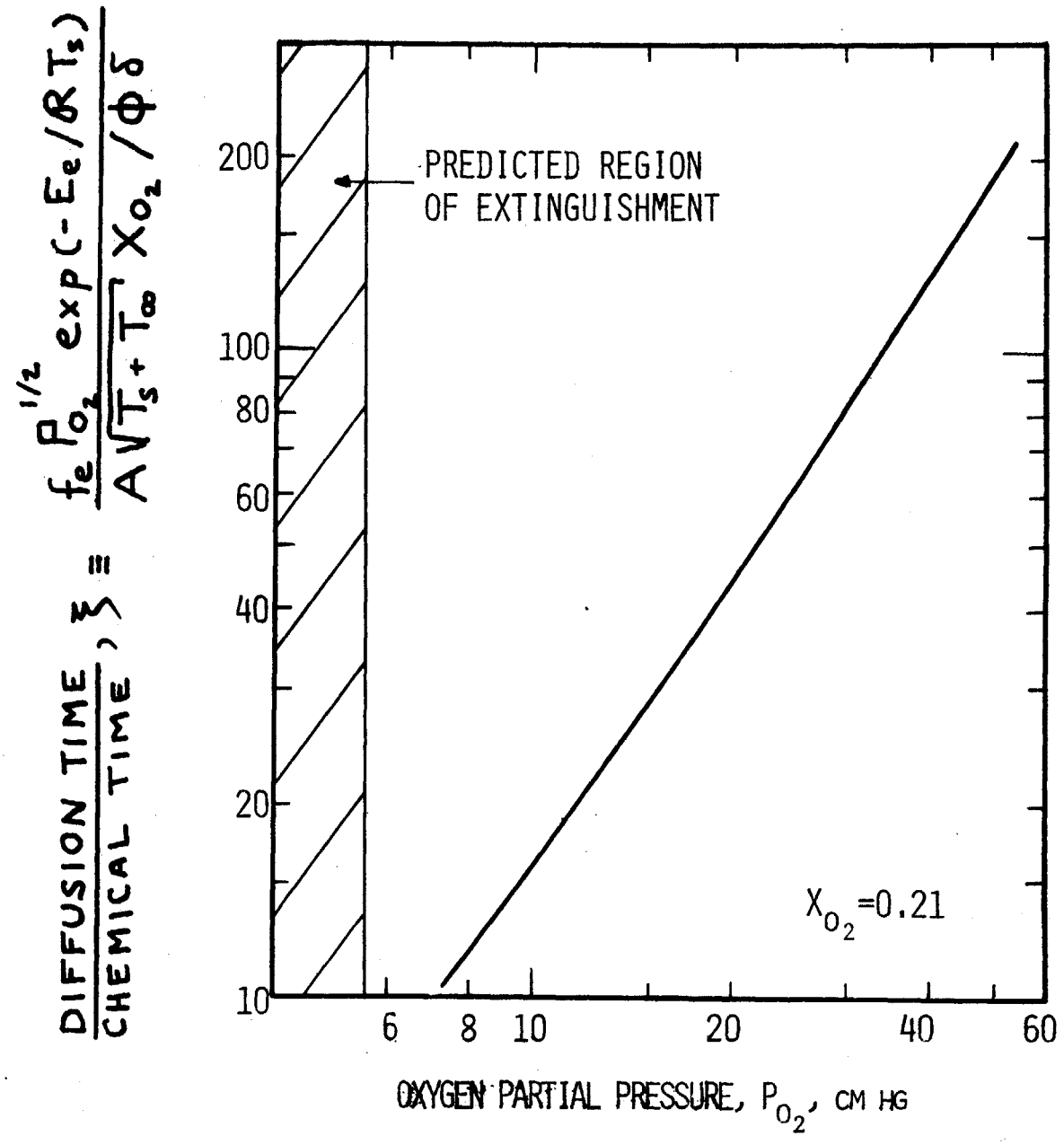


FIGURE 3.3.5 Predicted Ratio of Diffusion to Chemical Times versus Ambient Oxygen Partial Pressure at a Constant Oxygen Mole Fraction, X_{O_2}

In the case under study, steady smoldering is found to occur in the mixed and diffusion-limited regimes being even closer to the latter one. Thus, the predictions of speed and temperature for steady smoldering may not be very sensitive to the char-oxidation kinetics used in the calculations. However, these kinetics were needed to calculate the ratio of diffusion to chemical times (ξ) on the basis of which, the relative role of the two processes was determined. Thus, it was still necessary to determine the appropriate kinetics for this study as presented in section 3.2.4.

The finding, that smoldering is in a mixed regime and is closer to the diffusion limit has interesting practical applications. One can estimate an upper bound for the smoldering rate (useful for safety considerations) by assuming the process to be diffusion-limited. This bound can be obtained simply because the non-linearity of the kinetics are avoided, and the answer would not be too far off the exact one.

It is of note that the use of Emmons' kinetics instead of Aldrich's yields results about five times higher for the speed and about 20% lower for the temperature*. This is plausible because with Emmons' faster kinetics, the decomposition of cellulose into char and volatiles can be completed at a lower temperature. Furthermore, energy conservation requires a faster speed with a lower temperature as discussed in section 3.1.3.

---

* These values were obtained for some variations of the model presented in this thesis (namely, that with a constant boundary layer thickness). It is believed that the effects of using Emmons' kinetics will be essentially the same if the calculations were repeated on this model.

The preceding paragraphs presented the agreement between the main features of theory and experiment indicating the overall validity of the model developed in this study. It should be noted however, that the predicted numerical values for the smoldering speed are lower* than the measured values, as illustrated in Figs. 3.3.1 and 3.3.2. This may be due to an overestimation of the heat losses from the circumferential area because the theory assumes that the yarn surface temperature is the same as its inside temperature. In fact, the surface temperature is lower as presented in Appendix 3.2. Furthermore, the difference between the surface and inside temperatures becomes smaller at higher mole fraction (see Appendix 3.2). Thus, the overestimation of the heat-losses is expected to be less at high mole fraction, yielding a speed closer to the measured value. This is in fact observed in Fig. 3.3.1. A similar effect is not observed in Fig. 3.3.2 because the temperature changes little with oxygen partial pressure, as noted earlier.

Overestimation of the heat losses causes also errors in predicting the temperature. However, they are small and not very apparent in Figs. 3.3.1 and 3.3.2. This is plausible because small variations in temperature correspond to large variations in smoldering speed, due to the strong dependency of the pyrolysis kinetics on the temperature, see Fig. 3.1.9.

---

* By a maximum of about 90% which is still reasonable given the uncertainties in the material thermophysical properties, in the heat losses and in the rough estimates of the overall kinetic parameters (as obtained in this study).

In this connection, it is interesting to note that the losses from the char zone are mainly by radiation. Calculations show that radiation is two to eight times larger than natural convection for the range of this study.

3.4 CONCLUSIONS

On the basis of the agreement between theory and experiments, it can be concluded that the mechanism proposed in this thesis can interpret the main features of smoldering in cellulosic materials. This mechanism postulated an overall cellulose pyrolysis scheme leading to the formation of char and volatiles and subsequent char-oxidation yielding the energy needed to sustain pyrolysis.

The main features of smoldering determined in this study are as follows:

1. The existence of a region of steady-smoldering and an extinguishment limit, depending on the environment (namely the oxygen partial pressure and mole fraction).
2. In the region of steady-smoldering, the speed depends strongly on the environmental oxygen mole fraction and weakly on its partial pressure; and the corresponding dependencies of the maximum temperature in the smoldering zone are weak and negligible. Furthermore, there is a unique temperature-speed relationship governed by the fuel pyrolysis kinetics and thermophysical properties (related to conductive heat transfer within the fuel).

It is also concluded that for the purposes of studying smoldering, the use of overall kinetic schemes for cellulose pyrolysis and for char-oxidation is adequate. And, if appropriate kinetics are unavailable, they can be determined by critical matchings of theoretical predictions with experimental results. In this study, the pyrolysis kinetics were determined by matching the measured temperature-speed relationship,

at any environment, with theoretical predictions on the basis of specific kinetic parameters. Furthermore, the char-oxidation kinetics were determined by matching the observed extinguishment limit with theoretical predictions on the basis of specific kinetic parameters, combined with the pyrolysis kinetics determined above.

Finally, a closed-form expression yields the smoldering speed as functions of the imposed heat flux or the surface temperature, and the kinetics and thermophysical properties of the system.

RECOMMENDATIONS

The following problems are recommended for further study:

1. To incorporate volatiles-oxygen reactions in the model proposed in this thesis, so as to predict the observed spontaneous and induced transitions to flaming

2. To further evaluate the role of oxygen diffusion in smoldering by varying the transport properties of the inert diluent in the environment, and by comparing the measurements with the predictions of the model proposed in this thesis

3. To analyze species and heat diffusion in a free-convective boundary layer around a surface reacting heterogeneously.

4. To determine by theory and experiment the role of oxygen diffusion in the pores of the char under the conditions of smoldering.

5. To determine by theory and experiment the mechanism by which ambient oxygen enhances cellulose pyrolysis: whether by catalysis or by providing additional heat due to char-oxidation or by both processes.

6. To investigate by theory and experiment the dispersion and accumulation of the products of smoldering fires in confined enclosures and the ensueing hazards such as transitions to flaming, flash overs and explosions.

REFERENCES

Chapter I

1.1 National Fire Protection Agency, "Handbook of Fire Prevention", 13th ed., NFPA, Boston, Ma., 1969, pp. 1-2 to 1-24.

1.2 Twelfth Symposium (International) on Combustion, The Combustion Institute, 1969, Section on "Flame Spread and Mass Fires", pp. 215-276.

1.3 Thirteenth Symposium (International) on Combustion, The Combustion Institute, 1971, section on "Fire Spread", pp. 917-994.

1.4 Fifteenth Symposium (International) on Combustion, The Combustion Institute, 1975, Section on "Fire and Explosion Research and Safety", pp. 103-350.

1.5 National Fire Protection Association, "Los Angeles Fire Department Tests -- Fire Detection Systems in Dwellings". NFPA Quarterly, January, 1963, pp. 201-215.

1.6 Cohen, L. and Luft, N. W., "Combustion of Dust Layers in Still Air", Fuel, 34, London, 1955, pp. 154-161.

1.7 Palmer, K. N., "Smoldering Combustion in Dusts and Fibrous Materials", Combustion and Flame, Vol. 1, No. 2, 1957, pp. 129-154.

1.8 Egerton, Sir Alfred, et al., "The Mechanism of Smoldering of Cigarettes", Combustion and Flame, Vol. 7, No. 1, 1963, pp. 63-78.

1.9 Kinbara, T. et al., "Downward Propagation of Smoldering Combustion Through Solid Materials", Eleventh Symposium (Int.) on Combustion, The Combustion Inst.,Pittsburgh, Pa., 1967, pp. 525-531.

Chapter II

2.1 Fristrom, R. J. et al., "Fire Problems Research and Synthesis", The Johns Hopkins University, NSF/RANN meeting at Atlanta, Ga., May 28-29, 1974.

2.2 Moussa, N. A., Toong, T. Y., and Backer, S., "An Experimental Investigation of Flame-Spreading Mechanisms Over Textile Materials", Combustion Science and Technology, 1973, Vol. 8, pp. 165-175.

2.3 Ohlemiller, T. J., Rogers, F. E. and Summerfield, M., "Modeling the Generation of Toxic Gases by the Smoldering Combustion of Polyurethanes", Princeton University, Second Quarterly Progress Report to the National Bureau of Standards, Feb. 1975.

2.4 Backer, S., Tesoro, G., Toong, T. Y., and Moussa, N.A., Textile Fabric Flammability, MIT Press, Cambridge, Mass., in press.

Chapter III

3.1 Aldrich, D. C., "Kinetics of Cellulose Pyrolysis", Dept. of Chem. Eng. D. Sc. Thesis, M.I.T., Feb. 1974.

3.2 Shivadev, U. K., and Emmons, H. W., "Thermal Degradation and Spontaneous Ignition of Paper Sheets in Air by Irradiation ," Combustion and Flame, 22 (2), April 1974, pp. 223-236.

3.3 Kilzer, F. T. and Broido, A., "Speculations on the Nature of Cellulose Pyrolysis", Pyrodynamics, 2, 1965, pp. 151-163.

3.4 Roberts, A. F., "The Kinetic Behavior of Intermediate Compounds During the Pyrolysis of Cellulose," Journal of Applied Polymer Science, Vol. 14, 1970.

3.5 Roberts, A. F., "Ultimate Analysis of Partially Decomposed Wood Samples," Combustion and Flame, 8, p. 345, 1964.

3.6 Broido, A., and Nelson, M. A., "Char Yield on Pyrolysis of Cellulose", Combustion and Flame, 24, pp. 263-268, 1975.

3.7 Panton, R. L., and Rittmen, J. G., "Pyrolysis of a Slab of Porous Material", Thirteenth Symposium (International) on Combustion, The Combustion Institute, 1973, pp. 881-891.

3.8 Handbook of Fire Protection, 13th ed., published by the National Fire Protection Association, Boston, Massachusetts, 1969, section 4, chapter III.

3.9 McCarter, R. J., "The Pyrolysis of Cellulose at Rates Approaching Those in Burning", Textile Research Journal , V. 42, No. 12, Dec. 1972.

3.10 Tang, W., in Differential Thermal Analysis by MacKenzie, R. C., ed. Academic Press, London, 1972, chapter 45.

3.11 Moussa, N. A., Garris, C. A. and Toong, T. Y., "Early Behavior and Detection of Fire", Third Quarterly Progress Report submitted to the National Bureau of Standards, September, 1974.

3.12 Mulcahy, M. F. R., and Smith, I. W., "Kinetics of Combustion of Pulverized Fuel: A Review of Theory and Experiment", Rev. of Pure and Appl. Chem., 19, p 81, 1969.

3.13 Scala, Sinclair M., "The Ablation of Graphite in Dissociated Air", Pt. 1: Theory, Technical Information Series No. R62 SD72, Missile Space Division, General Electric Co., Sept. 1962.

3.14 Maahs, H. G., "Oxidation of Carbon at High Temperatures: Reaction-Rate Control on Transport Control", NASA TN D-6310, 1971.

3.15 Tu, C. M., Davis, H. and Hottel, H. C., "Combustion Rate of Carbon - Combustion of Spheres in Flowing Gas Streams", Industrial and Engineering Chemistry, Vol. 26, No. 7, pp. 749 - 757.

3.16 Parker, A. S., and Hottel, H. C., "Combustion Rate of Carbon - Study of Gas-film Structure by Microsampling", Industrial and Engineering Chemistry, Nov. 1936, pp. 1334 - 1341.

3.17 Howard, J. B., Class Notes

3.18 Appleton, J. P., "Soot Oxidation Kinetics at Combustion Temperatures", presented at the AGARD Propulsion and Energetics Panel 41st Meeting, London, England, April 1973.

3.19 Wiltshire, L. L., et. al., "Carbon Monoxide Production in Charcoal Briquette Fires", NOL TR 71-104, July 1971.

3.20 Rohsenow, W. M. and Choi, H. Y., Heat, Mass, and Momentum Transfer, Prentice-Hall, Inc., N. J., 1961.

3.21 Mc Adams, W. H., Heat Transmission, 2nd ed., Mc Graw-Hill, Inc., N.Y., 1942.

3.22 Lewis, B., and von Elbe, G., Combustion, Flames and Explosions of Gases, 2nd ed., Academic Press, 1961.

3.23 Hottel, H. C., and Sarofim, A. F., Radiative Transfer, Mc Graw-Hill, N.Y., 1967.

3.24 Frank-kamenetskii, D. A., Diffusion and Heat Transfer in Chemical Kinetics, Plenum Press, N.Y., 1969

3.25 Kreith, F., Principles of Heat Transfer, 2d ed., International Textbook, Scranton., Penn., 1969.

3.26 Bird, R. B., Steward, W. E., and Lightfoot, E. N., Transport Phenomena, John Wiley & Sons, Inc., N.Y., 1960.

3.27 Hermann,r., NACA, tm 1366, 1954.

APPENDICES

Appendix 2.1

EXPLORATORY EXPERIMENTS ON SMOLDERING

Because of the little knowledge on smoldering at the onset of this investigation, exploratory experiments were conducted to identify smoldering behaviors and test materials appropriate for further in-depth study. The results presented in this section are mainly qualitative in nature and there is no attempt to be rigorous or complete. (For brevity only the main features of each experiment are reported.) Still, these results represent a large body of new and useful information on smoldering.

Various materials were tested including cellulose, wood, nylon, wool, polyurethane and polyester-cotton blends (in the following compositions 50%-50% and 65%-35%), in various commercial forms such as fabrics, paddings, papers, piles of papers, threads, yarns, sawdust beds and foams. Tests were also performed on samples made of pure (fibrous and powder) α-cellulose compacted into cylindrical and dust-tray forms. Smoldering was initiated using a hot wire, a cigarette or a flame.

An early and unexpected discovery was that only some of these tested materials smoldered (even though they are all known to be otherwise combustible) and that an even fewer number did self-sustain smoldering. For the materials tested and for otherwise identical conditions, smoldering was observed for char-forming polymers (such as cellulose, wool and polyurethane) and not for non-char forming polymers (such as nylon, polyester, polystyrene, and cotton/polyester blends)*.

---

* See section 2.6 for the importance of char in smoldering.

Smoldering was characterized by pyrolysis, charring and glowing (sometimes erratic) without the formation of a flame. Grayish pyrolysis gases are generated and diffuse into the surrounding air. As described below, this process may or may not sustain itself -- after the removal of the heat source. Two distinctly different behaviors are observed (for material placed in a horizontal plane and with minimum external quenching):

1. A steady smoldering until complete consumption of the sample (as for cellulosic yarns, twines and threads varying in diameters from 1.3 to 8.6 mm).

2. A transient smoldering followed by extinguishment before the consumption of the sample (as for fabrics, papers, filter papers varying in thicknesses from 0.13 to 2.5 mm).

For the materials exhibiting transient smoldering, blowing air on the smoldering zone or changing the sample orientation in the gravity field did not lead to a self-sustained smoldering. However, increasing the thickness of a material, and varying the heat flux to the material from the external source led to significant changes as described below:

a. A cellulosic filter paper and a felt wool (with thickness of 0.94 and 4 mm, respectively) exhibited transient smoldering. However, when these sheets are rolled into solid cylinders (of 1.5 and 3 cm, respectively), they self-sustained smoldering when ignited.

b. A self-sustained smoldering was observed when a cigarette was "buried" in a block of polyurethane, but was not obtained under the other heating conditions used in this section.

c. Increasing the thickness of paper towel piles led to longer transient smoldering.

It was also noted that the addition of a little bleach, to a material, inhibited the sustainment of smoldering. Some of the tested commercial fuels could have been bleached during manufacturing. This might explain why they did not self-sustain smoldering, as reported above.

The very preliminary experiments presented above suggest the following:

1. Only char-forming polymers self-sustain smoldering.
2. The sustainment of smoldering is apparently very sensitive (when compared to that of flaming) to the heating rate from the external ignition source, the sample thickness and geometry, and the presence of bleach.

These experiments also identified elements that smoldered uniformly and repeatedly. These elements, namely cylindrical cellulosic yarns, were used for further in-depth study of smoldering.

Appendix 2.2

EXPERIMENTAL DATA ON THE EFFECTS OF ENVIRONMENT PRESSURE AND COMPOSITION

This is a listing of the experimental data obtained using the cotton yarn (dia = 0.86 cm, density = 0.06 $g.cm^3$) described in section 2.4. All Runs are in oxygen/nitrogen mixtures except for two runs in oxygen/Helium: Runs #54 and 67, as noted in the remark Column. The Remark Column specifies also if Flaming or Extinguishment occurred.

P = Mixture pressure, cm Hg

P_{O_2} = Oxygen partial pressure, cm Hg

T_s = Surface temperature, °K

E = Extinguishment

F = Flaming

X_{O_2} = Oxygen mole fraction

V = cm/min, ± 7%

$T_{i,2}$, $T_{i,1}$ = Temperature at center of yarn, °K, ± 7%

Run #	P cm Hg	X_{O_2} %	P_{O_2} cm Hg	V cm/min	T_s °K	$T_{i,1}$ °K	$T_{i,2}$ °K	REMARK
T1	76.	7.0	5.3	–	–	–	–	E } FIRST TRIAL RUNS
A2	75.7	21.	15.9	1.27	860	–	–	
T2	76.	14.1	10.7	–	–	–	–	E }
1.	76.4	19.0	14.5	0.91	–	–	–	
2	75.7	30.	23.	–	–	–	–	F
3	75.4	24.	18.1	1.43	–	–	–	
4	81.7	19.	15.5	1.08	–	–	–	
5	63.4	23.	14.3	1.27	–	–	–	
6	55.3	26.	14.4	1.44	–	–	–	
7	110.	13.1	14.4	–	–	–	–	E
8	34.6	42.	14.4	2.5	–	–	–	
9	76.0	42.	32.	–	–	–	–	F

Run #	P cm Hg	X_{O_2} %	P_{O_2} cm Hg	V cm/min	T_s °K	$T_{i,1}$ °K	$T_{i,2}$ °K	REMARK
10	90.1	16.0	14.4	0.79	–	–	–	
11	99.7	14.4	14.3	–	–	–	–	E
12	76.0	16.6	12.6	0.78	–	–	–	
13	55.3	19.3	10.6	0.86	–	–	–	
14	34.6	20.	7.0	–	–	–	–	E
14_a	35.1	20.	7.1	0.79	–	–	–	
15	34.5	30.	10.5	1.66	–	–	–	
16	76.9	21.	16.1	1.37	890	950	–	
17	142.	13.8	19.6	0.73	700	–	–	
18	76.8	21.	16.1	1.27	790	–	–	
19	142.	18.6	26.	1.23	850	–	–	

Run #	P cm Hg	X_{O_2} %	P_{O_2} cm Hg	V cm/min	T_s °K	$T_{i,1}$ °K	$T_{i,2}$ °K	REMARK
20	106.6	14.8	15.8	–	–	–	–	E
21	99.4	14.4	14.3	–	–	880	–	E
22	77.4	21.	16.3	1.23	780	980	–	
23	75.3	21.	15.8	1.34	770	860	–	
24	44.3	35.	15.5	2.3	–	1110	–	
25	26.	60.	15.7	3.2*	1110	1150	–	F
26	11.	95.	10.5	4.2*	–	1210	–	F
27	190.	11.1	21.	–	–	–	–	E
28	97.8	21.	21.	1.28	–	1010	970	
29	133.	21.	28.	1.40	–	1020	1050	
30	50.0	21.	10.5	0.96	–	1020	1040	

* This may be an unsteady speed because flaming eventually occured

Run #	P cm Hg	X_{O_2} %	P_{O_2} cm Hg	V cm/min	T_s °K	$T_{i,1}$ °K	$T_{i,2}$ °K	REMARK
31	142.	21.	30.	1.41	–	1040	1050	
32	69.0	21.	14.5	1.06	–	1040	1010	
33	185.	21.	39.	1.80	–	1010	1010	
34	13.7	80.	11.0	3.6	–	1180	–	
35	31.1	50.	15.6	2.4	–	1060	1140	
36	61.2	32.	19.4	2.1	–	1020	1180	
37	170.	12.4	21.	–	–	–	–	E
38	97.5	15.8	15.5	0.69	–	990	–	
39	56.0	28.	15.9	1.77	–	1040	1070	
40	–	–	–	–	–	–	–	
41	4.1	67.	2.8	2.1	–	1120	–	

Run #	P cm Hg	X_{O_2} %	P_{O_2} cm Hg	V cm/min	T_s °K	$T_{i,1}$ °K	$T_{i,2}$ °K	REMARK
42	20.	72.	14.4	–	–	–	–	F
43	31.7	49.	15.6	2.7	–	–	–	
44	86.7	18.1	15.7	0.99	–	–	–	
45	10.9	21.	2.3	–	–	–	–	E
46	51.5	21.	10.8	0.98	–	–	–	
47	32.7	21.	6.8	0.82	–	–	–	
48	30.	21.	6.2	–	–	–	–	E
59*	8.9	36.	3.2	1.30	–	1130	–	
60	7.9	35.	2.7	–	–	–	–	
63*	11.9	30.	3.6	1.08	–	–	–	

* Missing runs were conducted in helium/oxygen mixtures and can be found in a Master Thesis in preparation by Marcos Ortiz, Dept. of Mech. Eng., MIT.

Run #	P cm Hg	X_{O_2} %	P_{O_2} cm Hg	V cm/mm	T_s °K	$T_{i,1}$ °K	$T_{i,2}$ °K	REMARK
64	9.7	30.	2.9	0.97	–	–	–	
65	7.9	30.	2.3	–	–	–	–	E
54	35.4	36.	12.8	2.6	–	1180	–	HELIUM/ OXYGEN MIXTURES
67	48.6	41.	20.	2.9	–	1150	–	

Appendix 2.3

INVESTIGATION OF THE HAZARDS FROM SMOLDERING FIRES

This thesis focused on the study of the mechanism of smoldering in cellulosic materials. To make the study tractable, a simple geometry and a simple configuration were chosen, namely single cylindrical elements mounted horizontally in an infinite natural-convective field. These conditions simulate the early behavior of many fires when the smoldering zone is very small compared to the enclosure.

On the basis of the mechanism proposed in this thesis (see chapter III) one can predict whether smoldering will self-sustain or will go to extinguishment, from a knowledge of fuel and environmental characteristics. Furthermore, the propagation speed and the heat generation rate can be predicted, in the case of a steady smoldering.

On the basis of these predictions, effective means of detection and suppression of smoldering fires can be developed. However, to assess the overall hazards associated with smoldering fires, additional aspects need to be considered such as

1. Smoldering fires in confined enclosures
2. The likelihood of a transition to flaming under imposed convective flow, simulating air conditioning or venting units.
3. the case of smoldering suppression
4. the effects of chemical retardants on smoldering

In this section, experiments were conducted to explore these various important aspects of smoldering fires. The results presented below are all qualitative. They indicate the areas of study where further work seems fruitful.

Smoldering Fires in Confined Enclosures

Experiments were conducted in a confined enclosure to examine the dispersion and accumulation of the products of large smoldering fires, and the evolution of events critical to life hazards. Intuitively, such events may include the loss of visibility, the attainment of tolerance limits in temperature and toxicity and the transition to flaming, flash over or even explosion.

One such experiment simulating a large fire is described below. Smoldering is initiated with a hot coil at one end of a pile of 110 grams of cotton sliver. (Ratio of volume of cotton pile to volume of pressure vessel equals 0.01, the same as for, say, a sofa in a room). The concentration-time histories* for 0_2, CO and CH above the fire at the vessel ceiling are illustrated in Figure A.2.3. Crude subjective judgements of visibility** inside the vessel and standard tenability limits for CO and 0_2 from the Handbook of Fire Protection are also noted as functions of time. Temperature measurements inside the pile recorded a maximum temperature of 690°K. The linear smoldering speed was 0.7 cm/min. Extinguishment occurred before the total consumption of material, when the oxygen concentration dropped to a threshold value of about 15%. For a pressure of one atmosphere in the vessel, this value is in agreement with the extinguishment limit (for a different fuel) reported on in section 2.4.1.

---

* The oxygen profile is not complete due to malfunction of the 0_2 analyzer during part of the experiment.

** For the future, it is recommended to employ a photo-cell to measure light transmission.

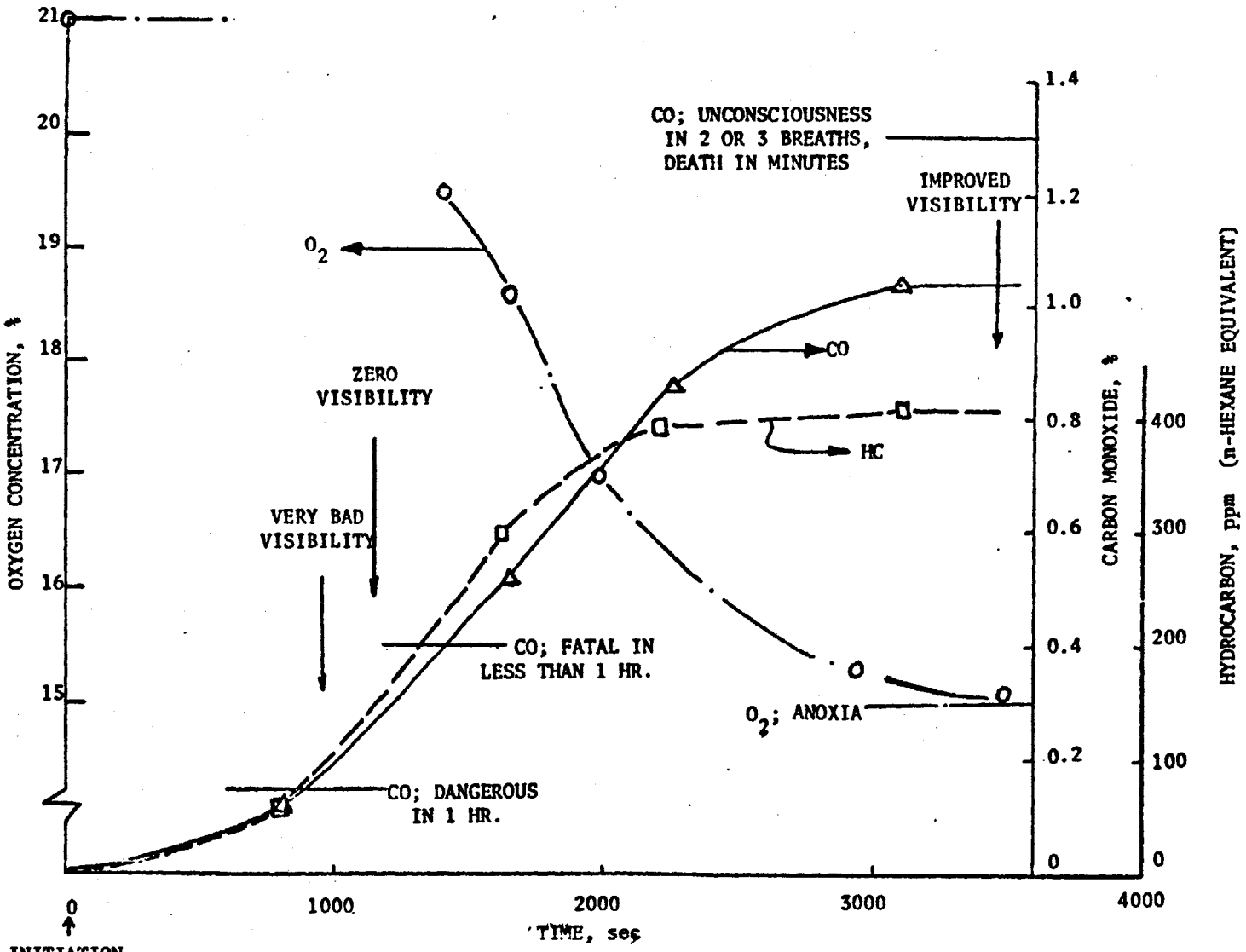


Fig. A.2.3. Oxygen, Carbon Monoxide and Hydrocarbon Concentration- time histories for a simulation of a large smoldering fire. Standard Tenability limits and crude subjective judgements on visivility are also noted.

The important finding from this experiment is that the dispersion of the smoldering products throughout the entire vessel occurred very rapidly because the in-depth smoldering led to the formation of multiple plumes which were only weakly buoyant. Furthermore, the rapid dispersion led to complete loss of visibility long before the tenability limits in CO and O_2 were reached, as indicated in Figure A.2.3.

Under the conditions of this experiment, a spontansous transition to flaming could not occur because of oxygen depletion. However, if the environment is initially oxygen-enriched (such as the hyperbaric chambers used in hospitals, in undersea exploration and in the space program), spontaneous transitions to flaming may occur as described in section 2.4.1. Furthermore, in standard atmospheric conditions, transitions to flaming can be induced if air flow is imposed on the smoldering zone (simulating air conditioning or venting units). Such experiments are described briefly in the following section.

Transition to Flaming Under Imposed Air Flow

The purpose of this study is to determine whether imposing an air flow would cause a transition from smoldering to flaming under realistic conditions of home fires. Thus, commercial household materials (described below) were tested and reasonable air flows were used, simulating air conditioning, fans or venting units.

When an air flow is imposed on a smoldering element, the boundary layer around the element becomes thinner. This increases the rate of arrival of oxygen to the surface and consequently, it increases the reaction rate. In fact, glowing is more intense. The smoldering products are swept with the imposed air flow close to the material surface. If transition to flaming occurs, the ignition of these gases is initiated within the hot charred zone. It is observed that the longer the charred zone, the more likely the occurrence of a transition. (The charred zone length increases with the material thickness.)

The following behaviors were observed when air flows (with varying velocities, up to 3cm/s) are imposed on samples smoldering in a horizontal place.

1. A transition to flaming occurred and the flame was sustained after the air flow was interrupted. This occurred for a sateen cotton fabric (thickness = 0.58 mm and mass/unit area = 7.89 oz/yd^2 or 267 g/m^2), for a 2 cm-thick coarse sawdust fuel bed, and for felt wool rolled in a cylinder (diameter = $\sim$ 3 cm).
2. A transition occurred only at intermittent gentle air-mouth blowing, but the flame did not self-sustain. This occurred

for cardboard and piles of filter paper, thickness up to 4 mm).

3. Glowing was enhanced but a transition did not occur. This was observed for the cylindrical cellulosic materials used in section 2.5 (of varying diameters, up to 8.6 mm) and for papers and filter papers (of varying thickness, up to 0.94 mm).

The important conclusions one can draw from such preliminary experiments is that transition to flaming can occur under realistic conditions of home fires. Such transition does not occur for all materials, however. Much work needs to be done to determine the factors governing such a transition.

Suppression of Smoldering

The results from the study of the effects of environmental parameters (section 2.4.1, and their interpretations in chapter III) indicate that pressurization with an inert gas can slow down and suppress smoldering. This has obvious applications in the space programs and in submarines. Pressurization can also prevent or delay the transition to flaming.

In fires where pressurization is not possible, experiments indicate that carbon-dioxide fire extinguishers and quenching with transite and metal heat sinks are not as effective as water in putting out smoldering cellulosic fires (despite their effectiveness in extinguishing flaming fires). It appears that the factors governing the suppression of smoldering are different from those in the case of flaming, and they are yet to be determined.

Effects of Chemical Retardants on Smoldering

Because of the increasing commercial importance of flame retardants, it is crucial to determine their effects on smoldering combustion. It would be very unfortunate if a chemical that retards flaming enhances smoldering (or vice versa), thus the motivation of the experiments in this section.

Tests on two commercial cotton fabrics of different weights (4.0 and 7.8 oz/yd^2 or 135 and 264 g/m^2) treated with the same flame retardant (Tetrakis hydroxymethyl phosphonium hydroxide/ammonia, polymerized in situ) yielded some interesting results. Upon removal of the heat source (a cigarette or a flame) to initiate the smoldering, the untreated fabric underwent transient smoldering for a short duration of a few minutes before extinguishment while the treated fabric did not sustain smoldering at all. A significantly greater amount of char was formed during the initiation in the case of treated fabrice. However this char did not glow under further heating as readily as the char obtained from untreated fabrics. Possibly, the flame retardant could have affected the pyrolysis reactions, leading to different amounts of char which has different reactivity.

For the conditions of these tests, one can conclude that: (1) the flame retardant used above retarded smoldering also, and (2) an increase in char formation does not necessarily mean an increase in smoldering tendency.

Appendix 3.1

REACTION OF A POROUS CHAR LAYER WITH AMBIENT OXYGEN

Physical Model

In a porous reacting surface, oxygen from the ambient atmosphere has to first diffuse through the boundary layer in the gas-phase, then diffuse through the pores while reacting with the sides of the pores.

Mathematical Model

The mathematical formulation presented below is taken from Frank-kamenetskii [3.24].

In the gaseous boundary layer, the flux of oxygen (j, mole/cm^2 -s) to the char layer is given by the following approximate expression:

$$j \simeq \frac{D(C_\infty - C_o)}{\delta} \qquad (1)$$

where

C_∞ = The oxygen concentration in the ambient atmosphere

C_o = The oxygen concentration at x = 0, i.e., at char surface

δ = Film thickness through which mass diffusion occurs. It depends on the pressure, temperature and the fluid thermo-physical properties in the boundary layer and on the size of the smoldering element.

and D = Diffusion coefficient.

Within the pores, the steady-state diffusion equation for a semi-infinite reacting medium is the following:

$$D'\frac{d^2C}{dx^2} = k'C^n \qquad (2)$$

where D' and k' are the diffusion coefficient and the specific reaction rate calculated on the basis of the true areas of diffusion and reaction within the porous structure. For a structure with cylindrical pores of diameter (h), tortuosity (τ) and a number of pores per unit external cross-sectional area (N), it can be shown that [3.24]:

$$D' = \frac{N\pi h^2}{4} D \qquad (3)$$

and

$$k' = \tau N \pi h k \qquad (4)$$

where D is the diffusion coefficient and k is the specific reaction rate for a same but non-porous material.

The boundary conditions are the following:

$$\text{at } x = 0, \qquad C = C_o \qquad (5)$$

$$\text{and} \quad \text{at } x \to \infty, \qquad C \to 0 \qquad (6)$$

The solution of the diffusion equation (2) subject to conditions (5) and (6) is the following:

$$C(x) = C_o\left(\frac{n-1}{\sqrt{2+n+1}}\sqrt{\frac{k'}{D'}C_o^{n-1}}\,x + 1\right)^{\frac{2}{1-n}} \qquad (7)$$

The macroscopic reaction rate (r, mole/cm^2 s) is equal to the flux of oxygen through the surface at x = 0, i.e.,

$$r = -D'\left(\frac{dC}{dx}\right)_{x=0} \qquad (8)$$

Using the solution (7), it yields:

$$r = \sqrt{\frac{2}{n+1} k'D'C_o^{n+1}} \tag{9}$$

From eqs. (1) and (9), the macroscopic reaction rate (r) can be expressed in terms of the ambient oxygen concentration (C_∞).

For first-order kinetics, eq. (7) becomes:

$$r = \sqrt{D'k'}\, C_o \tag{10}$$

Then, solving eqs. (1) and (10) is simply:

$$r = \frac{\frac{D}{\delta}\sqrt{D'k'}}{\frac{D}{\delta} + \sqrt{D'k'}} C_\infty \tag{11}$$

equivalently,

$$r = \frac{C_\infty}{\gamma} \tag{11a}$$

where

$$\gamma = \frac{\frac{D}{\delta} + \sqrt{D'k'}}{\frac{D}{\delta}\left(\sqrt{D'k'}\right)} \tag{13}$$

Note that γ is the equivalent of the two resistances for the two processes in series:

1. Resistance to diffusion in the boundary layer, $R_1 = \frac{\delta}{D}$ (14)
2. Resistance to diffusion through pore with reaction, $R_2 = \frac{1}{\sqrt{D'k'}}$ (15)

Note that when $R_1 >> R_2$, eq. (11) for the reaction rate reduces to eq. (1) (with $C_o \to 0$). This is the case limited by diffusion through the boundary layer.

When $R_2 >> R_1$, eq. (11) reduces to eq. (10) with $(C_o \to C_\infty)$. This is the case limited by processes occurring in the pores.

In the smoldering problem under investigation, the pores characteristics needed to determine the diffusion coefficient and the specific reaction rate within the pores, according to eqs. (3) and (4), are not available. (The "true"* kinetics needed for eq. (4) are also unavailable). Furthermore, these pores characteristics vary from one experiment to another and vary with time in each experiment. Consequently, we did not attempt to determine them. Instead, the overall "apparent"+ kinetics (appropriate for this study) were determined. And, to be consistent, they were used in a model that did not account for porosity (see sections 3.2.1 and 3.2.4).

---

* i.e., on the basis of the true surface area of the char, including its internal area.

\+ i.e., on the basis of the external area of the char assuming that it is not porous.

APPENDIX 3.2

NON-DIMENSIONAL PARAMETERS OF INTEREST TO THIS STUDY

Molecular diffusion and free convection times

1. Molecular diffusion time, t_{md} in the free convective boundary layer:

$$t_{md} \sim \frac{\delta^2}{D}$$

where δ = boundary Layer thickness $\simeq$ 0.2 cm

D = diffusion coefficient

$\simeq 0.8\ cm^2/s$ for $T_m = 600\ ^\circ K$, $P = 1$ atm

(T_m is arithmetic mean temperature in the boundary Layer)

$t_{md} \simeq 0.05$ sec

2. Free convection time, t_c :

$$t_c \sim \delta / u$$

where u = free-convective velocity $\sim \sqrt{g \beta \Delta T \delta}$

g = gravity constant

β = coefficient of expansion

$\Delta T = T_{surface} - T_{ambient}$

for $\Delta T = 600\ ^\circ K$ and $\delta \simeq 0.2$ cm,

$u \simeq 14$ cm/sec and $t_c \simeq 0.01$ sec

3. From (1) and (2) :

$$\frac{t_c}{t_{md}} \simeq \frac{0.01}{0.05} = \frac{1}{5}$$

Thus, molecular diffusion is much slower than free-convection and limits the arrival of oxygen to the surface.

Appendix 3.3

OXYGEN DIFFUSION FLUX TO CHAR SURFACE

The purpose of this appendix is to present an approximate expression for the oxygen diffusion flux to the char surface. In accordance with the approach taken in this thesis, the simplest realistic expression will be used. The large uncertainties in the pyrolysis and char-oxidation kinetics unwarrants refining any other aspect of the problem.

In the boundary layer of the smoldering element, oxygen and the smoldering products diffuse countercurrently. In the analysis below, it is assumed that oxygen diffuses through a stagnant layer of Nitrogen. At low oxygen mole fraction, the partial pressure of Nitrogen is high and this assumption is good. At higher oxygen mole fraction, the importance of the counterflow effect increases because larger fluxes of oxygen and smoldering products are involved (due to a higher reaction rate). The counterflow effect increases the resistance to the flow of oxygen and decreases the oxygen flux to the surface. Thus, the assumption of oxygen diffusing through a stagnant layer of nitrogen will overestimate the oxygen flux at the high oxygen mole fraction.

The argument given above might explain why the rate of increase of the measured smoldering speed declines at high oxygen mole fraction, as illustrated in Fig. 3.3.1. Note that heat losses (at high mole fraction) might also cause such a decline as discussed in section 3.3. The observed decline may be caused by either or both of these factors.

The oxygen flux is calculated on the basis of the external area of the char. Alternative areas were not chosen for the sake of simplicity. (For example, Tu, Davis and Hottel [3.15] suggest the use of the geometric mean film area, namely

$$\sqrt{\pi d^2 \cdot \pi(d + 2\delta)^2}$$

where d = diameter of element and length of reaction zone, see Section 3.2.3 and δ = thickness of the boundary layer).

The flux of oxygen (J_{O_2}, $g/cm^2 s$) is given by Fix's law:

$$J_{O_2} = -\rho D \nabla Y_{O_2} \tag{1a}$$

$$\text{or } J_{O_2} = -\frac{P}{R_{O_2} T} D \nabla X_{O_2}$$

where ρ = mixture density

D = diffusivity of O_2 through N_2

Y_{O_2} = Oxygen mass fraction

P = mixture pressure

T = Temperature

X_{O_2} = Oxygen mole fraction = P_{O_2}/P

R_{O_2} = Gas constant for oxygen

Assuming the pressure to be constant everywhere, then:

$$J_{O_2} = -\frac{D}{R_{O_2} T} \nabla P_{O_2}$$

Using the film theory approximation (see section 3.2.2), it yields:

$$J_{O_2} = \frac{D}{R_{O_2} T_m \delta} (P_{O_2,\infty} - P_{O_2,s}) \tag{2}$$

δ = film thickness

T_m = Arithmetic mean temperature of the film

Replacing the oxygen and nitrogen molecular weight and atomic volumes (from ref. [3.20]) in the Gilliland expression for D, eq. (3.2.5), yields:

$$D = 5.64 \times 10^{-5} \frac{T_m^{3/2}}{P} \qquad (3)$$

with D in cm^2/s

T_m in °K

P in atm

Replacing eq. (3) in eq. (2) yields:

$$J_{O_{2,s}} = 1.534 \times 10^{-5} \frac{\sqrt{T_s + T_\infty}}{P} \frac{(P_{O_{2,\infty}} - P_{O_{2,s}})}{\delta} \qquad (4)$$

Denoting the numerical factor in eq. (4) by A, then eq. (4) becomes identical to eq. (3.2.6) and

$$A = 1.534 \times 10^{-5} \text{ g of } O_2/\text{cm.s°K}^{1/2}$$

Appendix 3.4

HEAT TRANSFER CORRELATIONS FOR THE BOUNDARY LAYER THICKNESS

The purpose of this Appendix is to determine the thermal boundary layer thickness around a cylindrical smoldering element.

For semi-infinite cylinders, McAdams, [3.21], Kreith [3.25], Bird [3.26] and Rohsenow [3.20], give the following correlation for the laminar regime:

$$Nu = 0.525\ (Gr \cdot Pr)^{1/4}$$

$$\text{for } 10^3 < Gr < 10^8$$

where the nomenclature is defined in text, section 3.2.3, following eq. (3.2.16).

However, the Grashof Number range calculated for the present study is 5 - 6000. For this range, McAdams suggests the use of Fig. 126 in Ref. 3.21. The data in this figure were fitted by the following relationship:

$$Nu = 1.23\ (Gr \cdot Pr)^{0.15} \qquad (3.2.16)$$

$$\text{for } 1 < Gr < 5000$$

This correlation was used in this study to calculate the thickness of the boundary layer.

It should be noted that the length of the reaction zone is about 9 mm ($\pm$ 30%, from section 2.4.2), and the calculated boundary layer thickness varies from 1.6 mm to 4 mm for the range of this study. Thus, the problem is not strictly two-dimensional, especially for low pressures where the boundary layer is thick.

Based on data for three-dimensional flow fields, Kreith [3.25] suggests the use of the same correlations as for the two-dimensional case with a modification of the Grashof Number. The Grashof Number is then calculated on the basis of a new average length, L_{avg} given by:

$$\frac{1}{L_{avg}} = \frac{1}{L_1} + \frac{1}{L_2}$$

where L_1 and L_2 are the two physical lengths of the system. For the case under consideration: $L_1 \equiv d$ and $L_2 \equiv d$ (see section 2.4.2). Thus,

$$L_{avg} = \frac{d}{2}$$

If this new length is used, the boundary layer thickness will increase by only 30% because of its weak dependence on Gr.

Because of the uncertainties in these heat transfer correlation data, it was not warranted to include this new average length in our calculations. Accordingly, eq. (3.2.16) was used with the fuel diameter as the physical length. For a detailed study of free-convective boundary layers, the work of Hermann [3.27] is recommended.

Appendix 3.5
COMPUTER PROGRAMS

SIMPLEST PROGRAM TO CALCULATE EIGENVALUE, PROGRAM NO.1

```
C                                                                       HFCL0001
C                                                                       HFCL0002
C          SIMPLEST PROGRAM TO CALCULATE EIGENVALUE, PROGRAM NO.1       HFCL0003
C                                                                       HFCL0004
      EXTERNAL MMDEI                                                    HFCL0005
      NAMELIST/NIN/D,AEC,AEV,FR,C1,V1,H,QOV                             HFCL0006
      NAMELIST/N1/IERW,W,IERZ,ZZ/N2/IERX,X,IERY,ARGY,YY,QOV,V,TS,Q,VV,TI HFCL0007
      REAL*8 ARG,MMDEI,W,Z,X,Y                                          HFCL0008
      READ (5,NIN)                                                      HFCL0009
      WRITE (6,NIN)                                                     HFCL0010
      IOPT=1                                                            HFCL0011
      N=0                                                               HFCL0012
C                                                                       HFCL0013
    2 ARG=AEC                                                           HFCL0014
      W=MMDEI(IOPT,ARG,IER)                                             HFCL0015
      IERW=IER                                                          HFCL0016
C                                                                       HFCL0017
      ARG=AEV                                                           HFCL0018
      Z=MMDEI(IOPT,ARG,IER)                                             HFCL0019
      ZZ=FR*Z                                                           HFCL0020
      IERZ=IER                                                          HFCL0021
C                                                                       HFCL0022
      WRITE (6,N1)                                                      HFCL0023
C                                                                       HFCL0024
   10 ARG=(C1/(H+QOV))                                                  HFCL0025
      X=MMDEI(IOPT,ARG,IER)                                             HFCL0026
      IERX=IER                                                          HFCL0027
C                                                                       HFCL0028
      ARG=(V1/(H+QOV))                                                  HFCL0029
      Y=MMDEI(IOPT,ARG,IER)                                             HFCL0030
      YY=FR*Y                                                           HFCL0031
      IERY=IER                                                          HFCL0032
      ARGY=ARG                                                          HFCL0033
C                                                                       HFCL0034
      V=(D*(X+YY-W-ZZ))**0.5                                            HFCL0035
      Q=QOV*V                                                           HFCL0036
```

```
      VV=V*60.                                                          HFCL0037
      TS=300.+QOV*83.333                                                HFCL0038
      TI=1./TS                                                          HFCL0039
C                                                                       HFCL0040
      WRITE (6,N2)                                                      HFCL0041
      QOV=QOV*.966                                                      HFCL0042
      N=N+1                                                             HFCL0043
      IF(N.LT.30) GO TO 10                                              HFCL0044
C                                                                       HFCL0045
      END                                                               HFCL0046
C                                                                       HFCL0047
C *****     DATA                                                        HFCL0048
C                                                                       HFCL0049
 &NIN D=-722.,AEC=-44.4,AEV=-51.9,FR=50.,C1=-159.8,V1=-198.1,           HFCL0050
 H=3.6,QOV=16., &END                                                    HFCL0051
```

```
C                                                                       EIGC0001
C         PROGRAM NO.2                                                  EIGC0002
C                                                                       EIGC0003
C         DETERMINATION OF HEAT FLUX INTO MATERIAL                      EIGC0004
C                                                                       EIGC0005
C                                                                       EIGC0006
      REAL*8 XCEE,ETA,DMY,POS                                           EIGC0007
      NAMELIST/NI2/H,TA,F,AEK,SR,BL,A,Q,S                               EIGC0008
      NAMELIST/NO8/PO,FO,P,F                                            EIGC0009
      NAMELIST/NO6/TI,RR,QS,TS,X,XCEE,ETA,POS,GR,BL,HTC,QG,QR,QLR       EIGC0010
C                                                                       EIGC0011
      READ (5,NI2)                                                      EIGC0012
      WRITE (6,NI2)                                                     EIGC0013
      N1=9                                                              EIGC0014
      DO 30 N=1,N1                                                      EIGC0015
      READ (5,100) PO,FO,F                                              EIGC0016
  100 FORMAT (2F10.5,F16.2)                                             EIGC0017
    2 I=0                                                               EIGC0018
      P=PO/FO                                                           EIGC0019
      WRITE (6,NO8)                                                     EIGC0020
      QT=0.0                                                            EIGC0021
      X=2.0                                                             EIGC0022
C                                                                       EIGC0023
    1 TS=X*TA                                                           EIGC0024
      TAVG=(TS+TA)/2.                                                   EIGC0025
      TI=1./(X*TA)                                                      EIGC0026
C                                                                       EIGC0027
      VIS=1.709E-4*(TAVG/273.)**1.5*(393.0000000/(TAVG+120.))           EIGC0028
      COND=5.83E-5*(TAVG/273.)**0.82+5.55E-5*(PO/(FO*TAVG))**1.23       EIGC0029
C                                                                       EIGC0030
      GR=(77.83*(TS-TA)*PO**2)/(TAVG*(VIS*FO*TAVG)**2)                  EIGC0031
      BL=0.58/(1.0705*GR**0.15)                                         EIGC0032
      HTC=COND/BL                                                       EIGC0033
C                                                                       EIGC0034
      EXD=F*EXP(-AEK/X)                                                 EIGC0035
      XCEE=EXD*SR*BL*SQRT(PO)/(A*SQRT(TS+TA)*FO)                        EIGC0036
```

```
      DMY=1.+.5*XCEE**2                                                 EIGC0037
      ETA=DMY-DSQRT(DMY**2-1.0)                                         EIGC0038
      POS=ETA*PO                                                        EIGC0039
      RR=DSQRT(POS)*EXD                                                 EIGC0040
      QG=RR*Q                                                           EIGC0041
C                                                                       EIGC0042
      QR=1.356E-12*S*TS**4                                              EIGC0043
      QC=HTC*(TS-TA)                                                    EIGC0044
      QLR=QR/QC                                                         EIGC0045
C                                                                       EIGC0046
      QS=2*(QG-QR-QC)                                                   EIGC0047
C                                                                       EIGC0048
      IF (QS.GT.0.0) WRITE (6,N06)                                      EIGC0049
      IF (QS.GT.0.0) QT=QT+QS                                           EIGC0050
C                                                                       EIGC0051
C                                                                       EIGC0052
    5 I=I+1                                                             EIGC0053
      X=X+0.04                                                          EIGC0054
      IF (XCEE.GT.1000.0.AND.QS.LT.0.0) I=99                            EIGC0055
      IF (I.LT.99) GO TO 1                                              EIGC0056
C                                                                       EIGC0057
      IF (QT.EQ.0.0) GO TO 30                                           EIGC0058
      PO=PO*0.95                                                        EIGC0059
      GO TO 2                                                           EIGC0060
C                                                                       EIGC0061
   30 CONTINUE                                                          EIGC0062
      END                                                               EIGC0063
C                                                                       EIGC0064
C ******    DATA                                                        EIGC0065
C                                                                       EIGC0066
 &NI2 H=3.6,TA=300.,F=3.29E8,AEK=73.7,SR=2.67,BL=.1,A=1.534E-5,Q=7700,  EIGC0067
 S=0.9, &END                                                            EIGC0068
 .72       .1          100000000.                                       EIGC0069
 .384       .13        100000000.                                       EIGC0070
 .197       .15        100000000.                                       EIGC0071
 .145        .17       100000000.                                       EIGC0072
```

```
 .092        .21      100000000.                                    EIGC0073
 .066        .25      100000000.                                    EIGC0074
 .0422       .3       100000000.                                    EIGC0075
 .0263       .35      100000000.                                    EIGC0076
.0237        .4       100000000.                                    EIGC0077
```

NOMENCLATURE FOR COMPUTER PROGRAMS

The main variables in the computer programs are expressed in terms of the nomenclature introduced in chapter III. The listing below follows the order of appearance in the programs.

Program No. 1

MMDEI = exponential integral function

$D = \lambda f_c / \rho_\infty c \ln\beta$

$AEC = -E_c / \mathcal{R} T_\infty$

$AEV = -E_g / \mathcal{R} T_\infty$

$FR = f_c / f_g$

$C1 = -\rho_\infty c E_c / \mathcal{R}$

$V1 = -\rho_\infty c E_g / \mathcal{R}$

$H = \rho_\infty c T_\infty$

$Q = q_s$

$V = V$

$QOV = q_s / V$

$TS = T_s$

Program No. 2

XCEE = ξ , see eq. (3.2.9)

ETA = $P_{O_2,s} / P_{O_2,\infty}$

POS = $P_{O_2,s}$

H = $\rho_\infty c T_\infty$

F = f_e

AEK = E_e

SR = ϕ

BL = δ

A = A , see Appendix 3.3

Q = Q , heat of reaction

S = ϵ , emissivity

PO = $P_{O_2,\infty}$

FO = $X_{O_2,\infty}$

P = P

TI = Inverse temperature

TS = Surface temperature

X = T / T_∞

GR = Grashof Number

BL = δ

HTC = h , heat transfer coefficient

QG = heat flux generated by char oxidation

QR = heat flux lost by radiation

QC = heat flux lost by convection

QS = heat flux feedback

Appendix 3.6

NUMERICAL VALUES EMPLOYED IN THE THEORETICAL CALCULATIONS

For the pyrolysis study:

cellulose specific heat = 0.20 cal/gm °K

cellulose thermal conductivity = 1.2×10^{-4} cal/cm°Ks

sample density = 0.06 g/cm^3

ambient temperature = 300°K

For the char-oxidation study:

activation energy = 44 k cal/mole

frequency factor = 10^8 g of char/cm^2.s.$atm^{1/2}$

heat of combustion of char = 7700 cal/g of char

stoichiometric ratio = 2.67 g of O_2/g of char

emmissivity = 0.9 from Ref. [3.23].

A, from eq. (3.2.6) = 1.53×10^{-5} g of O_2/cm.s.$°K^{1/2}$